Flow Unit Characterization of the Early Cretaceous Missisauga Formation Using Venture B-13 Well

---

Lori Manoukian

Supervisor: Grant Wach

Submitted in Partial Fulfillment of the Requirements
for the Degree of Bachelor of Science, Honors

Department of Earth Science,

Dalhousie University, Halifax Nova Scotia

March 2013

Distribution License

DalSpace requires agreement to this non-exclusive distribution license before your item can appear on DalSpace.

NON-EXCLUSIVE DISTRIBUTION LICENSE

You (the author(s) or copyright owner) grant to Dalhousie University the non-exclusive right to reproduce and distribute your submission worldwide in any medium.

You agree that Dalhousie University may, without changing the content, reformat the submission for the purpose of preservation.

You also agree that Dalhousie University may keep more than one copy of this submission for purposes of security, back-up and preservation.

You agree that the submission is your original work, and that you have the right to grant the rights contained in this license. You also agree that your submission does not, to the best of your knowledge, infringe upon anyone's copyright.

If the submission contains material for which you do not hold copyright, you agree that you have obtained the unrestricted permission of the copyright owner to grant Dalhousie University the rights required by this license, and that such third-party owned material is clearly identified and acknowledged within the text or content of the submission.

If the submission is based upon work that has been sponsored or supported by an agency or organization other than Dalhousie University, you assert that you have fulfilled any right of review or other obligations required by such contract or agreement.

Dalhousie University will clearly identify your name(s) as the author(s) or owner(s) of the submission, and will not make any alteration to the content of the files that you have submitted.

If you have questions regarding this license please contact the repository manager at dalspace@dal.ca.

Grant the distribution license by signing and dating below.

______________________________	______________________________
Name of signatory	Date

DALHOUSIE
UNIVERSITY
Inspiring Minds

Department of Earth Sciences
Halifax, Nova Scotia
Canada B3H 4R2
(902) 494-2358
FAX (902) 494-6889

DATE: April 25, 2013

AUTHOR: Lori Manoukian

TITLE: Flow Unit Characterization of the Early Cretaceous Missisauga Formation Using Venture B-13 Well

Degree: BSc. Convocation: May Year: 2013

Permission is herewith granted to Dalhousie University to circulate and to have copied for non-commercial purposes, at its discretion, the above title upon the request of individuals or institutions.

THE AUTHOR RESERVES OTHER PUBLICATION RIGHTS, AND NEITHER THE THESIS NOR EXTENSIVE EXTRACTS FROM IT MAY BE PRINTED OR OTHERWISE REPRODUCED WITHOUT THE AUTHOR'S WRITTEN PERMISSION.

THE AUTHOR ATTESTS THAT PERMISSION HAS BEEN OBTAINED FOR THE USE OF ANY COPYRIGHTED MATERIAL APPEARING IN THIS THESIS (OTHER THAN BRIEF EXCERPTS REQUIRING ONLY PROPER ACKNOWLEDGEMENT IN SCHOLARLY WRITING) AND THAT ALL SUCH USE IS CLEARLY ACKNOWLEDGED.

Table of Contents

List of Figures .... **I**

List of Tables .... **III**

Acknowledgements .... **V**

Abstract .... **VI**

Chapter 1 .... **1**

1.1 Introduction 1

1.2 Problem Statement 2

1.3 Regional Geology 2

1.4 Stratigraphy 4

1.5 Mobil Texaco PEX Venture B-13 6

1.6 Missisauga Formation 8

1.7 Petroleum System Elements 8

1.7.1 Reservoir 8

1.7.2 Seals and Traps 9

1.7.3 Source Rocks and Migration 9

1.8 Diagenesis 9

1.9 Flow Units 11

Chapter 2 .... **13**

2.1 Lithofacies 13

2.2 Core Description Analysis 13

2.3 Methodology 13

2.3.1 Ranking Potential Differences in Flow Units 14

2.3.2 Flow Unit Strength: Influence on Preferential Flow 23

Chapter 3 .... **28**

3.1 Mobil Texaco Pex Venture B-13 Lithofacies: 28

3.1.1 Thin Section Classification 29

3.2 Lithofacies 1: Oolitic Limestone 29

3.2.1 Thin section analysis of facies 1 30

3.2.2 Lithofacies 1 Interpretation: Shallow marine, sub-tidal zone 35

3.3 Lithofacies 2: Shale 35

3.3.1 Thin section analysis of facies 2 36

3.3.1.1 Burrowed Clay 36

3.3.2 Lithofacies 2 Interpretation: Shallow Marine Open Shelf 37

3.4 Lithofacies 3: Heterolithic and Cyclic Sandstone and Shales 39

3.4.1 Thin section interpretation of facies 3 40

3.4.2 Lithofacies 3 Interpretation: Tide-Influenced Nearshore Shallow Marine Shelf Deposits 41

3.5 Lithofacies 4: Cross-Stratified Calcareous Micaceous Sandstone 42

3.5.1 Thin section interpretation of facies 4 44

3.5.2 Lithofacies 4 Interpretation: Shoreface Deposits 54

Chapter 4 55

4.1 Trace Fossils-Venture B-13 Well 55

4.1.1 Cruziana Ichnofacies 55

4.1.2 Skolithos Ichnofacies 58

4.2 Summary of Trace fossils 60

Chapter 5 61

5.1 Permeability in Venture B-13 Cores 61

5.1.1 TinyPermII 61

5.1.2 Core Plug Permeability 62

5.1.3 TinyPermII and Core Plug Permeability 62

5.2 Porosity in Venture B-13 68

5.3 Porosity vs. Permeability 71

Chapter 6 72

6.1 Results 72

6.1.1 Flow units 72

6.1.2 Flow Unit Strength: Influence on Preferential Flow 77

Chapter 7 90

7.1 Discussion 90

7.1.1 Porosity 90

7.1.2 Horizontal Permeability 90

7.1.3 Porosity vs. Permeability 91

7.1.4 Flow Unit Differentiation 91

7.1.5 Flow Unit Characterization 92

7.2 Conclusions 93

7.3 Future Work 95

References........ 97

Appendix A: Pictures of Core Boxes 101

Appendix B: Horizontal core plug data points 118

Appendix C: Thin section data points 119

List of Figures

Figure 1.1 Location map of eastern North America Atlantic margin 2

Figure 1.2 Location map of Offshore Nova Scotia 3

Figure 1.3 Location map of Sable Island area and wells 3

Figure 1.4 Stratigraphic column, Scotian Basin, offshore Nova Scotia 5

Figure 1.5 Venture B-13 stratigraphic column 6

Figure 1.6 Cores of Venture B-13 tied to petrophysical data 7

Figure 1.7 Image from Mayaro Beach, Trinidad demonstrating concept of second order flow units 11

Figure 1.8 Graphical representation of flow unit scales 12

Figure 2.1 Histogram of permeability values of well Venture B-13 15

Figure 2.2 Histogram of porosity values in Venture B-13 well 17

Figure 2.3 Visual representation and classification of bioturbation with increased grade & intensity 20

Figure 2.4 Chart for determining approximate modal percentages in rocks 22

Figure 2.5 Permeability values assigned to specific types of rocks 23

Figure 3.1 Folk's carbonate classification chart 29

Figure 3.2 Core photo of facies 1 oolitic limestone (4700.44m-4700.22m) 30

Figure 3.3 Crinoid shell fragments found in oolitic limestone of lithofacies 1 (4700.38m) 30

Figure 3.4 Thin section from a depth of 4692.2m 31

Figure 3.5 Thin section from a depth of 4695.62m (A) and (B) 32

Figure 3.6 Thin section from a depth of depth of 4693m 32

Figure 3.7 Thin section from a depth of 4704.85m 33

Figure 3.8 Thin section from a depth of 4695.62m 34

Figure 3.9 Core photo of lithofacies 2 shales from interval 4706.88m to 4706.67m 35

Figure 3.10 Thin section photo of facies 2 offshore muds from 4708.14 m 37

Figure 3.11 Interlayered heterolithic sands and shales from 4732 m 39

Figure 3.12 Thin section of facies 3 interbedded siltstone and intramicrite from 4708.14 m 40

Figure 3.13 Thin section of facies 3 interbedded siltstone and intramicrite from 4716.25m 41

Figure 3.14 Oscillatory-flow cross-laminations in lithofacies 4 42

Figure 3.15 Climbing ripples 42

Figure 3.16 Fine sands with parallel shale laminaee 42

Figure 3.17 Laminaeted argillaceous sands 42

Figure 3.18 Thin section from 4699.66m 45

Figure 3.19 Thin section from 4699.66m 45

Figure 3.20 Thin sections from 4695.62m 47

Figure 3.21 Thin section from 4693.64m 49

Figure 3.22 Flexible grain deformation 49

Figure 3.23 Thin section from 4693.64m 49

Figure 3.24 Thin section from 4708.20m 50

Figure 3.25 Thin section from 4707.40m 50

Figure 3.26 Thin section from 4711.95m 51

Figure 3.27 Thin section from 4730.20m 52

Figure 3.28 Thin section from 4708.20m 53

Figure 4.1 Trace fossils and their respective ichnofacies and environments 55

Figure 4.2 Sands and shales from facies 3 with *Planolites* burrows 57

Figure 4.3 *Rosselia socialis* burrow of the *Cruziana* ichnofacies 57

Figure 4.4 Coarse grained sandstone of facies 4 with 3 cm *Ophiomorpha nodosa* burrow 58

Figure 5.1 TinyPermII from New England Research Inc. 61

Figure 5.2 Core 1 depth (m) vs. permeability (mD) 64

Figure 5.3 Core 2 depth (m) vs. permeability (mD) 65

Figure 5.4 Core 3 depth (m) vs. permeability (mD) 66

Figure 5.5 Core 4 depth (m) vs. permeability (mD) 67

Figure 5.6 Porosity fraction of cores 1&2 plotted against well depth (m) 69

Figure 5.7 Porosity fraction of core 3 plotted against depth of well (m) 69

Figure 5.8 Porosity fraction of core 4 plotted against depth of well (m) 69

Figure 5.9 Porosity fraction versus permeability (mD) through Venture B-13 71

Figure 6.1 Colors assigned to flow unit strength values. 81

Figure 6.2 Core 1 description sheet 82

Figure 6.3 Core 2 description sheet 84

Figure 6.4 Core 3 description sheet 85

Figure 6.5 Core 4 description sheet 87

List of Tables

Table 1.1 Cores of Venture B-13 Well 6

Table 2.1 Permeability and assigned values for flow unit differentiation 15

Table 2.2 Porosity and assigned values for flow unit differentiation 17

Table 2.3 Udenn-Wentworth grain size chart 18

Table 2.4 Grain size and assigned values for flow unit differentiation 18

Table 2.5 Change in lithofacies and assigned values for flow unit differentiation 19

Table 2.6 Variation in bioturbation and assigned values for flow unit differentiation 19

Table 2.7 Variation in cementation and assigned values for flow unit differentiation 21

Table 2.8 Flow unit characterization Integration table 22

Table 2.9 Assigned values for amount of clay for flow unit characterization 24

Table 2.10 Assigned values for amount of cement for flow unit characterization 24

Table 2.11 Assigned values for grain size for flow unit characterization 25

Table 2.12 Assigned values for bioturbation index for flow unit characterization 25

Table 2.13 Assigned values for porosity for flow unit characterization 26

Table 2.14 Flow unit strength integration 27

Table 3.1 Thin section sample list 28

Table 3.2 Paragenesis of bio-oosparite and oobiosparite 35

Table 3.3 Paragenesis of burrowed clay microlithofacies 36

Table 3.4 Paragenesis of interbedded siltstone and clay microlithofacies 40

Table 3.5 Paragenesis of fine-grained calcareous sandstone with ooid fragments 46

Table 3.6 Paragenesis of very fine- to medium-grained calcareous sandstone 46

Table 3.7 Paragenesis of fine- to coarse-grained calcareous silt 53

Table 4.1 Trace fossils of Venture B-13 and ethology 59

Table 4.2 Trace fossils, associated lithofacies and average permeability measurements 59

Table 5.1 Physical size of TinyPermII parts 61

Table 5.2 Average permeability measurements of lithofacies from core plugs and range of values 63

Table 5.3 Average permeability measurements of lithofacies from TinyPermII and range of values 63

Table 5.4 Average porosity from core plugs for each lithofacies and the number of values 69

Table 6.1 Table ranking potential differences in flow units of core 1 73

Table 6.2 Table ranking potential differences in flow units of core 2 74

Table 6.3 Table ranking potential differences in flow units of core 3 75

Table 6.4 Table ranking potential differences in flow units of core 4 76

Table 6.5 Table demonstrating strength of flow units within core 1 77

Table 6.6 Table demonstrating strength of flow units within core 2 78

Table 6.7 Table demonstrating strength of flow units within core 3 79

Table 6.8 Table demonstrating strength of flow units within core 4 80

Table 7.1 Identified lithofacies within Venture B-13 and interpreted depositional environments 93

Table 7.2 Microlithofacies in Venture B-13 and associated lithofacies 94

Table 7.3 Average porosity and permeability measurements throughout Venture B-13 94

Acknowledgements

My sincere gratitude towards Dr. Martin Gibling who helped me throughout this thesis with his genuine interest and constructive feedback. I also want to thank Dr. Isabelle Coutand, my first geology teacher, who with her passion and dedication to sciences captivated me, stimulating my interest and propelling me into the field of Earth Sciences. Moreover, the successful completion and personal reward of this thesis could not have been achieved without the encouragement and constant support of my family. I give special credit to my wonderful brothers who continue to inspire and motivate me throughout my academic tenure. Finally, thank you to my friends and supervisor Dr. Grant Wach.

Flow Unit Characterization of the Early Cretaceous Missisauga Formation Using Cores From The Venture B-13 Well

By Lori Manoukian

Abstract

Reservoir characterization through the identification of flow units is an important step in resolving challenges faced in the production of oil and gas. This study investigated the vertical variations in reservoir quality and heterogeneity of the Lower Missisauga Formation, penetrated by the Venture B-13 Well of the Sable Subbasin, offshore Nova Scotia.

Core logging, thin section analysis, permeability and porosity data were used to: 1) identify lithofacies and microlithofacies within the Venture B-13 Well, 2) identify and analyse factors that lead to reservoir heterogeneity, and 3) recognize vertical permeability variations. Flow units could be defined on the basis of measurements of permeability and porosity corresponding to grain size, bioturbation, lithology, cementation, and clay content. A semi-quantitative system was designed to allow the factors to be rated relative to each other. Application allowed for detection of potential flow units and their individual strengths.

The Lower Missisauga Formation at Venture B-13 corresponds to four depositional environments. Lithofacies 1 consists of oolitic limestone interpreted to be of a shallow marine sub-tidal zone. Microlithofacies subgroups of lithofacies 1 include bio-oosparite and oobiosparite. Facies 2 contains shales of an interpreted shallow marine setting. Lithofacies 3 comprises interbedded sandstone and shale of a tide-influenced nearshore shallow marine setting. Lithofacies 4 consists cross-stratified calcareous and micaceous sandstone. Its depositional environment is interpreted as a low-energy shoreface. Associated microlithofacies range from medium-grained sandstone to fine grained silt, with a slight variation in mineralogy. A steady increase in porosity and permeability values from lithofacies 1 to 4 is observed. Facies 4 micaceous sandstones have the highest potential for reservoir rocks.

Fifty-six potential flow units and 48 major flow units were identified with a wide range of preferential flow values. Changes in permeability and porosity are attributed to a change in depositional environment, diagenetic processes and activity of paleo-organisms. Enhanced flow unit definition could allow for strategic drilling in order to improve long term hydrocarbon production rates.

Keywords: Lower Missisauga Formation, Sable Subbasin, Offshore Nova Scotia, permeability, diagenesis, lithofacies, microlithofacies.

Chapter 1

1.1 Introduction

The study area of this project is located in the Scotian Basin, specifically the Sable Subbasin located offshore of Nova Scotia (Fig. 1.1). The Scotian Basin was a sediment depositional center during the Mesozoic and Cenozoic and is a 125 to 225 km wide continental margin (Wade & MacLean, 1990). In terms of scale, the Scotian Basin covers an area of approximately 300 000 km ^{2}(Ings *et al*., 2005). Gas production by ExxonMobil's Sable Offshore Energy Project (SOEP) in the Sable Subbasin comes from five fields: Thebaud, Venture, North Triumph, South Venture, and Alma. These fields contain a significant amount of natural gas and crude oil (Mukhopadhyay *et al*., 2003). To date, a total of 205 wells have been drilled in the Scotian Basin: 124 exploration, 27 delineation, 51 production, and 5 exploration / development or other types (CNSOPB, 2013).

Although approximately 75% of the original gas-in-place reserves discovered offshore Nova Scotia are within the Missisauga Formation (Canada Nova Scotia Offshore Petroleum Board, 2013), only a few researchers have studied its sedimentology in great detail (eg. Cummings & Arnott, 2005). This thesis will discuss and examine the contributing factors to fluid flow characterisation and flow strength within the Lower Missisauga Formation. Evaluation criteria to conduct this analysis include grain size, permeability, bioturbation and cementation. Following a geological overview of the Scotian Shelf and Sable Subbasin (Chapter 1), critical examination of the hydrocarbon reservoir characteristics, methodology for flow unit analysis is thoroughly explained (Chapter 2). Core lithofacies and thin section microlithofacies are identified (Chapter 3), trace fossils and individual abundance are analysed (Chapter 4) and this information is used in identification and classification of flow units within the Missisauga Formation (Chapter 5).

1.2 Problem Statement

Since 2009, gas production from the five SOEP fields has been in continuous decline (Canada Nova Scotia Offshore Petroleum Board, 2013). This thesis specifically analyses and critically assesses the Lower Missisauga Formation at well Venture B-13 to highlight and resolves fundamental limitations in the conventional permeability modeling workflow. Core and thin sections from Venture B-13 are analysed to thoroughly define and characterise flow units providing details about reservoir characteristics and the depositional environment. This study further serves to develop best practices for future projects in the areas of high resolution reservoir modeling of the greater Scotian Basin.

1.3 Regional Geology

The Scotian Basin demonstrates distinctive geology that is a product of tectonic cyclicity. Extensional faulting in this region was the result of the rifting that separated Africa from North America during the breakup of Pangea (Sable Offshore Energy, 1996). This rifting was initiated approximately 225 million years ago when the region of Nova Scotia bordered present day Morocco. Prior to the breakup of supercontinent Pangea, Nova Scotia was located at ~15°N in a semi-arid, subtropical to humid climate (Kidston *et al.,* 2005).

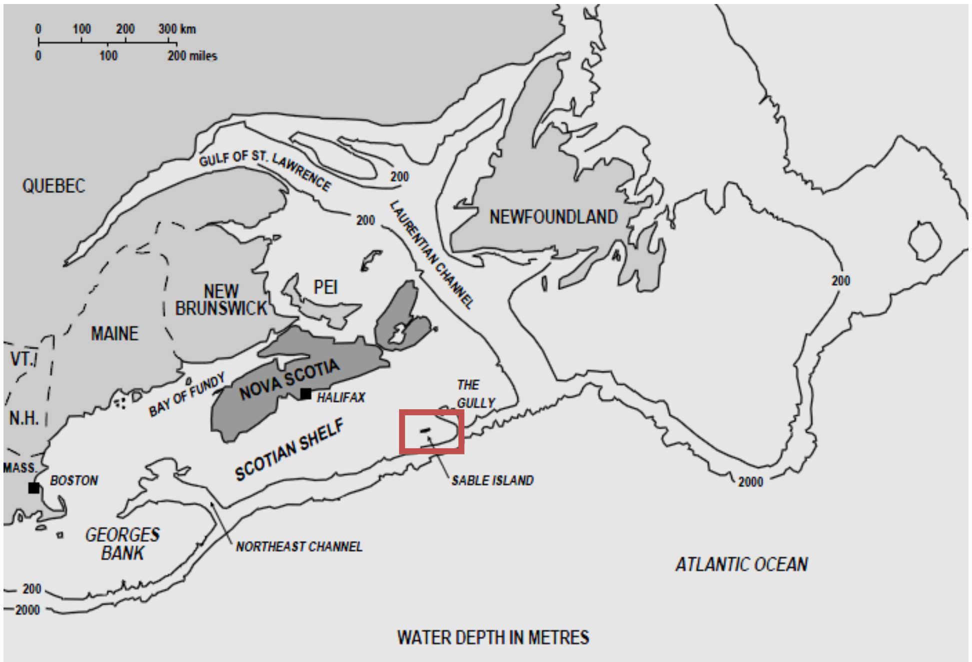
0 100 200 300 km
0 100 200 miles
QUEBEC
GULF OF ST. LAWRENCE
200
200
LAURENTIAN CHANNEL
NEWFOUNDLAND
NEW BRUNSWICK
PEI
MAINE
VT.
N.H.
MASS.
BOSTON
BAY OF FUNDY
NOVA SCOTIA
HALIFAX
THE GULLY
SCOTIAN SHELF
SABLE ISLAND
200
2000
GEORGES BANK
NORTHEAST CHANNEL
ATLANTIC OCEAN
200
2000
WATER DEPTH IN METRES

Figure 1.1. Map of the continental margin of northeastern United States and Atlantic Canada showing location of Sable Island (Sable Offshore Energy, 1996).

Within the Scotian Basin, ridge and platform tectonic elements define the subsidiary subbasins and grabens; e.g. La Have and Banquereau platforms, Orpheus Graben, and the Sable, Shelburne, Abenaki and Laurentian subbasins (CNSOPB, 2013).Interestingly, the boundaries of these subbasins are thought to be rooted in oceanic fracture zones (Welsink *et al.,* 1990).

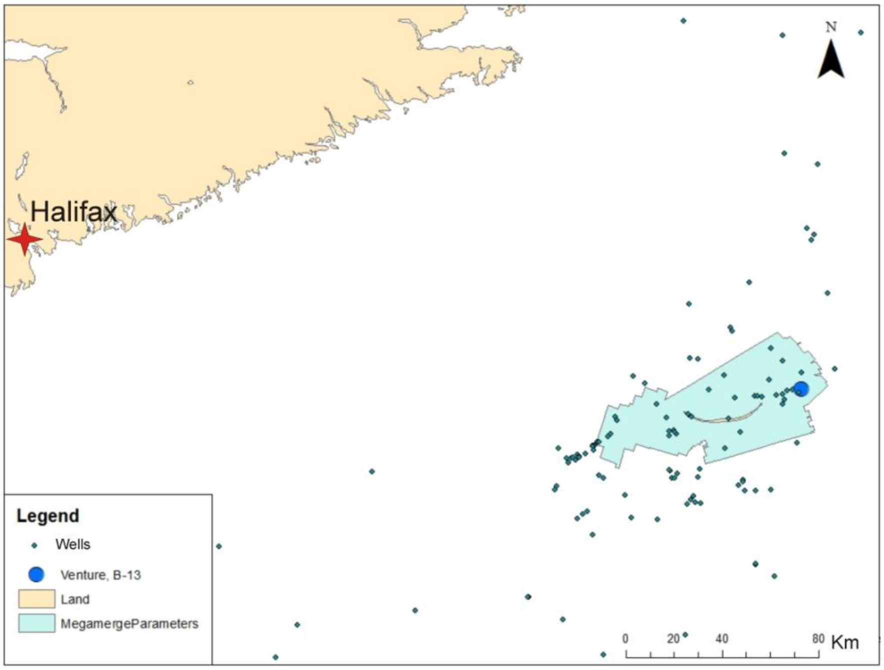
N
Halifax
Legend
Wells
Venture, B-13
Land
MegamergeParameters
0
20
40
80
Km

Figure 1.2. Location map for the central Scotian Shelf, offshore Nova Scotia.

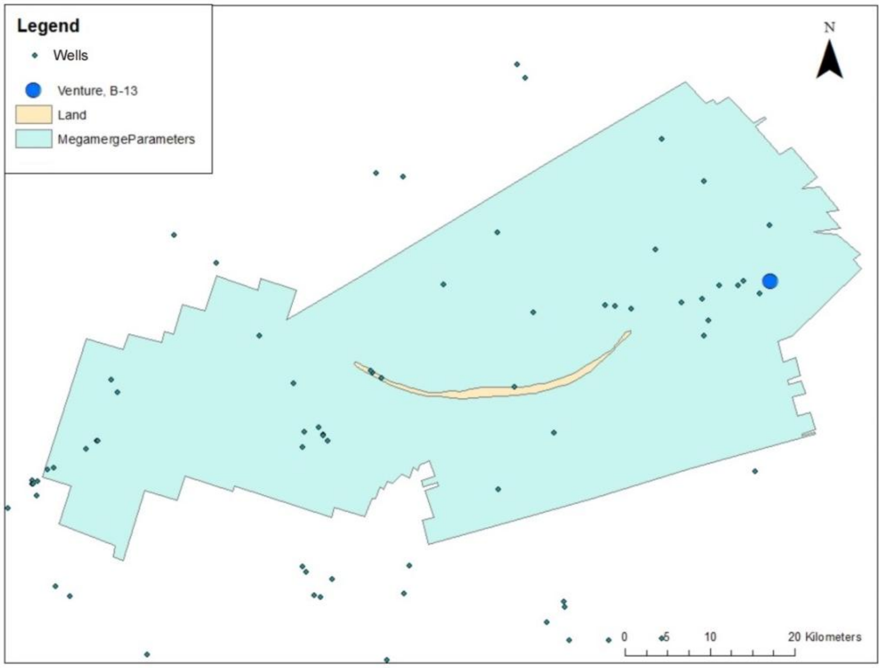
Legend
Wells
Venture, B-13
Land
MegamergeParameters
N
0
5
10
20 Kilometers

Figure 1.3. Map of Sable Island area showing the location of the ExxonMobil 3D seismic Megamerge, Venture B-13 and surrounding wells.

1.4 Stratigraphy

Stratigraphic units of the Scotian Basin were first defined by McIver (1972). Minor changes were made to the regional stratigraphy in 1975 and 1995 by Jansa and Wade (1975), Wade and MacLean (1990) and Wade *et al*., (1995). Cambro-Ordovician metamorphosed sediments, as well as Devonian granites form the basement of the Scotian Shelf and Mesozoic-Cenozoic sediments compose the cover (Sable Offshore Energy, 1996). The Argo and Eurydice formations were deposited during Late Triassic to Early Jurassic and comprise mainly evaporites and siliciclastic strata. Following continental breakup, rift grabens that formed during the synrift of the Upper Triassic were subsequently filled with continental clastics of the Mohican Formation and dolomites of the Iroquois Formation (Wade and MacLean, 1990). The Middle to Late Jurassic Abenaki Formation was deposited when marine conditions were predominant in the southwest margin and comprises reefal and platformal carbonates and shales.

During the post-breakup stage, the Late Jurassic to Early Cretaceous Mic Mac, Missisauga and Logan Canyon formations were deposited as a progradational sequence (Wade and MacLean, 1990). The Mic Mac Formation is representative of the first phase of the delta progradation. Distributary channels and delta front sands interfinger with the Verrill Canyon Shales (Kidston *et al.,* 2005). The "O" Marker is a regional seismic marker of variable thickness (up to 122 metres) composed of a series of shallow water oolitic limestones and calcareous sandstones (CNSOPB, 2013). It is found within the Missisauga Formation and is relatively continuous throughout the basin, pinching out towards the northwest. The Late Cretaceous Dawson Canyon Formation shales and limestones are overlain by the Wyandot Formation which consists of limestone with chalk intervals. The marine shelf mudstones, shelf sands and conglomerates forming the Banquereau Formation later covered the Wyandot Formation.

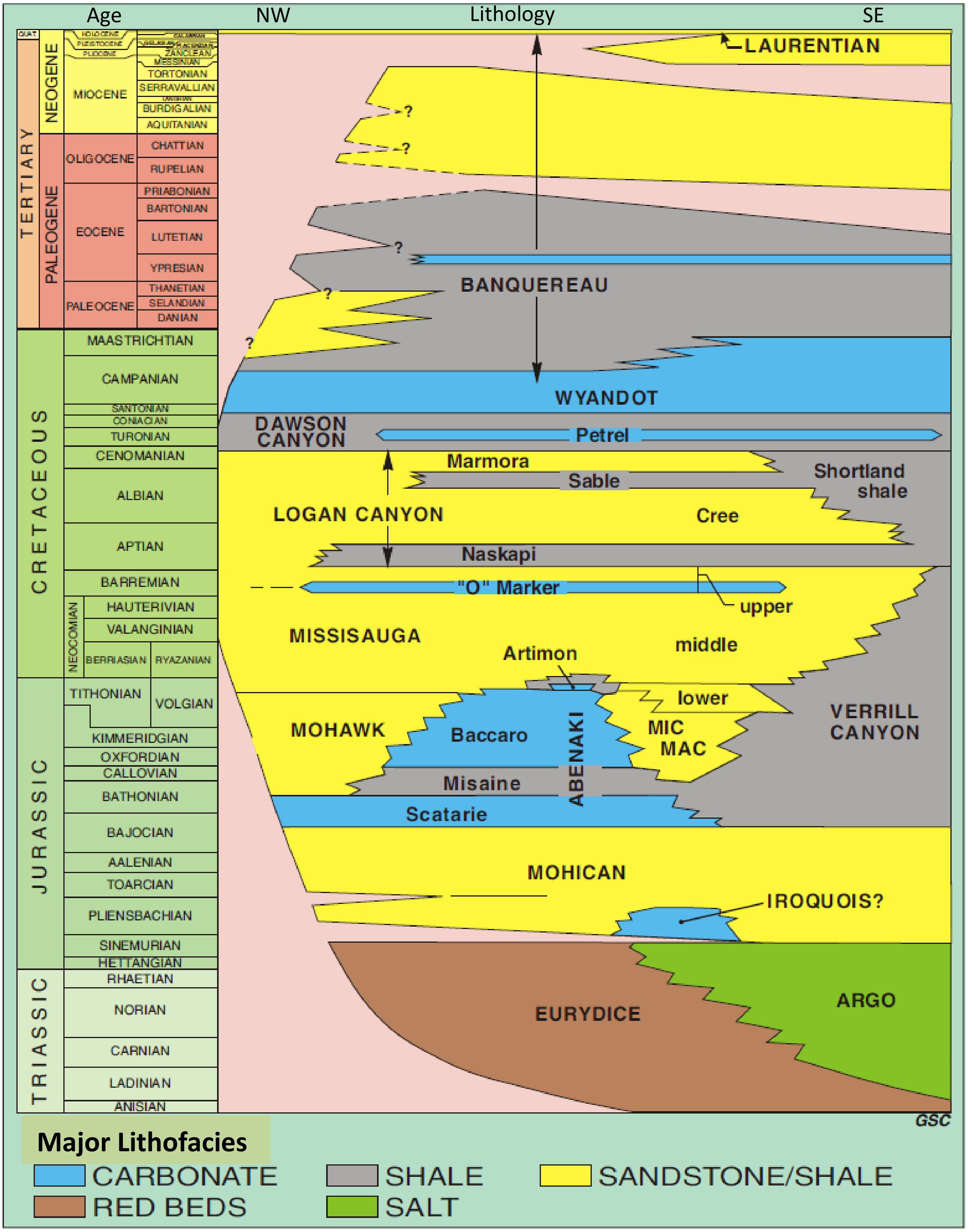

Figure 1.4. Stratigraphic chart of offshore Nova Scotia showing lithological units from NW to SE. Progradation, aggradation and retrogradation of units may be observed (Fensome *et al.*, 2008).

1.5 Mobil Texaco PEX Venture B-13

Mobil Texaco PEX Venture B-13 was operated by Mobil Oil Limited and is located north-northwest of Sable Island at coordinates 44° 02’ 11.6’’ N and 59° 32’ 3.5’’W. Drilling began in August 1980 and the well was plugged and abandoned in February 1981. The total driller’s depth reached was 5368 m and total logger’s depth reached 5227m. Four conventional cores were cut in the Missisauga Formation (details in Table 1.1) and stored in Calgary and at the Canada Nova Scotia Offshore Petroleum Board's Geoscience Research Centre in Dartmouth, Nova Scotia.

		Depth	**Recovered**
Core # 1	🟥	4692.7-4710.0m	17.3m
Core # 2	🟨	4710.4-4716.2m	5.8m
Core # 3	🟩	4716.2-4734.4m	18.0m
Core # 4	🟦	4949.0-4967.3m	18.3m

Table 1.1 Cores of Venture B-13 Well

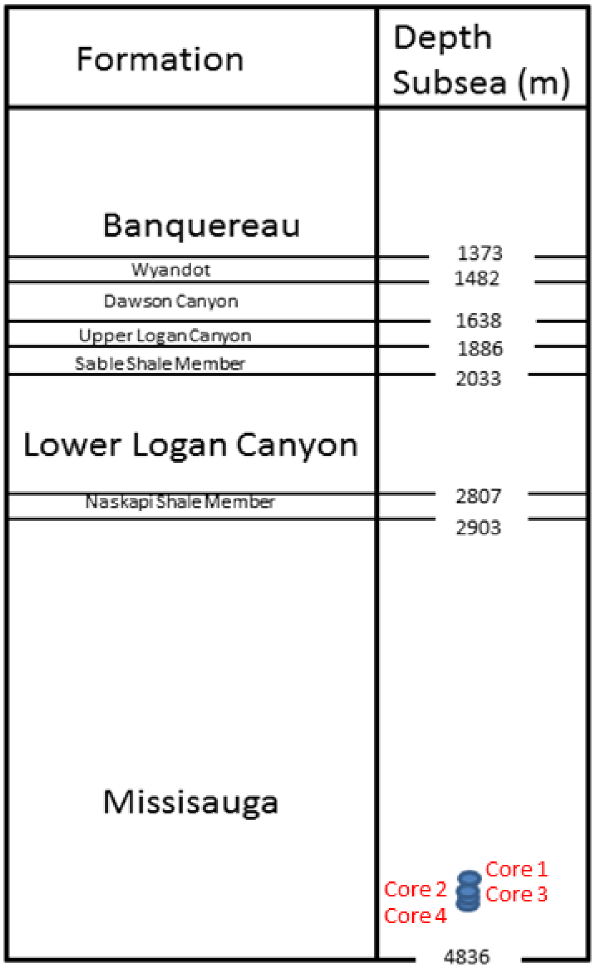
Formation
Depth Subsea (m)
Banquereau
Wyandot
Dawson Canyon
Upper Logan Canyon
Sable Shale Member
Lower Logan Canyon
Naskapi Shale Member
Missisauga
1373
1482
1638
1886
2033
2807
2903
Core 1
Core 3
Core 2
Core 4
4836

Figure 1.5. Formation depths in the Venture B-13 well. Core locations are indicated by the blue circles (Sable Offshore Energy, 1996).

VENTURE B-13

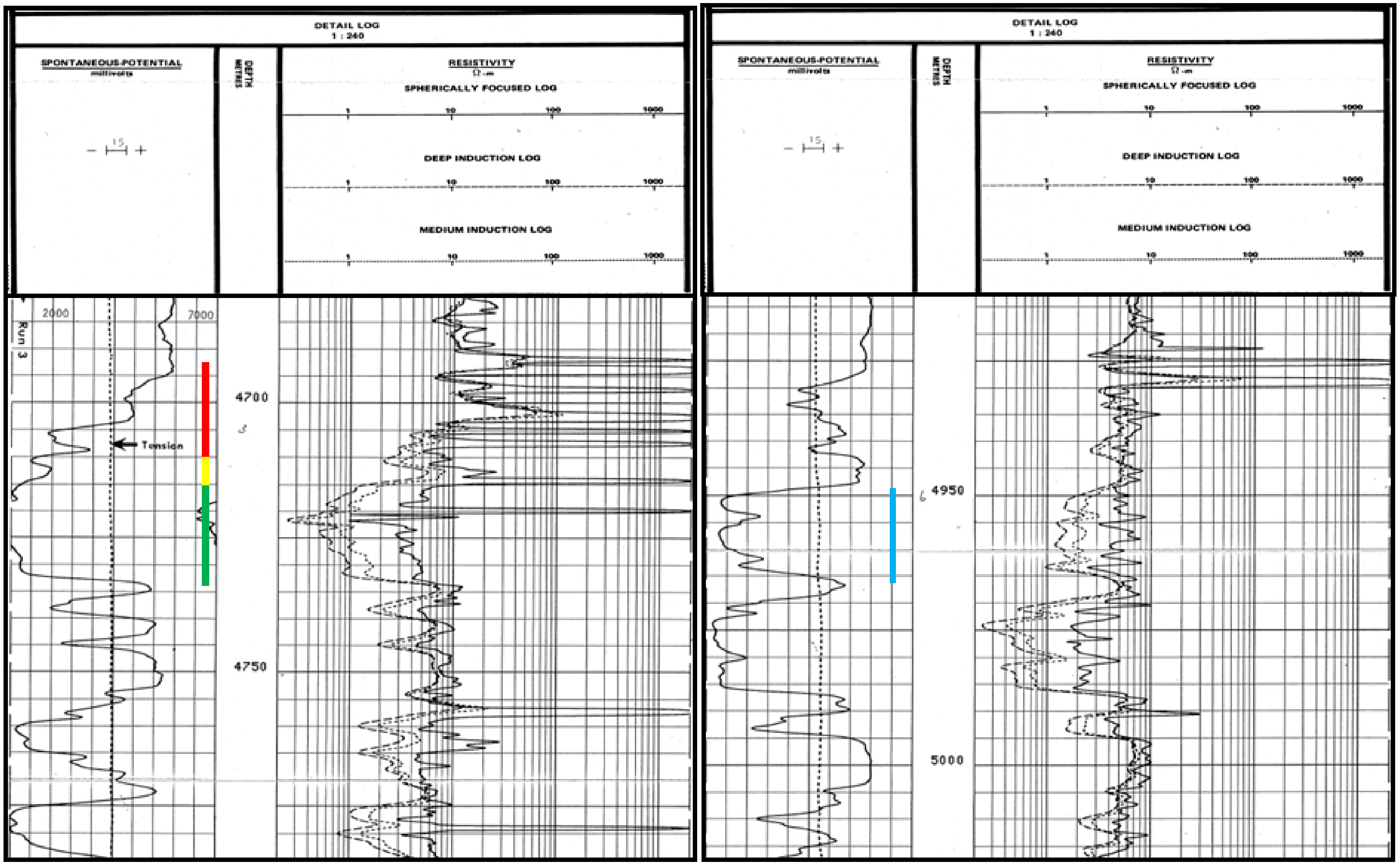

Figure 1.6. Spontaneous potential and resistivity measurements are tied to cores 1 through 4. Spontaneous potential curve measures the natural electric potential of a rock volume. It deviates towards the left from the shale base line to indicate clean sand. The resistivity of the pore fluid is measured by these logs. Cores #1, 2, and 3 demonstrate a wet fining upward sand package with possible barriers to flow in shallower sections. Core #4 demonstrates wet aggradational sands with interbedded shales.

1.6 Missisauga Formation

As previously mentioned, the Sable Subbasin is a Mesozoic to Cenozoic depositional center that is part of a passive-margin basin offshore Nova Scotia (Wade, 1991). The Venture Field is found in a rollover anticline that was formed by syndepositional listric growth faults within this basin (Wade, 1991). Named after the North American Native tribe Mississauga, the Kimmeridgian to Barremian Missisauga Formation is bounded by bounded below and above by the Mic Mac and Logan Canyon formations respectively and interfingers with the Verrill Canyon (Wade, 1991).

The Missisauga Formation comprises upper, middle and lower members (Wade, 1991). The Lower Missisauga Formation is analysed in detail in this thesis. The lower member contains the reservoir sands of the Venture Field and ranges from the shale beds to limestone beds of the MicMac Formation. The middle member ranges from the base of the “O” Marker to the top of Berriasian-Valanginian shales and the upper member ranges from the top of the formation to the base of the “O” marker. The main gas reservoirs are found between 4406 m to 5101 m (Karim *et al*., 2011). The deeper reservoirs are known to be overpressured. The “O” Marker is representative of a succession of Hauterivian-Barremian limestones and calcareous shales(Wade, 1991). It is generally found at a depth of 300 m from the top of the Missisauga Formation and is about 46 m thick. In the Sable Subbasin, over 2270 meters of the Missisauga Formation have been drilled in about 200 wells. The Missisauga Formation is represented by a succession of argillaceous sandstones that are separated by shale and siltstone beds deposited in a deltaic depositional sequence (Williams *et al.*, 1985) at the terminus of a river system drained the northeastern part of the Canadian Shield (Wade, 1991).

1.7 Petroleum System Elements

1.7.1 Reservoir

The main gas reservoirs of the Sable Delta complex are within the Mic Mac and Missisauga Formations. This research focuses on the Lower Mississauga Formation. The sands of the Mic Mac and

Missisauga formations were deposited in a delta that prograded towards the south (Sable Offshore Energy, 1996). With change in sediment supply and direction, and relative sea level, the Sable Delta complex varied in morphology, and advanced and retreated numerous times. The reservoirs show coarsening-upward successions (Sable Offshore Energy, 1996).

1.7.2 Seals and Traps

The seals present in the petroleum system are Late Jurassic shales of the Mic Mac Formation, Cretaceous Naskapi Member/Logan Canyon formations and the Tertiary Banquereau Formation. Syn-depositional listric growth faults are present throughout the Sable Subbasin creating rollover anticlinal traps. These syndepositional growth faults were created after deposition of the Mic Mac and Missisauga formations increasing sediment loading.

1.7.3 Source Rocks and Migration

The source rocks of this region are identified as the Verrill Canyon Shales (Sable Offshore Energy, 1996). As observed on the stratigraphic chart (Fig. 1.4), these shales occur in a more distal marine setting to the proximal and coeval Missisauga and Mic Mac formations (Sable Offshore Energy, 1996). The Verrill Canyon Shales have low total organic content (TOC) values (average ~1.0%), are gas and condensate-prone and are Type III source rocks (Mukhopahyay & Brown, 2003). These source rocks contain terrestrially-derived organic matter deposited in a slightly anoxic environment (Mukhopahyay & Brown, 2003). Deep reservoirs of the Thebaud, Venture and South Venture are overpressured (Sable Offshore Energy, 1996). Previous research suggests that there have been three stages of hydrocarbon generation and migration at 150-130 Ma, 110-90 Ma, and 70-50 Ma (Sable Offshore Energy, 1996).

1.8 Diagenesis

Diagenesis is defined as the chemical, physical or biological post-depositional change that sediments undergo at low temperatures and pressures as a result of burial and compaction (Boggs, 2006). Porosity values decrease as a result of diagenesis and some minerals may be dissolved. In effect, silica overgrowths on detrital quartz grains are present throughout the Venture Field, except where chlorite rims are present (Karim *et al.,* 2009).

Sandstones and siltstones of the lower Missisauga Formation have been subjected to variable degrees of diagenesis with pores filled with illite, chlorite and carbonates reducing their original porosity and permeability. The process of compaction, cementation and dissolution of the original rock fabric degraded the horizontal and vertical variations in reservoir quality of the Lower Missisauga Formation.

The products of physical and chemical changes related to diagenesis were analysed for nine wells and studies have determined the influence of cements and framework minerals on reservoir rocks (Karim *et al*., 2009). They suggested, by linking the “distribution of diagenetic minerals to depositional facies and sequence stratigraphy” researchers can “predict the spatial and temporal evolution of diagenetic minerals in reservoir rocks” and concluded that depositional lithofacies, sea-level changes, chemistry of basinal sediments and fluid flux during burial were influencing factors of diagenesis for offshore Nova Scotia (Karim *et a.l*, 2009). This research and analysis was conducted with the use of optical petrography, back-scattered electron images and the electron microprobe.

Higher porosity intervals were determined to be directly related to the formation of chlorite rims, specifically in the Missisauga Formation because they prevent silica overgrowths (Jansa & Noguera, 1990). Lower porosity in reservoirs is related to cementation by quartz, kaolinite or carbonates. In the Sable Subbasin, siderite is abundant in carbonates and is common in prodelta facies due to the high amount of iron released when ilmenite is broken down (Karim *et al*., 2009). Interestingly, in certain locations siderite has contributed to the increase in porosity because it has been dissolved as a result of diagenesis. However, the presence of Fe-rich carbonates prevents the formation of quartz overgrowths during early diagenesis and may be related to transgressive systems tracts (Karim *et al.,* 2009).

1.9 Flow Units

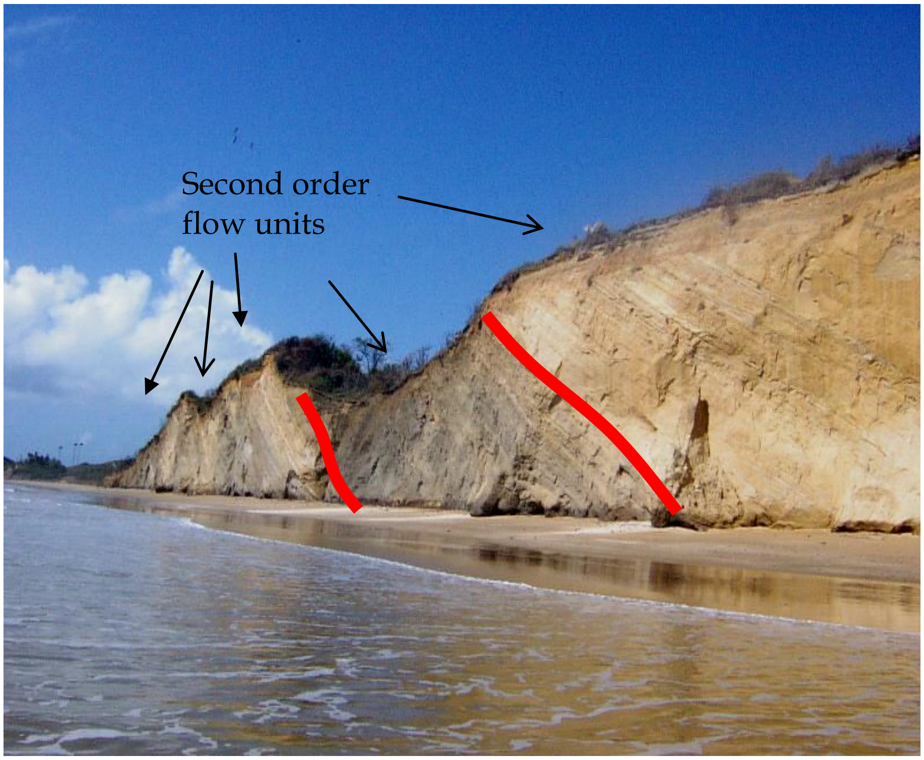

Figure 1.7. Image from Mayaro Beach, Trinidad demonstrating concept of second order, outcrop scale flow units. A clear change in lithology is observed (Modified from Wach et al., 2007).

A flow unit is a rock volume with identifiable fluid flow characteristics that can be modeled (Schlumberger, 2013). In other words, flow units are volumes of rock that are internally consistent yet predictably different from properties of other rock volumes. A difference in grain size, permeability, porosity, mineralogy and bioturbation is observed between flow units of a reservoir. For example, the image along Mayaro Beach in Trinidad of delta front and prodelta sediments of the Pliocene Mayaro Formation illustrate (Fig. 1.7) outcrop-scale flow units that show a clear change in grain size, permeability and lithology (Wach *et al*., 2007). Flow units are primarily analysed on a scale of a few decimeters to meters (core) and are supplemented with an understanding on a much finer millimetre scale, based on thin sections analysis.

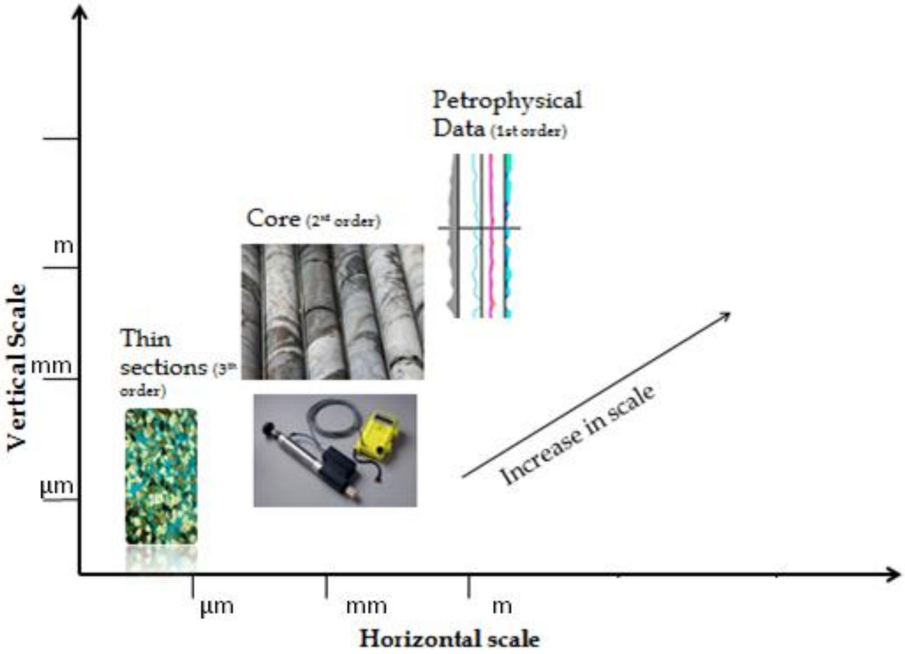
Petrophysical Data (1st order)
Core (2nd order)
Thin sections (3th order)
Increase in scale
Vertical Scale
m
mm
µm
Horizontal scale
µm
mm
m

Figure 1.8. Graphical representation of flow unit scale resolution. Second order and third order flow units will be analysed in this research. Petrophysical data is not analysed in this thesis.

Chapter 2

2.1 Lithofacies

A facies is described by Reading (1978) as a body of rock with specified characteristics such as colour, bedding, composition, sedimentary structures and fossil assemblage. A geologist must define lithofacies objectively based on physical lithological evidence and features that may be measured (Reading, 1978). No concrete rules exist for the selection of lithofacies since variation occurs for all sets of rocks and boundaries; however, each lithofacies must be defined objectively on observable and measurable features. For this thesis, lithofacies were defined within Venture B-13 through core description and interpretations of depositional environments were made.

2.2 Core Description Analysis

Approximately 57.3 m of core were described at the Canada Nova Scotia Petroleum Board Geoscience Data Centre in Dartmouth, Nova Scotia. Sedimentary structures, ichnofacies, lithofacies and potential flow units were identified. Detailed photographs of core were taken and Corel Draw was used to create a graphic interpretation of the core description.

Numerous steps are required to carry out a thorough description of the cores in order to identify lithofacies and define a depositional environment. Once physical and biogenic sedimentary structures, surfaces, grain size, and lithology were described, lithofacies were assigned to specific intervals of strata (Reading, 1978). Well-log data, seismic data and trace fossils may be used to define and assign a depositional environment to the lithofacies. Retrogradational, progradational or aggradational parasequences may be identified to aid in the prediction of the distribution of depositional environments.

2.3 Methodology

Flow units are defined as volumes of rock that are internally consistent yet predictably different from surrounding rocks (Shepherd, 2009). Reservoir properties that influence flow units include grain size, porosity, permeability, and lithology. In this section, the importance of each component will be discussed with regards to their influence on identification and quality of flow units.

This approach to understanding flow units was developed for this research as data were collected and evaluated. It became apparent that flow units could be defined on the basis of measurements of permeability and porosity corresponding to grain size, bioturbation, lithology, cementation, and clay content.

These data were available for specific log intervals that were assigned to sedimentological lithofacies identified in the cores. However, in order to understand more fully the relative contributions of numerous factors to potential fluid flow, a semi-quantitative system was designed to allow the factors to be rated relative to each other. The numerical system set out below for the Lower Missisauga Formation is relative, based on analysis of the available data for each factor.

Specifically, this methodology is separated into two parts. The first part identifies potential flow units and their associated depths, and the second critically evaluates the flow potential of each unit. Values were assigned to intervals typically of 0.92m thickness. Working upward through the core data allows intervals with strong potential changes in flow character to be identified and understood. The method also allows the thickness of flow units to be assessed.

2.3.1 Ranking Potential Differences in Flow Units

The following section explains how grain size, permeability, porosity, clay content, cementation and bioturbation data were key in understanding how to differentiate flow units. These data were assigned values relative to their impact on change of flow unit. Summing these scores, a relative ranking of flow units was created. This number indicated the relative probability of having different flow units in a specific section of the well based on the top and lower boundary. It does not rank the ability of fluid to flow in each flow unit.

2.3.1.1 Permeability

Permeability is the key factor affecting movement of fluids through a volume of rock. For this thesis, permeability was measured with TinyPermII and values of core plug permeability data from previous Venture B-13 core analyses (Venture B-13 Well History Report, CNSOPB Data Management Centre).

A histogram was created demonstrating the frequency of core plug permeability values of the Lower Missisauga Formation within Venture B-13 (Fig. 2.1). Ranges assigned to “Amount of variation in permeability” in Table 2.1 were chosen from this histogram (Fig. 2.1). Units were assigned values relative to the change of permeability they display. The assigned permeability values for the overlying and underlying rock volumes were added to give a value for a specific volume of rock. A unit showing >50mD difference in permeability with overlaying and underlying units received a value of 8.

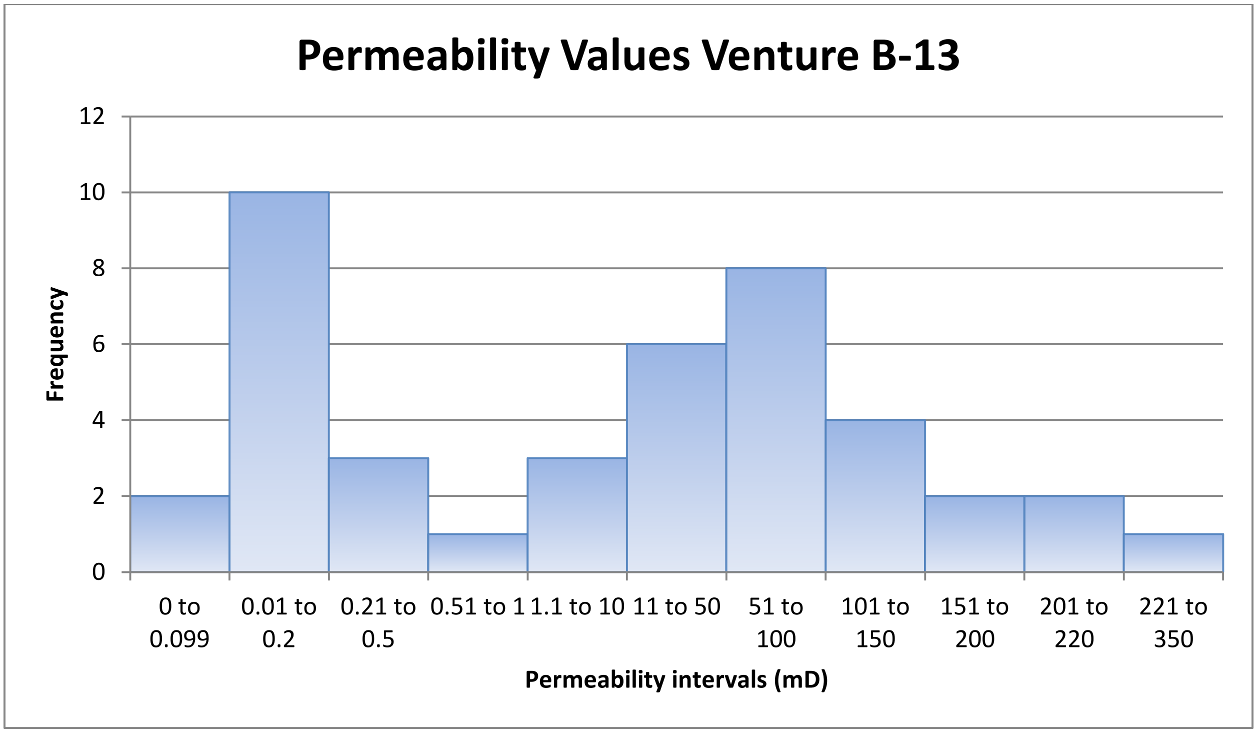

Figure 2.1. Histogram of permeability values of well Venture B-13.

PERMEABILITY	
Assigned value	**Amount of variation in permeability**
0	No variation in permeability
1	Difference of 0.01 to 0.51 mD between potential flow units
2	Difference of 1 to 10 mD between potential flow units
3	Difference of 11- 50 mD between potential flow units
4	Difference of >50 mD between potential flow units

Table 2.1. Permeability and assigned values for flow unit differentiation.

2.3.1.2 Porosity

Porosity is the void space in a volume of rock and is measured by dividing the volume of void space V_V by the total volume of material (V_t): $\Phi=V_V/V_t$

Porosity can be described as primary, secondary, intergranular, intragranular. Intergranular porosity means there is porosity between grains whereas intragranular porosity defines porosity inside sedimentary grains (Ramm & Bjorlykke, 1993). Primary porosity is the original pore space created during deposition. Secondary porosity is pore space formed as a result of dissolution or fracturing (Ramm & Bjorlykke, 1993). However, porosity observed in this research was primary intergranular and secondary intergranular and intragranular. Variation of porosity in a vertical section is representative of different flow units. A histogram was created demonstrating the frequency of porosity values of the Lower Missisauga Formation within Venture B-13 (Fig. 2.2). These values were then used in assigning values for the ranges in Table 2.2. Volumes of rock that show great amounts of variation in porosity were assigned higher values than rocks that show little variation in porosity. The assigned porosity values for the overlying and underlying rock volumes were added to give a maximum value of 8 for a specific unit.

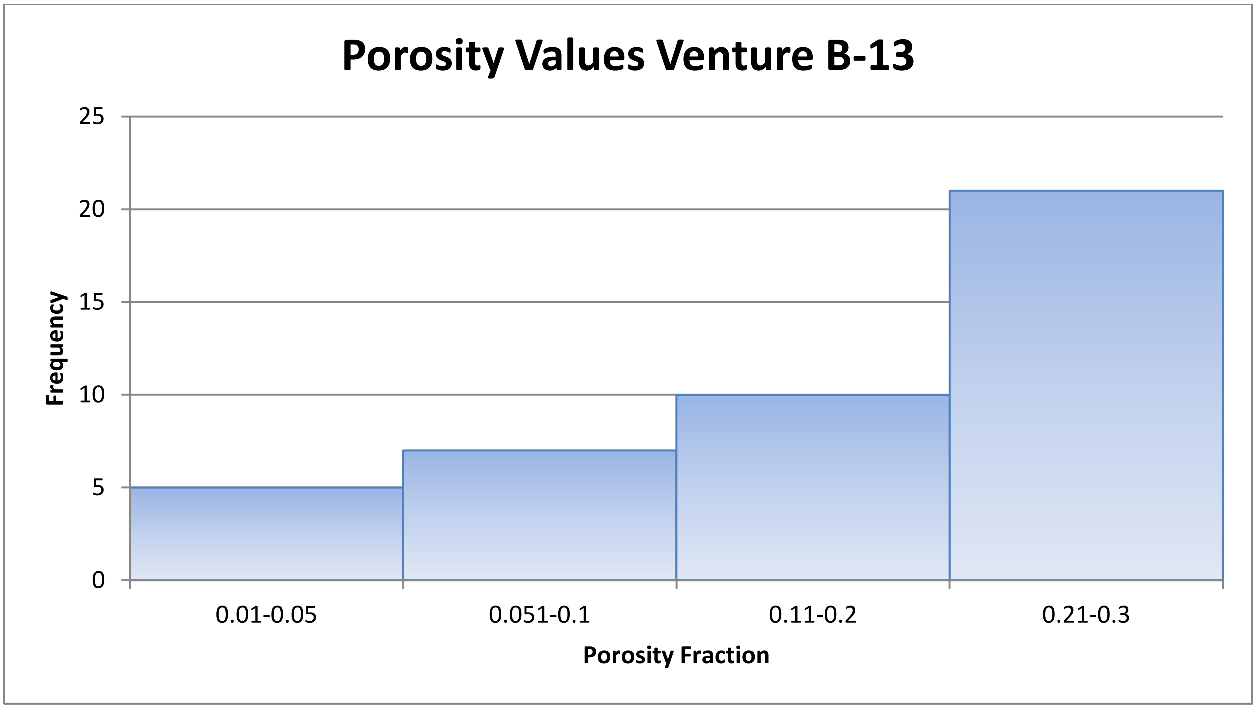

Figure 2.2. Histogram of porosity values in Venture B-13 well.

POROSITY	
Assigned value	**Amount of variation in porosity**
0	No variation in porosity
1	Difference of 1 to 5 % between potential flow units
2	Difference of 5.1 to 10% between potential flow units
3	Difference of 11 to 20% between potential flow units
4	Difference of 21 to 30% and above between potential flow units

Table 2.2. Porosity and assigned values for flow unit differentiation

2.3.1.3 Grain Size

Grain size and permeability are normally correlated (Boggs, 2006). An increased grain size is equivalent to an increase in permeability when cementation is not involved (Boggs, 2006). Moreover, a change in grain size and permeability in the reservoir is indicative of change in flow unit. A greater grain size or permeability value will yield better flow units. Grain sizes distribution was analysed throughout the Lower Missisauga Formation of Venture B-13 well and were compared against rock type classifications (Table 2.3).

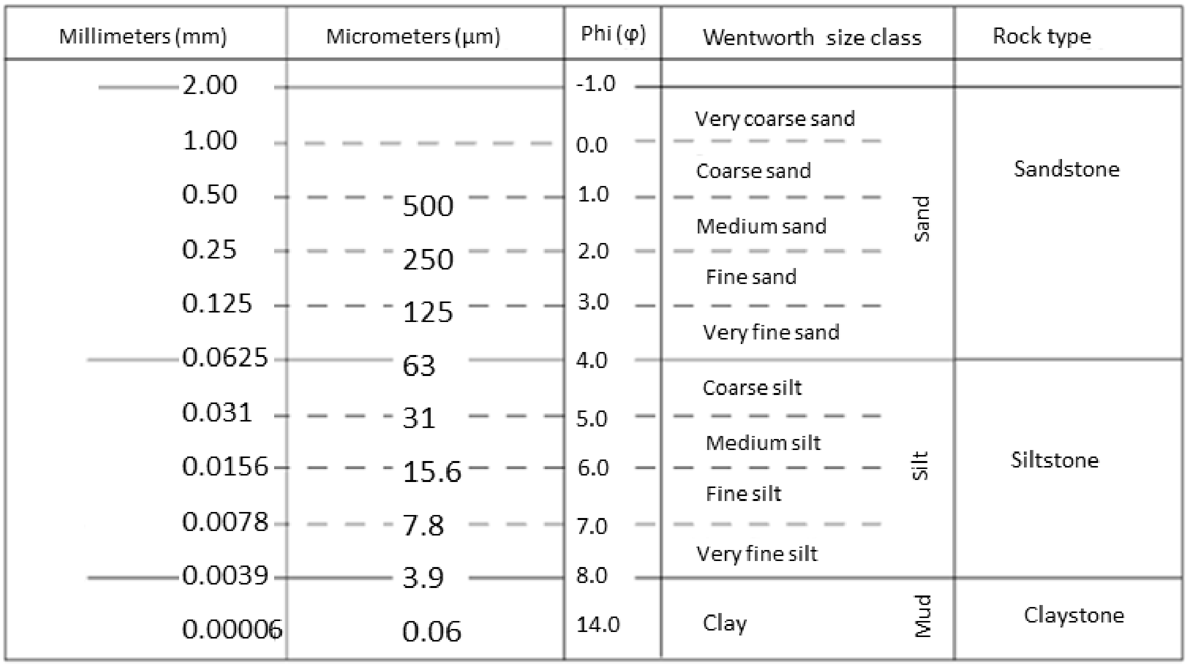

Millimeters (mm)	Micrometers (µm)	Phi (φ)	Wentworth size class		Rock type
2.00		-1.0			
1.00		0.0	Very coarse sand	Sand	Sandstone
0.50	500	1.0	Coarse sand		
0.25	250	2.0	Medium sand		
0.125	125	3.0	Fine sand		
0.0625	63	4.0	Very fine sand		
0.031	31	5.0	Coarse silt	Silt	Siltstone
0.0156	15.6	6.0	Medium silt		
0.0078	7.8	7.0	Fine silt		
0.0039	3.9	8.0	Very fine silt		
0.00006	0.06	14.0	Clay	Mud	Claystone

Table 2.3. Udenn-Wentworth grain size chart showing ranges in grain size and associated rock types (Modified from Boggs, 2006).

Values from 0 to 4 were assigned to volumes of rock relative to the amount of grain size change with bordering units. A higher value is indicative of evident change of grain size from one unit to another (Table 2.4). A value of 0 is indicative of similar grain size from unit to another. The assigned grain size values for the overlying and underlying rock volumes were both added to give a value for a specific volume of rock. Therefore, a flow unit could be assigned a minimum value of 0 and a maximum of 8

Grain size	
Assigned value	**Amount of variation in size class**
0	Same grain size (top and bottom lithology)
1	Change in one size class
2	Change in two size classes
3	Change in three size classes
4	Change in four or more size classes

Table 2.4. Grain size and assigned values for flow unit differentiation.

2.3.1.4 Lithofacies

Since the Lower Missisauga Formation is not homogeneous, changes in lithologies must be annotated. The assigned change in lithofacies values for the overlying and underlying rocks were added to give a maximum value of 8 for a specific unit. Lithofacies of Venture B-13 will be further discussed in Chapter 3.

Lithofacies	
Assigned value	**Change in lithofacies**
0	Recurring lithofacies between potential flow units
2	Different lithofacies below, same lithofacies on top or vice versa
4	Clear change in lithofacies between potential flow units

Table 2.5. Change in lithofacies and assigned values for flow unit differentiation

2.3.1.5 Bioturbation

The bioturbation index (BI) (Fig. 2.3) was used to characterize the influence of bioturbation on potential flow units. Degree of variation of bioturbation between potential flow units was assigned values with higher numbers indicating an increasing change in bioturbation. The assigned bioturbation values for the overlying and underlying rock volumes were added to give a maximum value of 8 for a specific volume of rock. An increased intensity of bioturbation mixes sand and mud laminaee, thus bringing finer matrix into coarser beds and reducing porosity.

Bioturbation	
Assigned value	**Bioturbation**
0	No variation in bioturbation
1	Difference of 1 BI between potential flow units
2	Difference of 2 BI between potential flow units
3	Difference of 3 BI between potential flow units
4	Difference of 4 BI between potential flow units

Table 2.6. Variation in bioturbation and assigned values for flow unit differentiation.

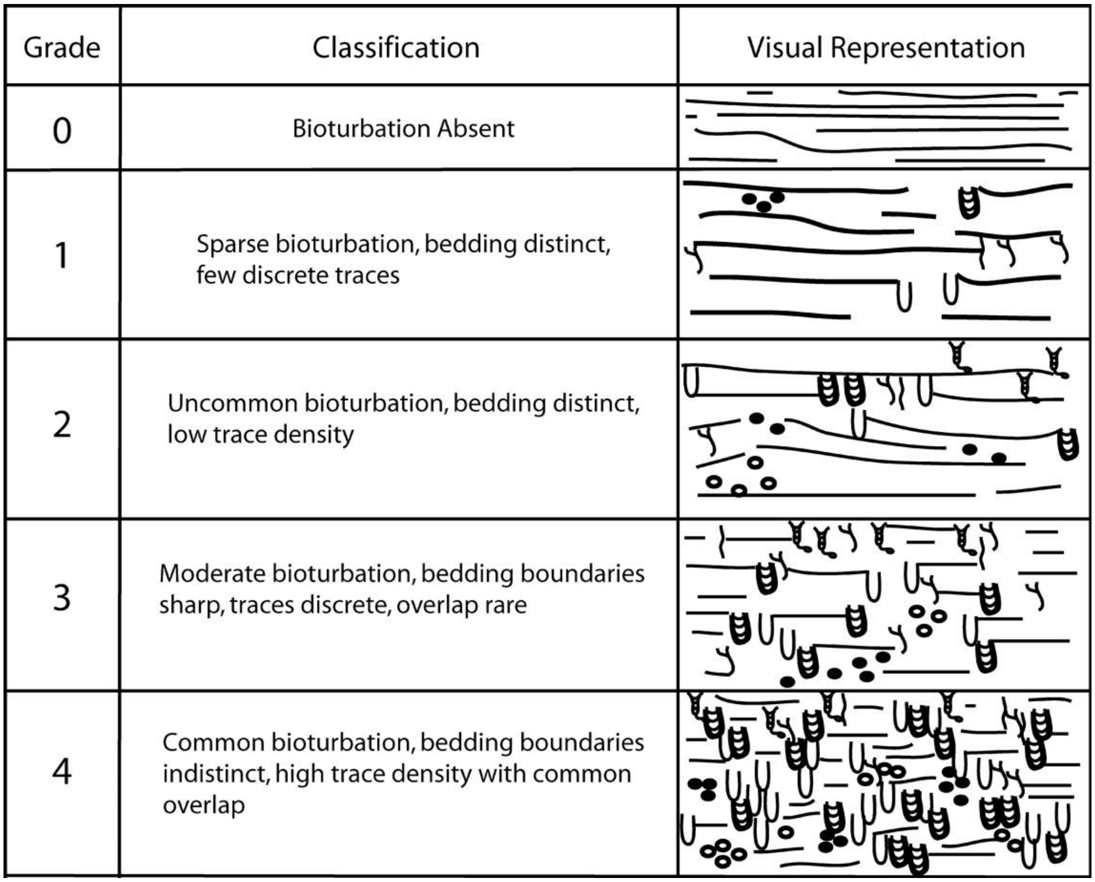

Grade	Classification	Visual Representation
0	Bioturbation Absent	
1	Sparse bioturbation, bedding distinct, few discrete traces	
2	Uncommon bioturbation, bedding distinct, low trace density	
3	Moderate bioturbation, bedding boundaries sharp, traces discrete, overlap rare	
4	Common bioturbation, bedding boundaries indistinct, high trace density with common overlap	

Figure 2.3. Visual representation and classification bioturbation with increased grade and intensity (Modified from Pearson & Gingras, 2006).

2.3.1.6 Cementation

Cementation, a diagenetic process, involves the chemical precipitation of ions forming new crystalline material between grains (Boggs, 2006), thereby lowering porosity and degrading flow units' reservoir properties. Variability of cementation leads to varying zones of permeability. Cementation ranges were picked on the basis of average cementation values in thin sections (Chapter 3).The assigned cementation values for the overlying and underlying rock volumes were added to give a maximum value for a specific volume of rock.

Cementation	
Assigned value	**Variation in cement percentage**
0	No variation in percentage of cement between potential flow units
1	1-10% variation of cement between potential flow units
2	11-20% variation of cement between potential flow units
3	21-30% variation of cement between potential flow units
4	≥31% variation of cement between potential flow units

Table 2.7. Variation in cementation and assigned values for flow unit differentiation

Estimating Percentages

Throughout thin section analysis, mineral, porosity and cementation percentages were estimated with the use of the following chart (Fig. 2.4).

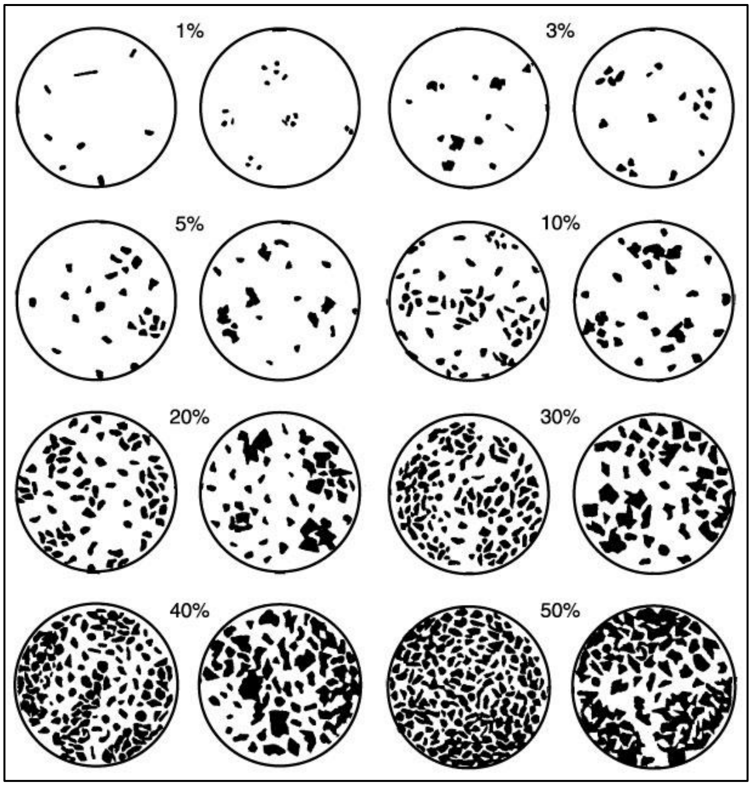

Figure 2.4. Chart for determining approximate modal percentages in rocks. (Terry et al., 1955)

2.3.2 Ranking values

Once values were assigned for changes in lithology, grain size, permeability, cementation, porosity and bioturbation, they were summed to give a value indicative of the relative ranking of a flow unit (Table 2.8). Values close to 48 are indicative definite change in flow units, whereas those closer to 0 indicate that there is no change of flow units with given depth change.

Depth		**Lithology**	**Grain Size**	**Porosity**	**Permeability**	**Cementation**	**Bioturbation**	**Rel. Ranking of flow unit out of 48**
Top	**Bottom**							

Table 2.8. Tabulation of flow unit ranking parameters used for the differentiation of flow units.

2.3.2 Flow Unit Strength: Influence on Preferential Flow

The following section explains how the interrelationships between grain size, permeability, porosity, clay content, cementation and bioturbation data are keys to understanding the strength of flow units. Flow unit strength is mainly controlled by permeability which is most accurately measured by core plugs. For a total of 57.3 m of core, 42 core plug permeability measurements were taken. This subject is further discussed in Chapter 5.

Generally, large grain size, high porosity, low bioturbation, low clay content and low cementation contribute to high permeability values and an increased flow potential. For this research, it was assumed that all these criteria equally contributed in equal parts to permeability variation. Therefore all criteria were assigned a maximum value of 4. Oil reservoir rocks have permeability measurements from 100 to 10,000 mD, other sandstones have permeability measurements from 1 to 10 mD and limestones 0.01 to 0.1mD (Bjorlykke, 1993).

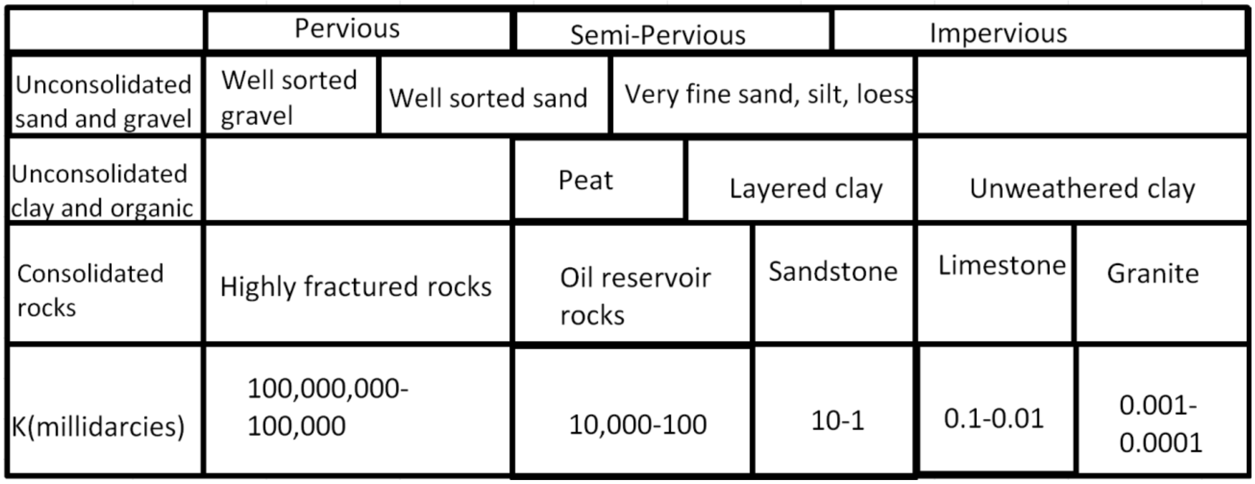

	Pervious		Semi-Pervious		Impervious	
Unconsolidated sand and gravel	Well sorted gravel	Well sorted sand	Very fine sand, silt, loess			
Unconsolidated clay and organic			Peat	Layered clay	Unweathered clay	
Consolidated rocks	Highly fractured rocks		Oil reservoir rocks	Sandstone	Limestone	Granite
K(millidarcies)	100,000,000-100,000		10,000-100	10-1	0.1-0.01	0.001-0.0001

Figure 2.5. Permeability values assigned to specific types of rocks (Modified from Geomore, 2012).

Areas of higher and lower permeability are identified throughout Venture B-13 core indicative of excellent to poor quality flow units. Barriers to flow include interbedded shales and stylolitic horizons. Clay content, cementation, grain size and bioturbation were analysed to understand the degree of difference between adjacent rock volumes. Permeability values were compared to values of other parameters in order to determine why differences in flow potential exist.

2.3.2.1 Clay Content

Authigenic and detrital clays in the Missisauga Formation have contributed to the reduction of primary porosity (Karim *et al.,* 2009). Clay minerals identified in thin section include chlorite, muscovite, biotite. Research by Jansa and Noguera (1990) states that kaolinite is also present; however, this was not observed in thin section. A rock with 100% clay content will be a very poor flow unit and a rock with no clay will likely be a good flow unit. Since a maximum value of 4 and a minimum value of 0 can be assigned to clay content, ranges were subdivided into five groups (Table 2.9). A higher amount of clay corresponds to a lower assigned value.

Clay content	
Assigned value	**Amount of clay**
0	100%-80%
1	80%-60%
2	60%-40%
3	40%-20%
4	20%-0%

Table 2.9. Assigned value for amount of clay for flow unit characterization.

2.3.2.2 Cementation

Increased cementation decreases porosity and permeability. Low percentages of cementation are assigned higher values. A rock with 100% cementation will be a very poor flow unit and a rock with no cementation will be a good flow unit. Since a maximum value of 4 and a minimum value of 0 can be assigned to cementation, ranges were subdivided into five groups (Table 2.10).

Cementation	
Assigned value	**Amount of cementation**
0	100%-80%
1	80%-60%
2	60%-40%
3	40%-20%
4	20%-0%

Table 2.10. Assigned values for amount of cement for flow unit characterization.

2.3.2.3 Grain Size

An increase in grain size leads to increased permeability. Finer particles are assigned lower values than coarser particles.

Grain Size	
Assigned value	**Grain size**
0	Clay
1	Fine silt- coarse silt
2	Fine sand
3	Medium sand
4	Coarse sand

Table 2.11. Assigned values for grain size for flow unit characterization.

2.3.2.4 Bioturbation

In marine sedimentary rocks, three-dimensional burrow connectivity can increase the amount of fluid-flow pathways through rock (LaCroix *et al*., 2012). However, analysis of Venture B-13 cores has demonstrated that bioturbation has decreased permeability as a result of sediment mixing. As such, a higher bioturbation index has a lower assigned value.

Bioturbation	
Assigned value	**Bioturbation index (BI)**
0	4
1	3
2	2
3	1
4	0

Table 2.12. Assigned values for bioturbation index for flow unit characterization.

2.3.2.5 Porosity

Increased porosity in a volume of rock accompanied by high permeability, leads to an increased amount of preferential flow through the unit. Reservoir rock porosity values range from 5-40% (Ramm & Bjorlykke, 1993). Values between 0-5% are considered insignificant, 5-10% poor, 10-15% fair, 15-20% good and porosity values above 20% are considered excellent (Hyne, 2001).

Porosity		
Assigned value	**Percentage of Porosity**	**Rank**
0	0-5%	Insignificant
1	5-10%	Poor
2	10-15%	Fair
3	15-20%	Good
4	>20%	Excellent

Table 2.13. Assigned values for porosity for flow unit characterization.

2.3.2.6 Ranking Flow Unit Strength

Once values were assigned for grain size, clay content, bioturbation and cementation, these values were summed to represent the strength of a flow unit. These numbers were then compared to permeability values (Table 2.14).

Flow units		Permeability	Grain Size	Porosity	Clay Content	Bioturbation	Cementation	Ability to flow within unit
Top	Bottom							

Table 2.14. Tabulation of flow unit ranking parameters used for the differentiation of flow units. Flow unit strength criteria are assigned values, summed, and given a value out of 20 that represents their strength as a flow unit. These numbers were then compared to average permeability value of lithofacies. For this reason, “ability to flow within unit” and “permability” values were highlighted in red. The objective of this research is to determine whether the permeability values correlate with quantified flow unit strengths.

Chapter 3

3.1 Mobil Texaco Pex Venture B-13 Lithofacies:

This study integrates core descriptions (57.3 m), thin section analysis (21 thin sections) and paleontological data (details in Chapter 4). Venture B-13 well core was described in ~3cm detail, four specific lithofacies were identified characteristic of various depositional settings, and sedimentary textures and trace fossils were noted. Thin section analysis allowed a better understanding of mineralogical composition of lithofacies and diagenesis. Photos of characteristic features in thin sections were taken under plain-polarized and cross-polarized light. Table 3.1 provides details on each available thin section studied. Thin sections have a width of approximately 3 mm, are unstained but are impregnated with orange epoxy to highlight porosity. The following section will qualitatively analyse identified lithofacies and associated microlithofacies in cores from the Venture B-13 well.

Sample	Core	Depth (m)
1	1	4692.2
2	1	4693
3	1	4693.64
4	1	4695.62
5	1	4698
6	1	4699.66
7	1	4703.01
8	1	4704.85
9	1	4707.40
10	1	4707.80
11	1	4708.14
12	1	4708.20
13	2	4711.40
14	2	4711.95
15	3	4716.25
16	3	4718.70
17	3	4718.75
18	3	4727.60
19	3	4730.20
20	3	4730.67
21	3	4749.76

Table 3.1. Thin section sample list.

3.1.1 Thin Section Classification

The lithofacies identified from core analysis overlook certain characteristic microscopic features. As such, thin sections descriptions identifying microscopic features supplemented core descriptions and gave rise to microlithofacies assemblages discussed in the following section. Folk's classification (Boggs, 2006) for limestones was used in naming carbonate lithofacies. Where two or more of the constituents that form the basis for Folk's classification were used, names were combined. For example, if both intraclasts (70%) and ooids (30%) are present with sparite, the lithology will be called an intra-oosparite.

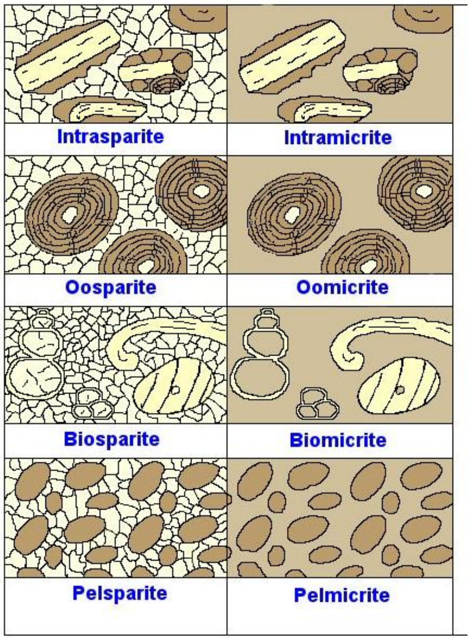

Figure 3.1. Folk's classification chart (Modified from Boggs, 2006)

3.2 Lithofacies 1: Oolitic Limestone

This lithofacies is composed of black, grey and dark brown oolitic limestone. Rounded ooids of calcium carbonate are the dominant feature of facies 1. Nuclei of ooids are upper to lower coarse grain size quartz or shell fragments. Intergranular calcite, small amounts of detrital chlorite, and traces of intergranular porosity are present. As such, there is a strong to medium reaction with hydrochloric acid. Crinoids, shell fragments and laminaee are found throughout this facies.

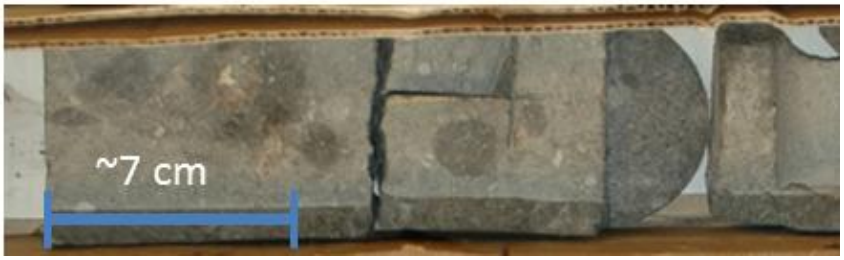

Figure 3.2. Core photo of lithofacies 1 oolitic limestone at a depth of 4700.4m to approximately 4700.2m.

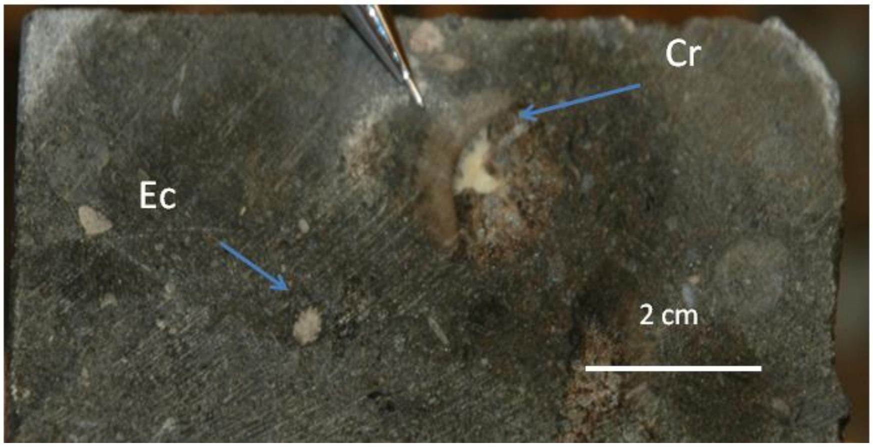

Figure 3.3. Crinoid (Cr) shell fragments found in oolitic limestone layer (lithofacies 1) in Venture B-13 at a depth of 4700.38m. The core in this photo has been sprayed with water to make the shell fragments more evident. Echinoderm (Ec) spines are evident as well.

3.2.1 Thin section analysis of facies 1

3.2.1.1 Bio-oosparite

Thin sections from Core 1 from sample points 4692.2m, 4693 m, 4695.62 m, 4698 m.

This is a sedimentary rock that contains ooids (20%), shell fragments (25-27%), mud (3-14%), intragranular micritic(minor) and sparry calcite (15-35%), quartz (13-20%), chlorite (0-2%), framboidal pyrite (2%), and muscovite (0-2%). Composition and ooid size is slightly variable throughout four thin sections. Calcite cement totals about 15-30% representing the original volume of porosity before cementation.

Rounded to subrounded ooids are the dominant features of this microlithofacies. Concentric layering is evident in most ooids that are typically 1-2mm in diameter and are cemented with sparry calcite. About 1% of the ooids display radial features yet have maintained relict concentric layering. This is likely isopachous cementation which is representative of a seafloor diagenetic environment (Boggs, 2006). Nuclei of ooids are composed of quartz or bioclastic fragments. Different shell fragments include pelmatozoans, crinoids, foraminifera, bivalves and bryozoans.

Degree of packing varies throughout the thin section as some areas are grain-supported, whereas others are matrix-supported. Sparite cement shows two phases of formation. The finer-sized phase formed first around ooids, minerals and bioclasts, and a later coarser phase formed within particle voids. A minimal amount of micrite matrix is also present. Intergranular voids that were filled with mud at an earlier stage were not affected by the carbonate infill. Patchy replacement of some fossils by botryoidal or blocky calcite is evident.

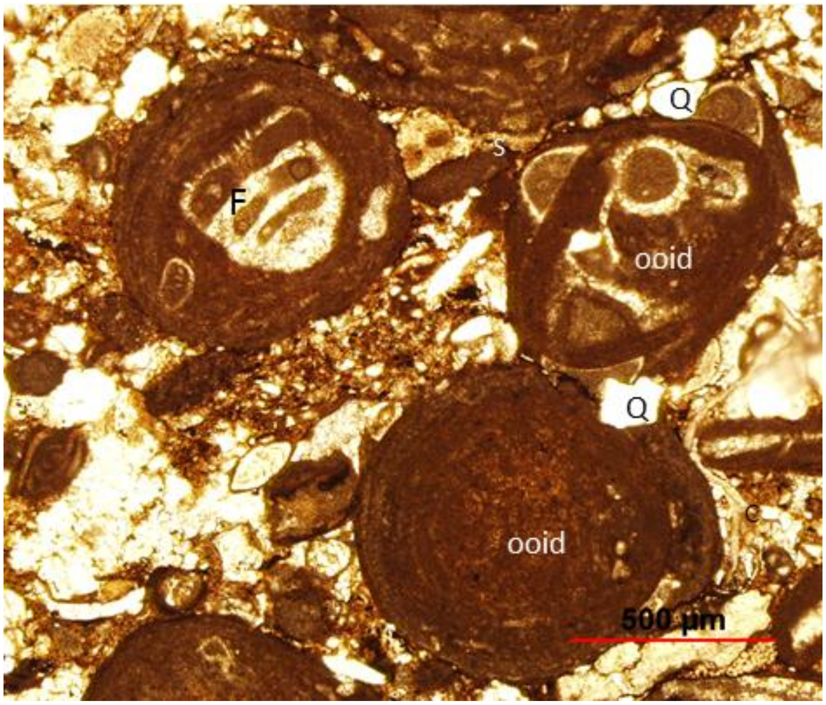

Figure 3.4. Sample 1 (Core 1, 4692.2 m) under plain-polarized light. Foraminifera (F) is identified as a nucleus of ooid creating intragranular porosity. Quartz grains show evidence for compaction as they indent into ooids. Micritic muds present between grains. Detrital chlorite grains(C) on the bottom right of the photo show ductile deformation as a result of compaction.

Ooids were dissolved as a result of diagenesis but quartz grains were not. Evidence for sediment compaction is observed where quartz grains indent into the ooids. Stylolites, which are carbonate dissolution features, are evident throughout the sample. Minimal grain distortion of platy minerals (chlorite, muscovite) was also observed. Dark micritic rims or envelopes around fossils fragments and some detrital quartz are results of fine micrite and siderite packing around the grains. Lastly, framboidal pyrite, an early diagenetic mineral commonly occurring in anaerobic marine sediments, was abundant in thin sections (Boggs, 2006). It is a product of microbial reduction within shallow buried sediments.

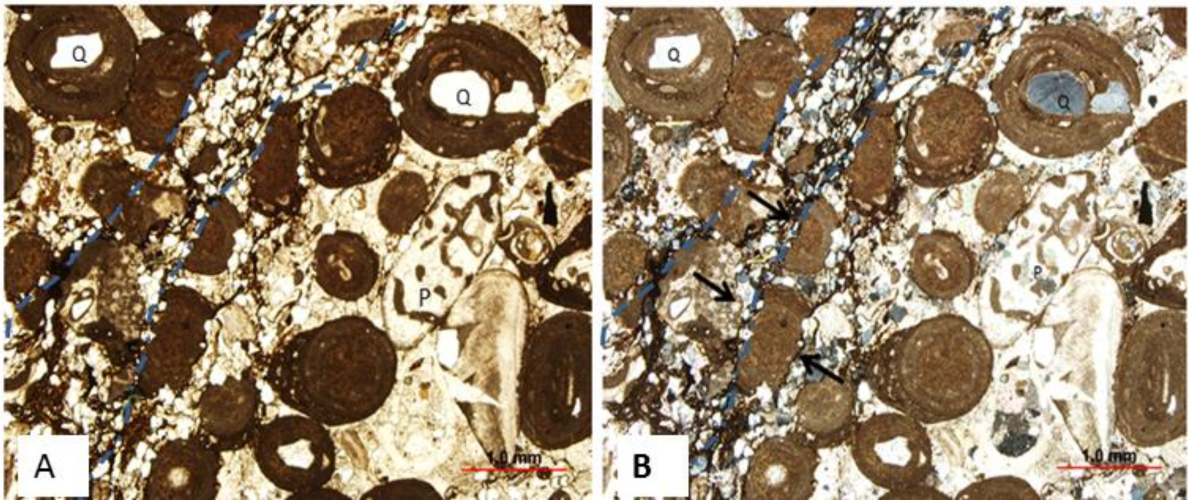

Figure 3.5. Photo of thin section under plain-polarized light (A) and cross-polarized light (B) of Sample 4 (Core 1, 4695.62m). Carbonate ooids with quartz nucleus(Q) and shelly fragments are characteristic of lithofacies 1. A set of stylolites, indicative of dissolution after lithification, are identified between two blue dashed lines. Black arrows point at partially dissolved ooids.

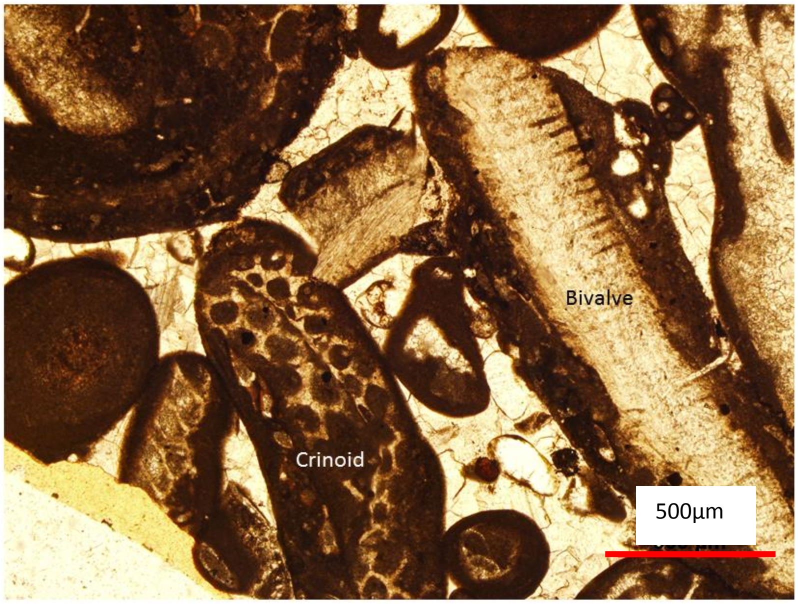

Figure 3.6. Thin section under plain-polarized of Sample 2 (Core 1, 4693 m) shows evident crinoid and bivalve shell fragments and intergranular sparry cement. Quartz grains and shell fragments are enclosed in a thin layer of Fe-rich muds.

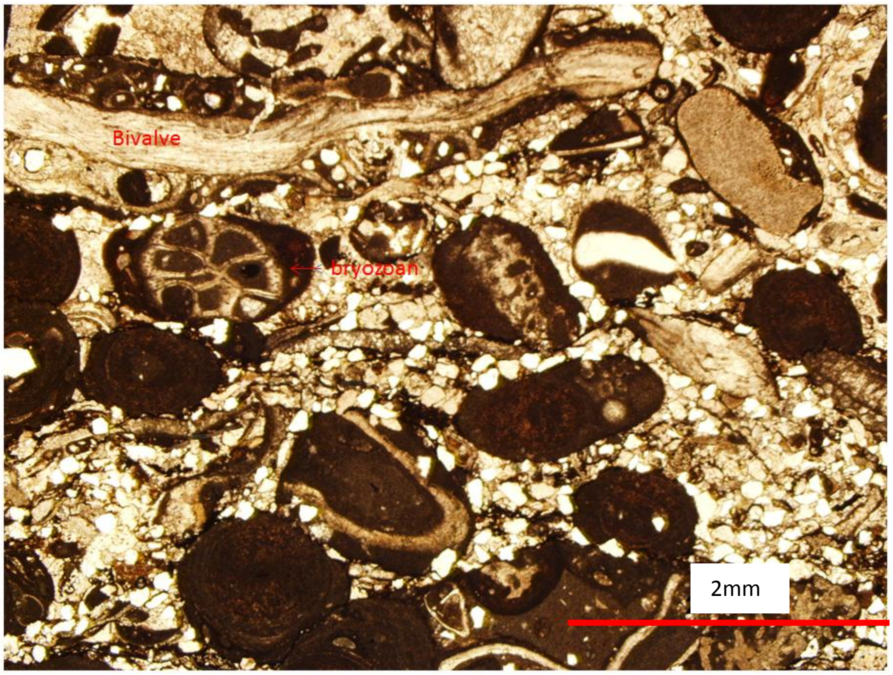

Figure 3.7. Sample 4 (Core 1, 4695.62 m) under plain-polarized light. Bryozoan, bivalve and other unidentifiable shell fragments are observed. Microscopic stylolites, dissolved ooids and quartz grains indenting into ooids serve as evidence of mid-diagenetic stage of sample.

3.2.1.2 Oobiosparite

Thin sections from Core 1 from sample points 4704.85m and 4711.40m

Thin sections representative of oobiosparite lithofacies have similar textures, features and paragenesis as bio-oosparite microlithofacies; however, the ooid to bioclast ratio is higher. These two thin section are composed of muscovite and biotite (5%), pyrite (5%), quartz(20-40%), ooids(20-40%), sparry intragranular calcite(25%), and bioclasts(5%).The quartz grains forming the nucleus of ooids in these thin sections are slightly larger than the bio-oosparite nuclei.

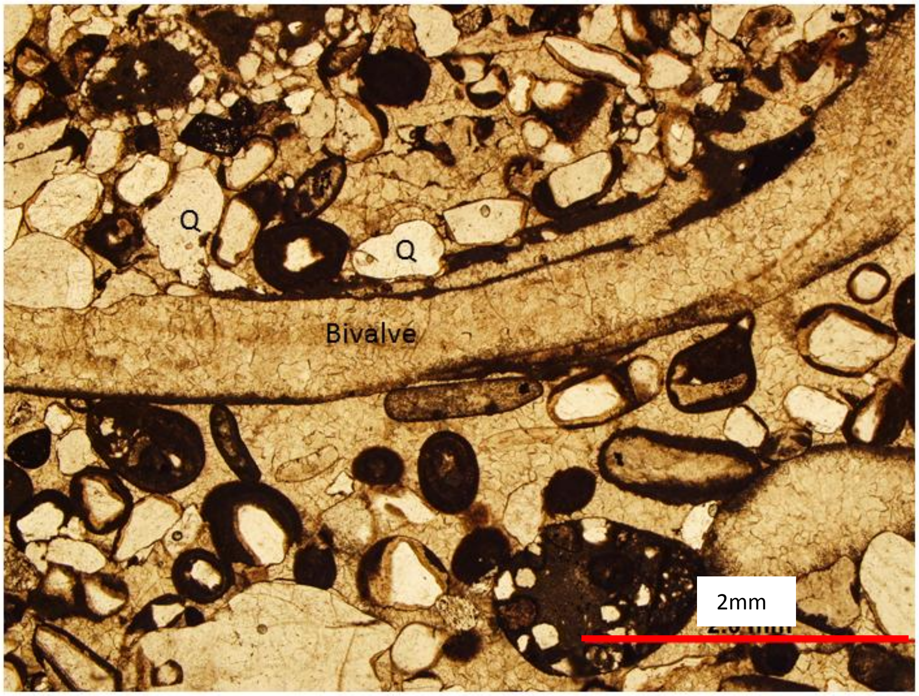

Figure 3.8. Thin section from a depth of 4704.85 m under plane-polarized light. A bivalve shell is surrounded by <1mm quartz grains that are enclosed by Fe-rich muds as a result of compaction. Sparry cement has infilled the original pore space. Lastly, the original fabric of the bivalve has been replaced by sparry carbonate.

Time	Paragenesis
1	Deposition of sediments and organism shells and ooid formation as a result of suitable water chemistry and environmental factors
2	Primary minor carbonate cemention
3	Formation of pyrite in reducing environment
4	Physical compaction, where grain packing occurs and porosity is reduced
5	Chemical compaction, partial dissolution of ooids and shell fragments and creation of stylolites
6	Secondary precipitation of carbonate cement between pore spaces
7	Mineral replacement of some shell fragments and quartz nuclei by botryoidal or blocky calcite.

Table 3.2. Diagenetic history of bio-oosparite and oobiosparite microlithofacies. After deposition of sediments and shells, minor early cements (carbonate and pyrite) were formed. Chemical compaction followed physical compaction. Secondary precipitation of carbonate cements and mineral replacements are representative of later stages of diagenesis.

3.2.2 Lithofacies 1 Interpretation: Shallow marine, sub-tidal zone

The depositional environment of this lithofacies is a shallow marine, agitated and probably tide dominated setting. Shell fragments or small quartz grains form a nucleus for growth of ooids. When currents start to wash the nucleus back and forth, precipitated calcite accumulates on the nucleus in a concentric fashion. The shallow tidal zone is always submerged by water except during low tide (Boggs, 2006). As such, various organisms such as crinoids and other metazoans are able to thrive in this type of setting.

3.3 Lithofacies 2: Shale

This facies comprises fissile and micaceous black to dark grey shale. Bioturbation caused mainly by *Planolites* and *Thalassinoides*, and burrows are filled with fine upper and fine lower grey calcareous sands. Bioturbation index varies from 0 to 3 throughout this facies. Muddy linings of these trace fossils are approximately 1 to 2 mm thick. The siltstone does not always react with hydrochloric acid. Bedding surfaces were not clearly identifiable. These muds have parallel layers with surfaces variably at angles of 0°-5°, indicative of depositional dips. Sedimentary structures were not observed within this facies. This facies occurs in thinner intervals than the other lithofacies.

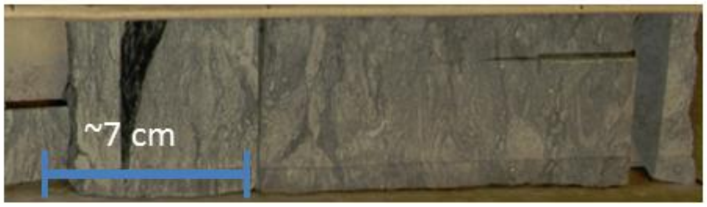

Figure 3.9. Core photo from Venture B-13 well showing lithofacies 2 shale between 4706.88m to 4706.67m.

3.3.1 Thin section analysis of facies 2

3.3.1.1 Burrowed Shale

Thin section from Core 1 from sample 4708.14m

This microlithofacies is comprised solely of microscopic clay grains (<0.062mm) and demonstrates minimal bioturbation. The grains are not visible in thin section and no additional information can be obtained. The proposed diagenetic history (Table 3.3) suggests that reworked sediments were deposited in a low energy environment followed by some physical compaction, burrowing and lithification of the mud-rich material. It is important to note that physical compaction increases with depth.

Time	Paragenesis
1	Deposition of reworked sediments in a low energy environment
2	Minimal physical compaction
3	Burrowing
4	Physical compaction
5	Lithification of mud-rich material

Table 3.3. Diagenetic history of burrowed clay microlithofacies. After deposition of muds and minimal compaction, organisms were able to burrow through the microlithofacies. Physical compaction is continuous throughout paragenesis.

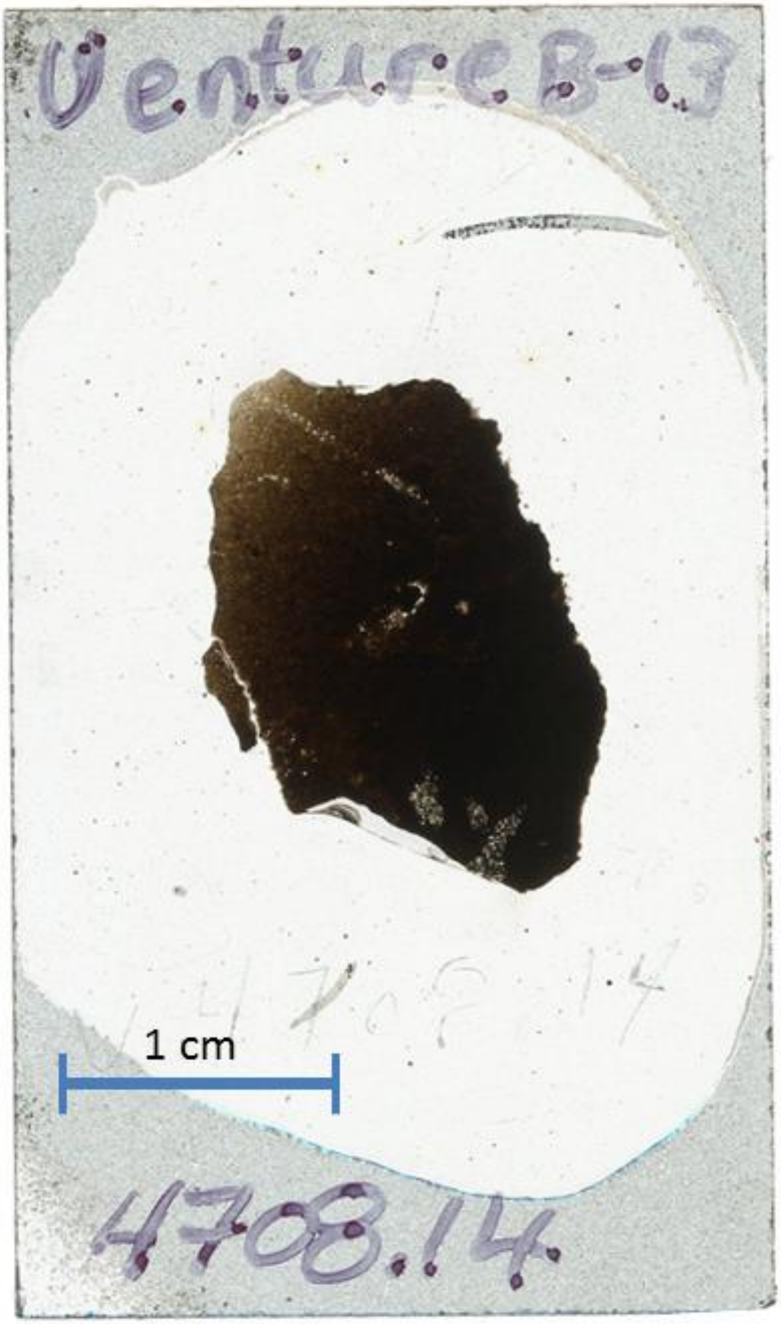

Figure 3.10. Thin section of facies 2 offshore muds illustrating microscopic burrows in the sediments (Sample11, Core 1, 4708.14m).

3.3.2 Lithofacies 2 Interpretation: Shallow Marine Open Shelf

Lithofacies 2 is interpreted as muds that have been deposited in a submerged, low energy setting. Based on presence of regular parallel laminaetions, these muds seem to have been gradually deposited out of suspension, in a shallow marine open shelf setting or potentially as part of the prodelta bottomset. Bioturbation is variable in intensity perhaps indicating change in sedimentation rate or variation in environmental stresses such as salinity, oxygen or acidity. Low bioturbation intensities are indicative of rapid sedimentation rates, whereas high bioturbation intensities indicate slow sedimentation rates. From the apparent absence of erosional surfaces and bedforms, this facies was deposited below fair-weather and storm wave base. Trace fossils in lithofacies 2 are not indicative of a specific environment. *Planolites* burrows can be found in virtually all environments, from freshwater to deep marine, and *Ophiomorpha* burrows are found in numerous marine shoreface environments (Pemberton *et al.*,1992).

3.4 Lithofacies 3: Heterolithic and Cyclic Sandstone and Shales

This heterolithic lithofacies is composed primarily of massive and parallel laminaeted sandstone and shale. No vertical grain size trends are observed; however, shale laminae show upward thickness change from ~5 mm to ≤1mm over 15 cm. Sands are moderately to well-sorted with the presence of some wavey beds. Calcareous and argillaceous red mudstone is common and garnet grains are also observed in thin laminae. Detrital garnets generally lie on top of cross-stratified calcareous sands of facies 4. Scour surfaces separate lithofacies 3 and 4 where detrital garnets are present. These heterolithic sands and shales show low-angles of repose with low intensity (0-3) bioturbation index (Fig. 2.3). Organisms forming *Planolites*, *Skolithos*, and *Ophiomorpha* are present. Micro-syndepositional slumping and microfaults have generated interesting pinch-off structures named loop bedding are observable in Figure 3.11 (Calvo *et al*., 1998).

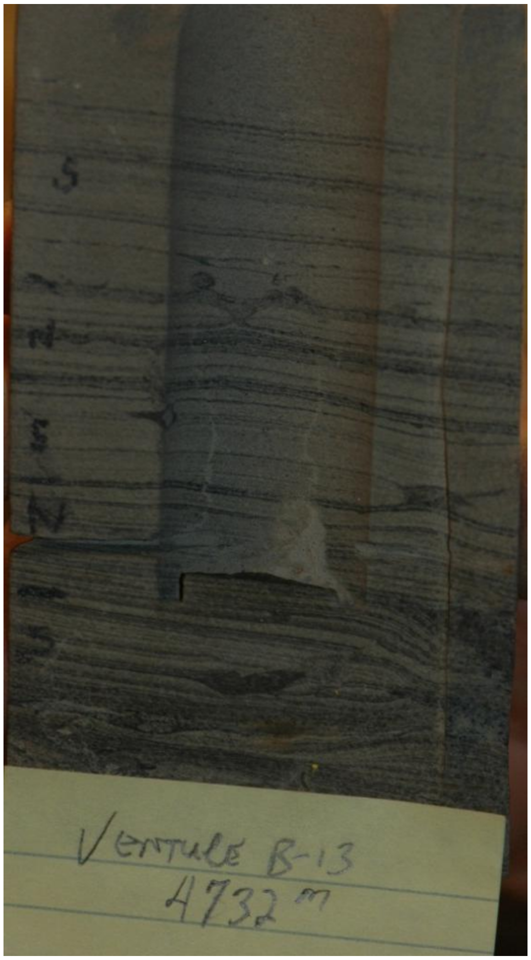

Figure 3.11. Interlayered heterolithic sands and shales from Core 1 (4732 m- 4731.80m) Venture B-13 well of facies 3 showing possible spring and neap cycles. Paired mud drapes on the top of this core sample. Thickening and thinning of beds and laminaee are representative of these spring and neap bundles. Microfaults have generated pinch-off structures termed loop bedding.

3.4.1 Thin section interpretation of facies 3

3.4.1.1 Interbedded siltstone and clay

Thin sections from Core 1 from sample point 4708.14m and Core 2, sample point 4716.25m

This rock is composed of separate quartz rich and mica rich bands. Bedding and parallel accumulation of clays are both observed in these samples. The quartz rich bands comprise quartz (60%), intergranular micritic calcite cement (30%), chlorite and muscovite (8%), and pyrite (2%).

The brown bands comprise primarily of microscopic platy minerals(75%), quartz grains (15%), pyrite (5%) and possibly organic matter(5%). Physical compaction is evident in these thin sections; however, chemical compaction is nearly nonexistent. As such, these samples have undergone a low degree of diagenesis.

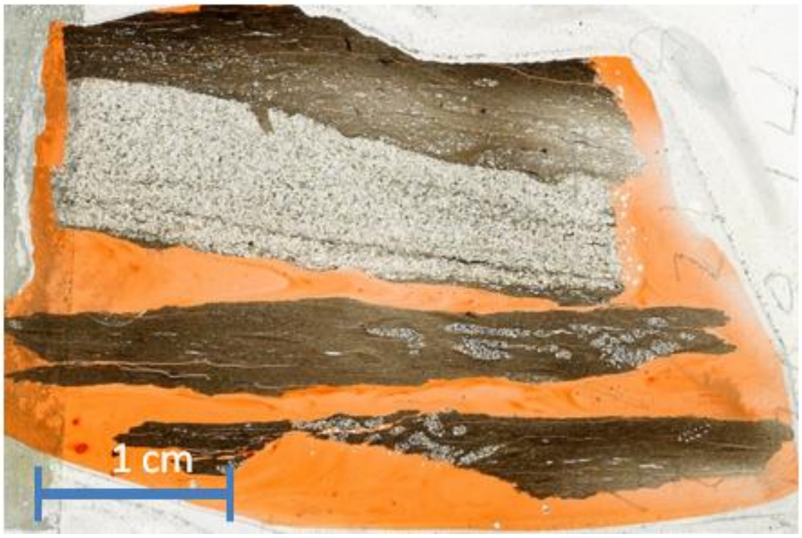

Figure 3.12. Thin section of facies 3 interbedded siltstone and intramicrite Sample 11 (Core 1, 4708.14 m).

Time	Paragenesis
1	Successive deposition of coarser and finersediments
2	Formation of authigenic pyrite in a reducing environment
3	Physical compaction of grains, alignment of platy minerals
4	Cementation by precipitation of carbonates in coarser bands

Table 3.4. Paragenesis of interbedded siltstone and clay microlithofacies. After deposition of sediments, minor early cements (carbonate and pyrite) were formed. Physical compaction and cementation are the final stages of diagenesis observed.

3.4.2 Lithofacies 3 Interpretation: Tide-Influenced Nearshore Shallow Marine Shelf Deposits

The nature and diversity of trace fossils is indicative of marine conditions and the cyclic appearance of sands and shales provides evidence of a tidally influenced setting. The heterolithic and cyclic nature of the sediments in this facies, with some systematic variation in laminae thickness, is suggestive of spring and neap tidal bundles, although bundles are not well defined. Loop bedding, as observed on Figure 24, is representative of compaction followed by microdeformation near the boundary between the ductile-brittle deformation fields (Calvo *et al.*, 1998). Appearance of garnets in thin (~2-4mm) laminaee suggests events capable concentrate these denser minerals during the deposition of lithofacies 3. Provenance of heavy minerals in the Scotian Basin is likely from the dominantly metamorphic Meguma Terrane of the Appalachians (Tsikouras *et al.*, 2011).

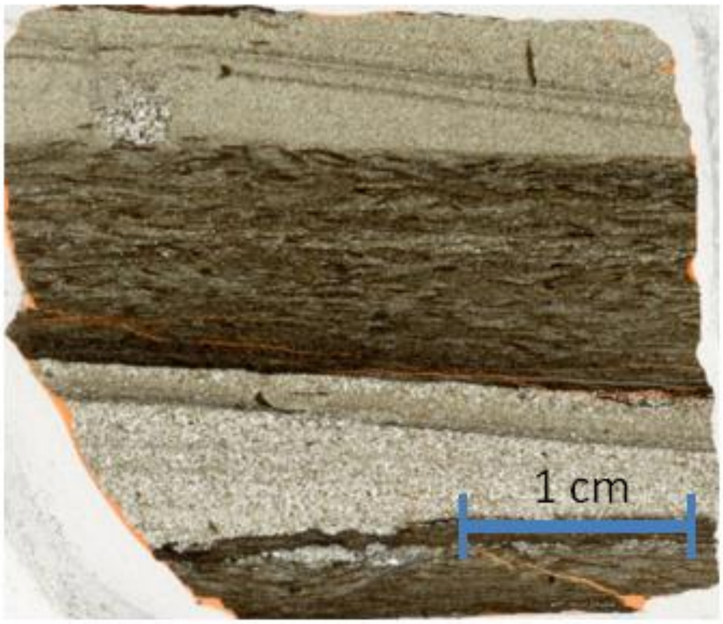

Figure 3.13. Thin section of facies 3 interbedded siltstone and intramicrite of Sample 15 (Core 3, 4716.25m).

3.5 Lithofacies 4: Cross-Stratified Calcareous Micaceous Sandstone

This lithofacies is composed of relatively clean, micaceous sands with calcareous cement. Thin dark-grey to black siltstone interbeds are present throughout this lithofacies with common detrital and authigenic chlorite. These sands are moderately to well sorted and rarely show coarsening upward laminae and beds. Argillaceous red mudstones are rarely present. Slightly finer grained sands overlie organic laminaee (~2mm) (Fig. 3.16). Low angle oscillatory-flow cross-laminaetion, truncated surfaces, and ripple-drift cross-stratification are present throughout the facies. *Ophiomorpha nodosa* and *Rosselia* socialis burrows are observed in the clean sandy intervals.

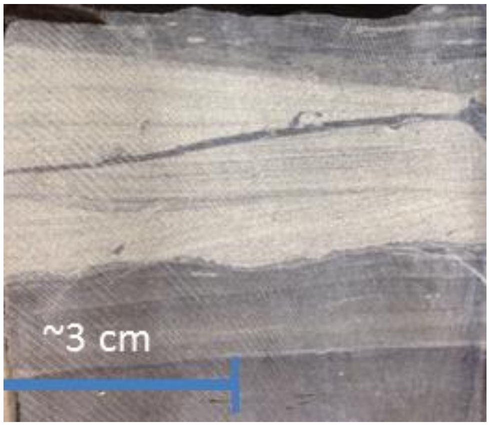

Figure 3.14. Oscillatory-flow cross-laminaetion observed in sands of facies 4 between 4719.73-4719.66m from Core 3. The base of the sandstone shows evidence of scouring and is bounded by facies 2 shale beds. Low angle truncations are present within the sandstone.

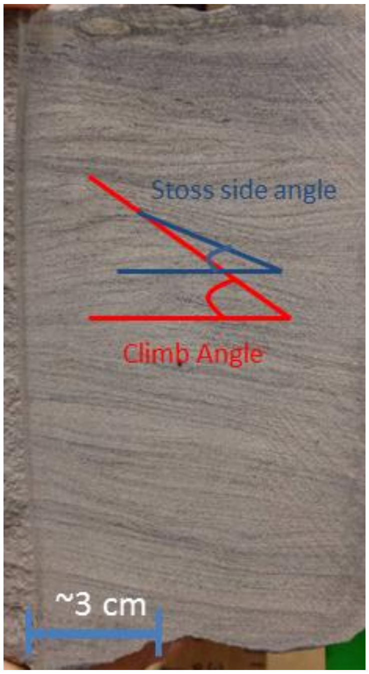

Figure 3.15. Calcareous micromicaceous sands of facies 4 showing symmetrical inclined layers and climbing ripples/ ripple-drift cross-stratification. Since the angle of climb is greater than the stoss side angle, these are called supercritical climbing ripples (Boggs, 2006).

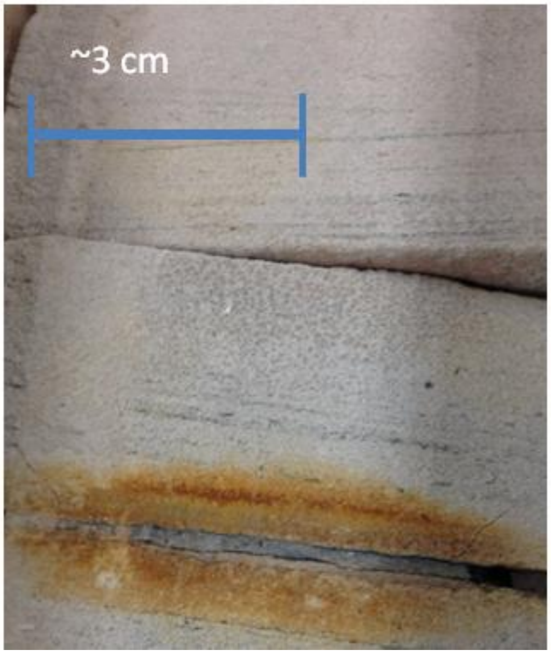

Figure 3.16. Calcareous fine-grain sand with shale laminaee having a less than 5o dip with possible organic debris within. This section is found between 4728.5m and 4728.17m.

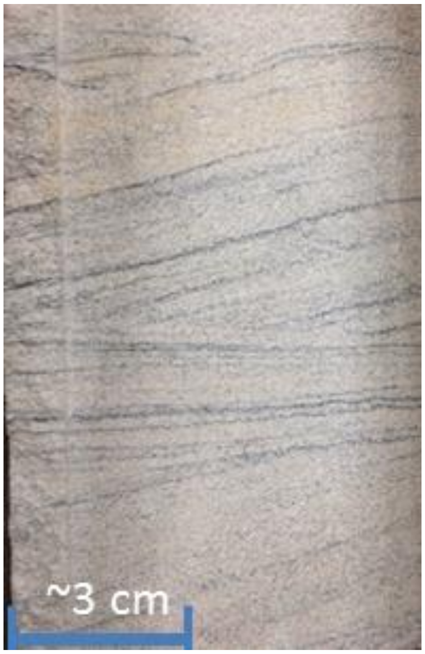

Figure 3.17. Medium to coarse grained argillaceous sands, laminated with minor tabular cross-bedding and minor bioturbation. Some cryptoturbation is identified along the shale laminae that is rich in organic material for opportunistic feeding organisms.

Intervals of lithofacies 4 bedsets may reach meters (>3m) in thickness. Some shale laminaee with low angle dips (~0-5°) were observed. Bioturbation index is variable (0-3 intensity range) throughout this lithofacies. Where bioturbation occurs, *Asterosoma*, *Skolithos*, *Ophiomorpha*, *Rosselia* and *Cylindrichnus* are present. *Asterosoma* shows groups of concentric banding around the central shaft (Pemberton *et al*, 1992) whereas *Ophiomorpha* burrows are lined with dark shales. *Planolites* burrows are evident in the siltstone interbeds.

3.5.1 Thin section interpretation of facies 4

3.5.1.1 Fine to medium-grained calcareous sandstone with ooids and shell fragments

Thin sections from core 1 from sample points 4699.66 m, 4703.01m

These thin sections comprise quartz grains (50-70%), shell fragments (bivalve fragments, crinoids and echinoid spines) (5-10%), ooids (5-15%), lime mud clasts (5%), muds (6%), intragranular micritic calcite cement (10-18%), pyrite (0-2%), chlorite (0-2%), muscovite and biotite (0-2%)

The average grain size in both thin sections ranges from 0.15 to 0.25 mm. Although larger grains (≥0.25mm) are found in 4703.01m, both samples are grain-supported and contain lime mud. The average ooid size is 0.2mm. Quartz grains are rounded (4703.01) to subrounded (4699.66m) and samples are generally well sorted. Platy minerals such as chlorite, muscovite and biotite have been deformed as a result of compaction. Burrows with mud linings are observed in Sample 7 (Core 1, 4703.01m).

Although both thin sections are part of the same microlithofacies, it is evident that Sample 6 (Core 1, 4699.66m) has undergone an increased amount of diagenesis. Whereas replacement of quartz by calcite is observed in Sample 6 (Core 1, 4699.66m) by nibbled grain contacts, this diagenetic feature is absent in Sample 7 (Core 1, 4703.01m). As silica is released, it becomes available for diagenesis. Dark micritic rims around quartz grains and fossils, as a result of iron rich carbonates packing around grains during compaction and burial, are present in both thin sections.

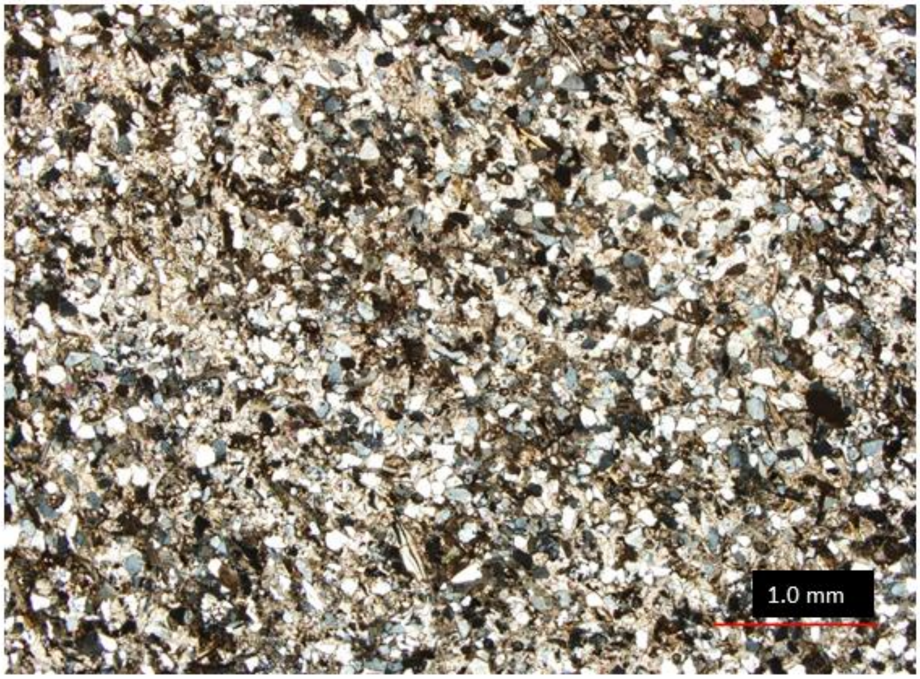

Figure 3.18. Thin section of Sample 6 (Core 1, 4699.66m) under cross-polarized light. Quartz grains and micritic calcite infilling the intergranular pore space. Calcite replacement of quartz grains is evident by observation of curved/nibbled quartz grains. These are evidence of late stage diagenesis.

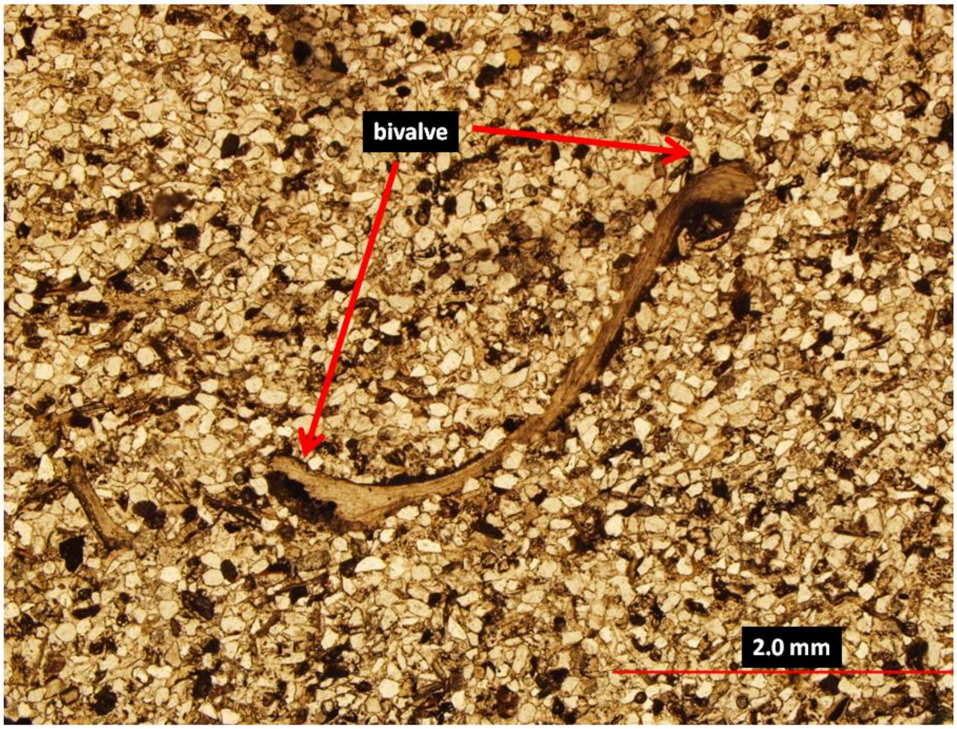

Figure 3.19. Thin section of Sample 6 (Core 1, 4699.66m) under plain-polarized light. Bivalve shell with fibrous unaltered texture is surrounded by embedded quartz grains. Calcite cement lies within pore spaces, and darker material is siderite. Quartz fragments indent bivalve shell as a result of compaction.

Time	Paragenesis
1	Deposition of sediments and shell fragments
2	Bioturbation creating mottled bedding
3	Formation of micritic rims around quartz creating embedded grains
4	Formation of authigenic pyrite in a reducing environment
5	Physical compaction and increased grain packing
6	Precipitation of calcium carbonate in intragranular spaces
7	Minimal replacement of quartz by calcium carbonate (only in 4699.66 m)

Table 3.5. Paragenesis of fine-grained calcareous sandstone with ooid fragments. After deposition of sediments, and minor physical compaction, organisms create burrows and minor early cements (carbonate and pyrite) are formed. Physical compaction, cementation and replacement of quartz by calcium carbonate are the final stages of diagenesis observed.

3.5.1.2 Very fine- to medium-grained calcareous sandstone

Thin sections from Core 3 from samples 4718.70m and 4718.75m

This rock is composed of quartz (85%), intergranular micritic calcite (10%), a few small ooids (5%), pyrite (3%), and microcline (2%).

Quartz grains demonstrate sub-rounded, convex/concave grain boundaries. Their size is variable throughout the thin sections, from very fine- to fine-grained sand (0.091mm-0.227mm). Some of the quartz grains in these thin sections are microcrystalline. Some coherent patches of the samples show carbonate cementation. Intergranular secondary porosity of about 25% is evident. Finally, early clay mineral (chlorite) growth over quartz grains is observed.

Time	Paragenesis
1	Deposition of sediments
2	Early clay mineral growth
3	Formation of authigenic pyrite in a reducing environment
4	Physical compaction of grains
5	Chemical compaction of grains where silicate grains are partially dissolved
6	Cementation by precipitation of carbonates
7	Minor dissolution by pore fluids

Table 3.6. Paragenesis of very fine- to medium-grained calcareous sandstone. After deposition of sediments, and minor physical compaction, minor early cements (carbonate and pyrite) are formed. Physical compaction, cementation and dissolution by pore fluids are the final stages of diagenesis observed.

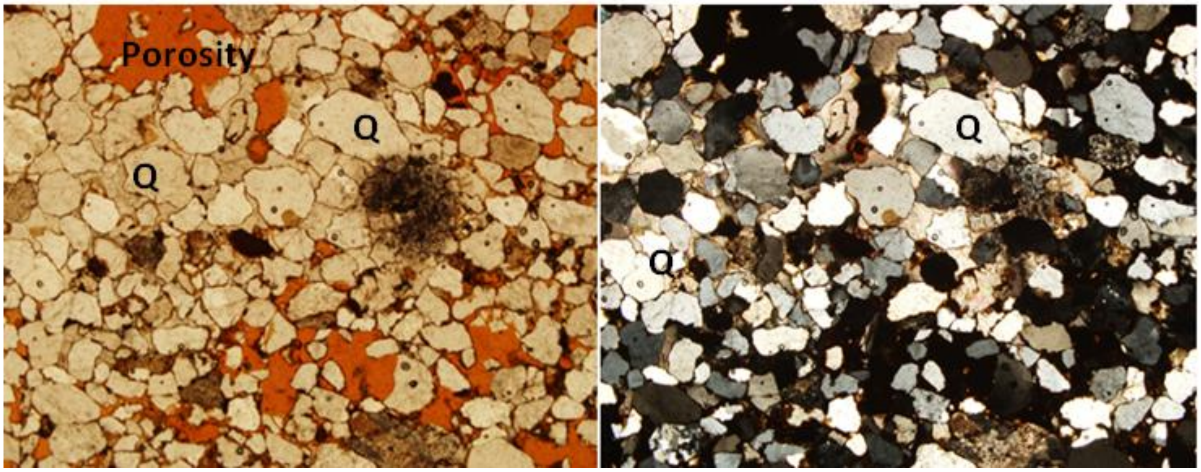

Figure 3.20. Sample 4 (Core1, 4695.62m) under plain-polarized and cross-polarized light showing quartz grains and high amount of secondary or ineffective porosity highlighted by orange resin.

3.5.1.3 Fine- to coarse-grained calcareous silt

Thin sections from Core 1 from samples 4693.64 m, 4707.80m, 4708.20m, from Core 2 from sample 4711.95m, from Core 3 from samples 4727.60m, 4730.20 m, 4730.67m, 4749.76

Quartz (40-70%) predominates, with detrital chlorite (10%), framboidal pyrite (1-7%), muscovite (4-7%), biotite (0-5%), plagioclase (0-5%), and micritic cement mixed in with mud (10%-26%). No bioclasts or ooids are observed in these thin sections. Sample 19 (Core 3, 4730.20m) and Sample 20 (Core 3, 4730.67m) have a bioturbation index of 3 (Fig. 2.3.) whereas the rest of the thin sections are unbioturbated. Pyrite seems to be lining these burrow walls. Grain size is variable from fine silt (0.0078 mm) to coarse silt (0.053mm). Muscovite and biotite grains are aligned forming microscopic laminaee, particularly in Sample 14 (Core 2, 4711.95m). Grains in all thin sections are subrounded to angular and moderately sorted. Opaque material in thin sections (Fig. 3.24) is likely siderite, an iron-rich calcite cement, or organic debris mixed with pyrite.

The plagioclase present is the calcium-rich end member, anorthite, which is identified by an average extinction angle of 49-63^{o} of polysynthetic twinning. These minerals have not been albitized as fluids were likely not able to penetrate these grains. Replacement of quartz by calcite is present, creating irregular “nibbled” contacts along the grain boundary. In all thin sections except in Sample 10 (Core 1, 4707.80m), flexible deformation of platy minerals such as chlorite, biotite and muscovite was observed throughout thin sections (Fig. 3.22). Chloritized bands of sediments are present in Sample 10 (Core 1, 4707.80m) as a result of mineral replacement. Specifically in this thin section, detrital chlorite grains are not present. Instead, chlorite is present as fine rims around detrital quartz grains. Finally, secondary porosity is observed in Sample 12 (Core 1, 4708.20m) as a result of dissolution by pore fluids (Fig. 3.28).

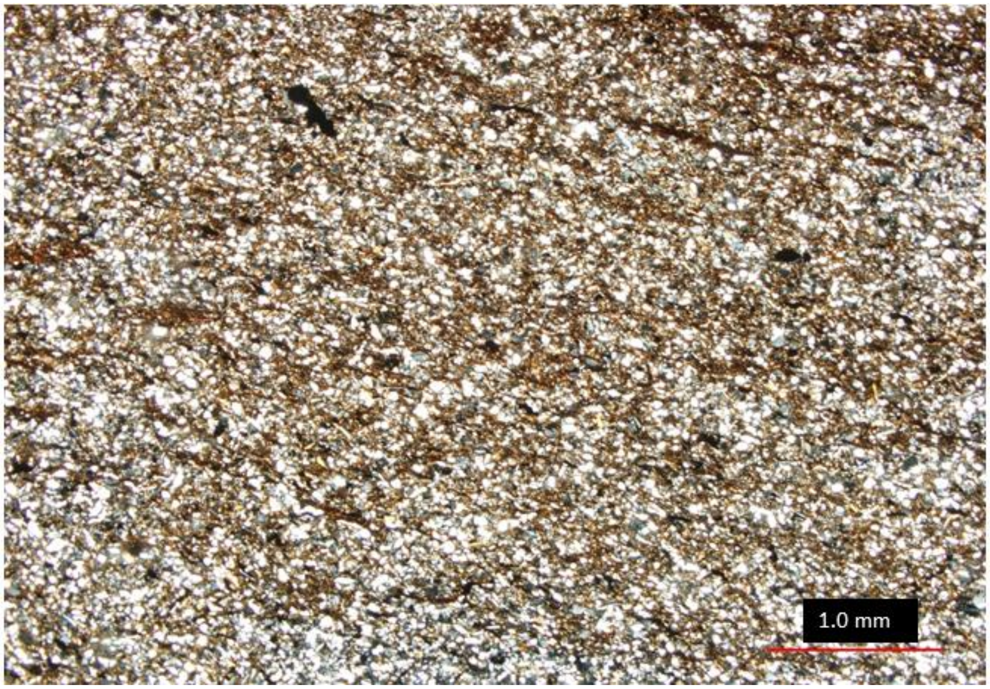

Figure 3.21. Thin section of Sample 3 (Core 1, 4693.64m) of fine- to coarse-grain calcareous siltstone under plain polarized light. The opaque material is likely pyrite. Note that the micaceous minerals display no preferential alignment.

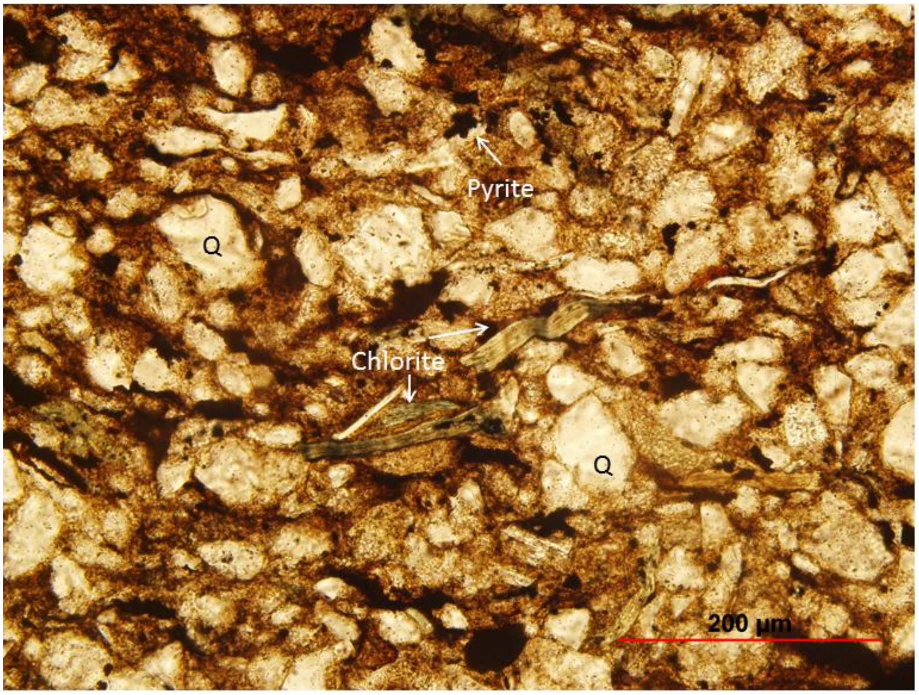

Figure 3.22. Sample 3(Core 1, 4693.64m) under plain polarized light demonstrating early signs of early diagenesis with chlorite deformation. Framboidal pyrite also found throughout.

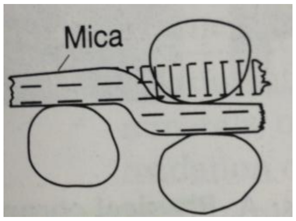

Figure 3.23. Flexible grain deformation identical to what is observed in Figure 35 as shown by Boggs (2006)

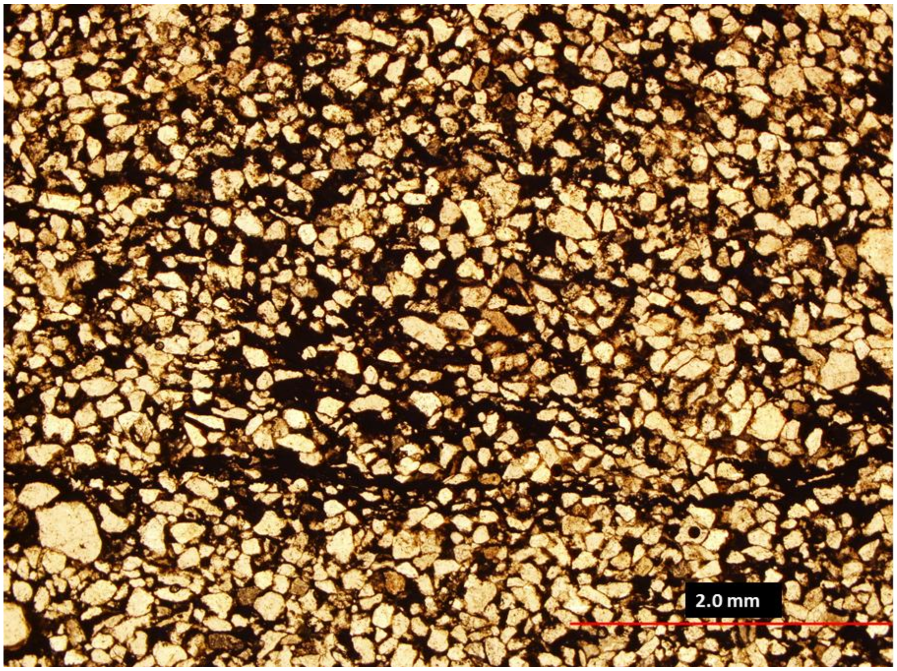

Figure 3.24. Thin section of fine-grain sandstone from Sample 12 (Core 1, 4708.2m) under plain polarized light. Quartz grains and organic fragments are cemented with siderite. Although secondary porosity is observed in this thin section, none is seen in this particular area.

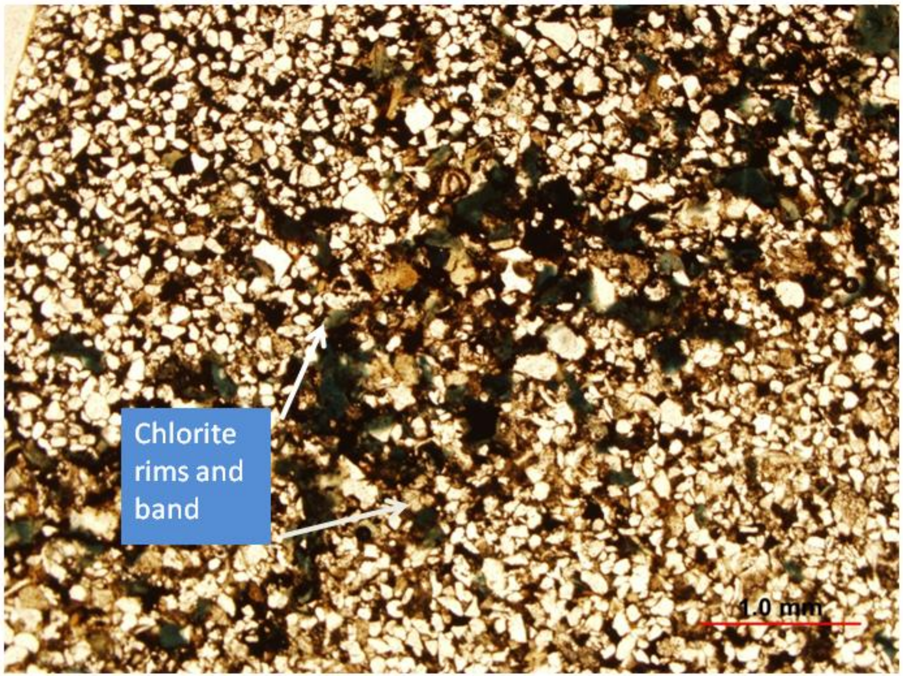

Figure 3.25. Thin section of fine-grain sandstone from Sample 9 (Core 1, 4707.4m) under plain polarized light. The presence of authigenic chlorite bands and rims around quartz veins are the result of early diagenesis. Porosity is observed to be greater in these chlorite-rich bands.

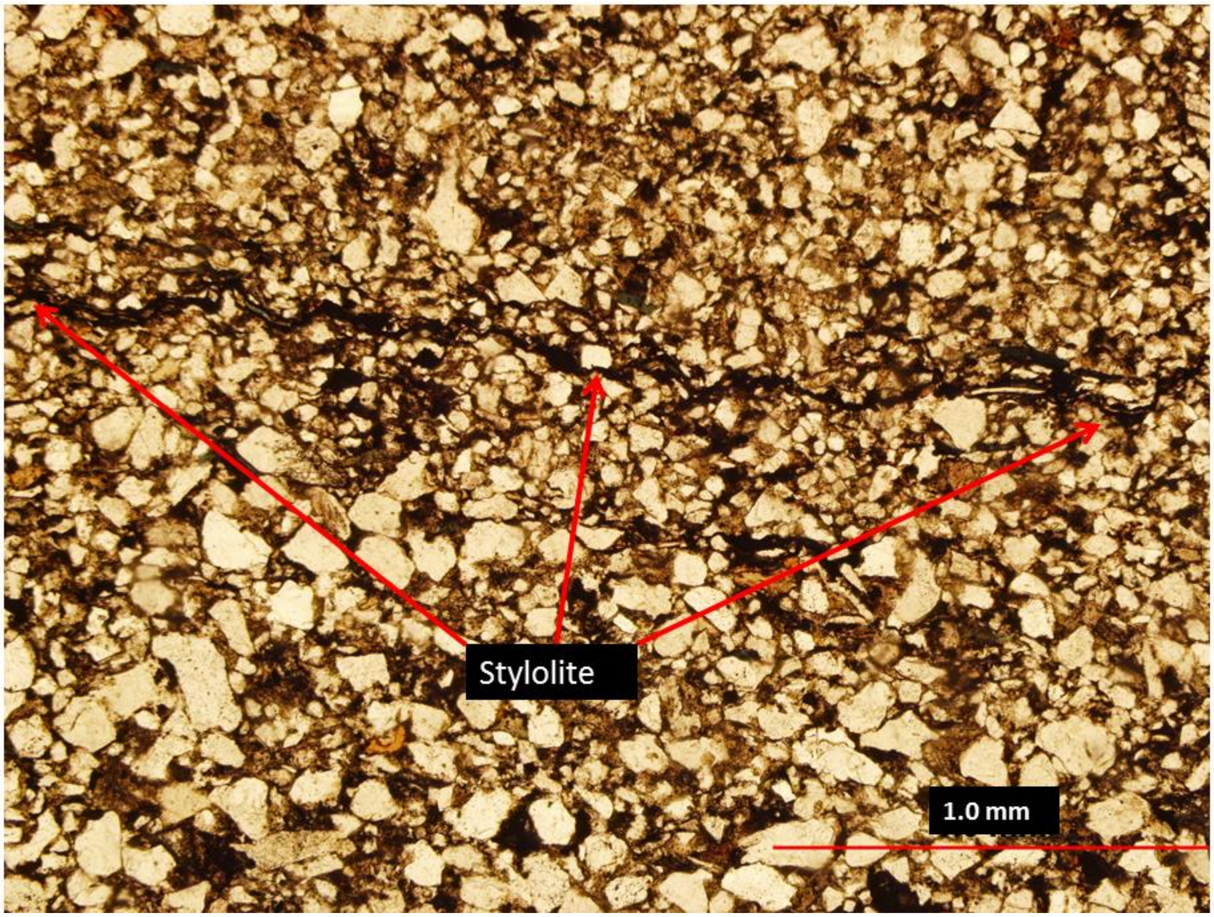

Figure 3.26. Thin section of sandstone from Sample 14 (Core 2, 4711.95m) under plain polarized light. Note the stylolites are present, carbonates have been dissolved, pyrite is concentrated in these zones and quartz grains remain intact. This thin section shows moderate to poor sorting.

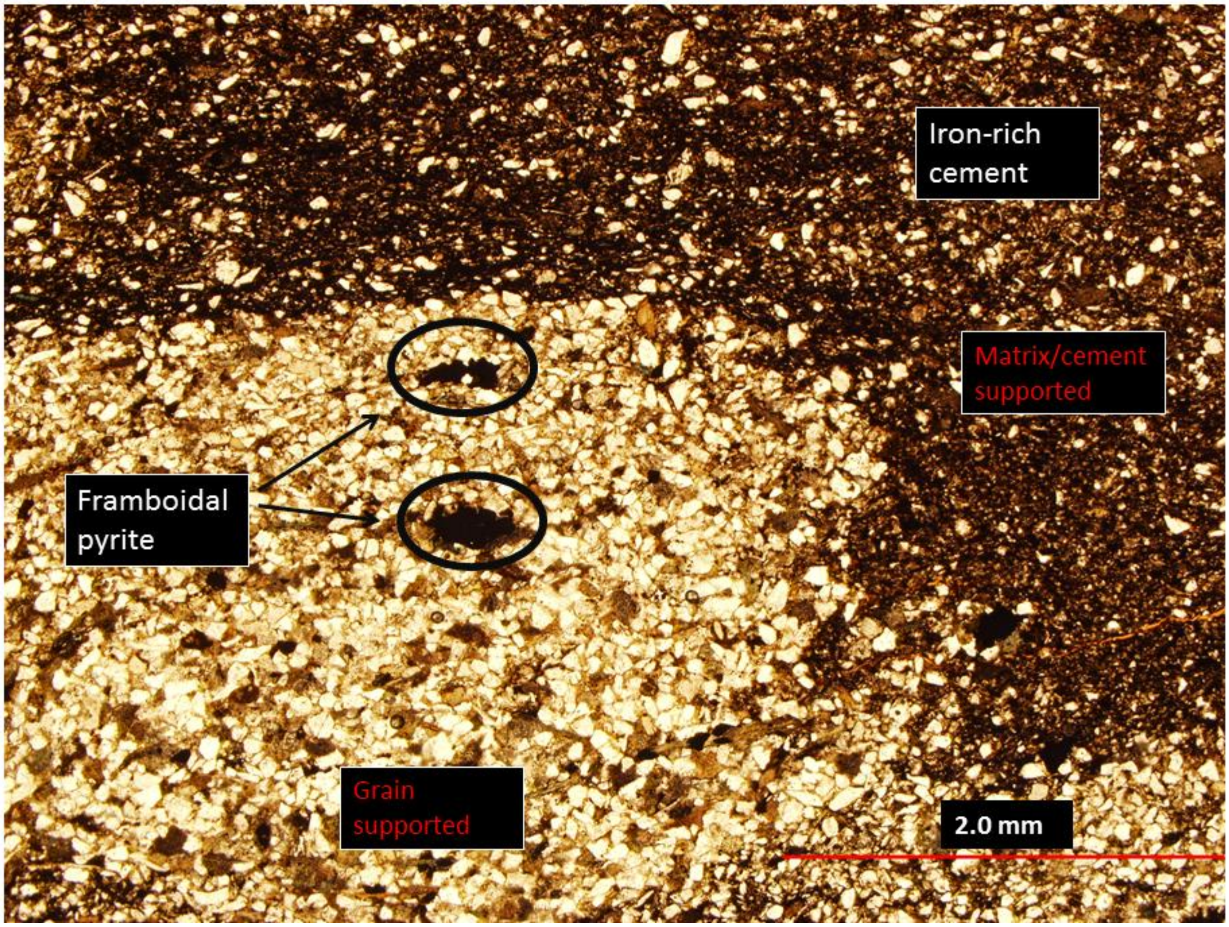
Iron-rich cement
Matrix/cement supported
Framboidal pyrite
Grain supported
2.0 mm

Figure 3.27. Thin section of sandstone from Sample 19 (Core 3, 4730.2m) under plain polarized light that reveals the contrast between grain-supported and matrix- and cement-supported sediments. Framboidal pyrite is found throughout this thin section.

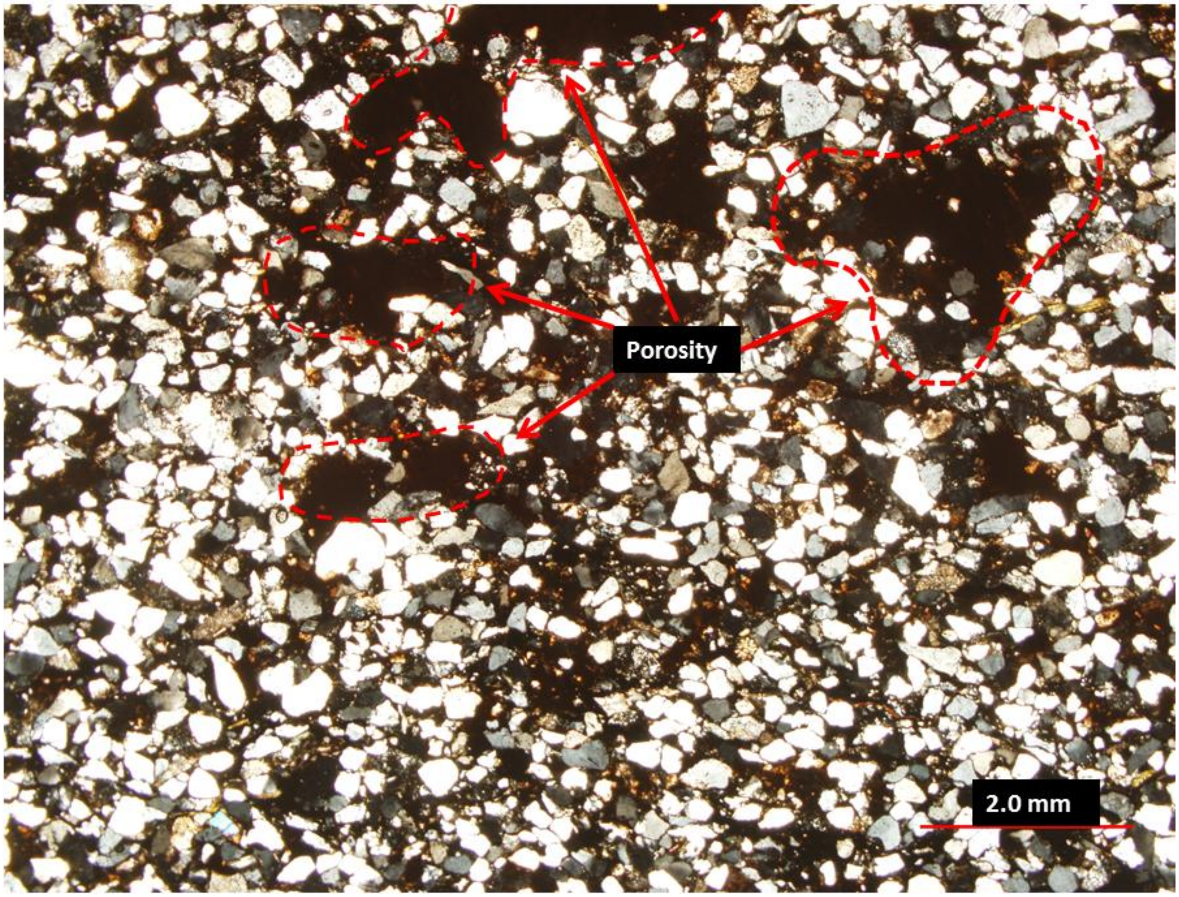

Figure 3.28. Thin section of micaceous sands of lithofacies 4 from Sample 12 (Core 1, 4708.2m) under crossed polarized light. The sample is quartz rich, well sorted with subrounded grains. Secondary porosity is also observed.

Time	Paragenesis
1	Deposition of sediments
2	Early clay mineral growth
3	Formation of authigenic pyrite in a reducing environment
4	Physical compaction of grains, alignment of platy minerals
5	Cementation by precipitation of carbonates
6	Slight dissolution by movement of pore fluids

Table 3.7. Paragenesis of fine- to coarse-grained calcareous silt. After deposition of sediments, and minor physical compaction, minor early chlorite minerals were able to form followed be the formation of cements (carbonate and pyrite). Physical compaction, cementation and dissolution by pore fluids are the final stages of diagenesis observed. Physical compaction occurs as a result of diagenesis.

3.5.2 Lithofacies 4 Interpretation: Shoreface Deposits

This facies is representative of a dynamic part of a shoreface. The presence of oscillatory-flow cross-stratification is evidence of a bidirectional paleocurrent during sediment deposition. Similar to facies 3, the presence of diverse burrows such as *Ophiomorpha nodosa* and *Rosselia socialis,* as well as diverse shell organisms suggest fully marine conditions during deposition. Horizontal laminaee, planar cross-beds, current and climbing ripples further suggest that these are of the lower flow regime with possible low to medium water velocity. Ripple-drift evidence could also be representative of storms or tides affecting shoreface deposits.

Chapter 4

4.1 Trace Fossils-Venture B-13 Well

The trace fossils observed in Venture B-13 cores were key components in understanding biofacies and depositional environments. The *Cruziana* and *Skolithos* ichnofacies were identified in the B-13 cores, and evidence presented below will show that bioturbation affects sediments**.**

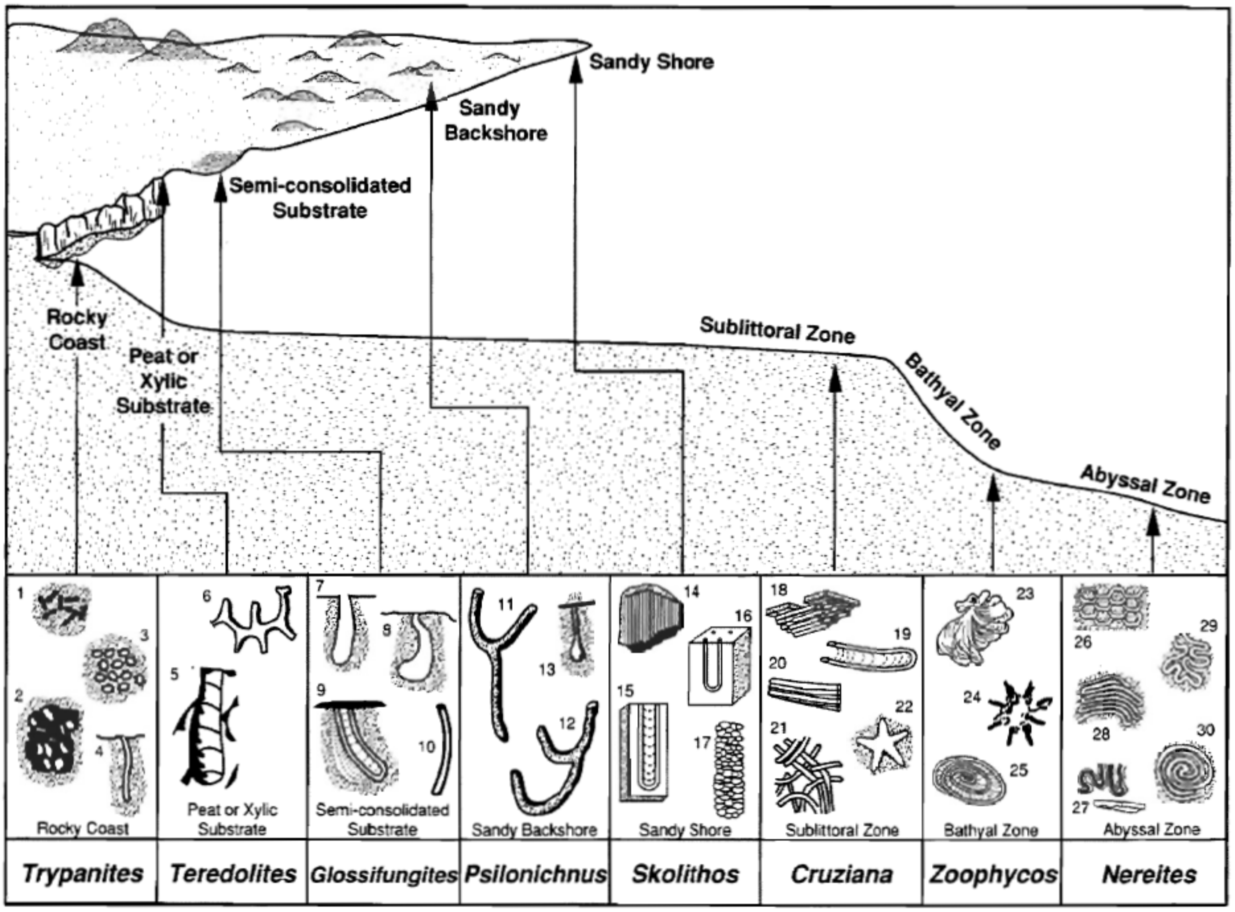
Sandy Shore
Sandy Backshore
Semi-consolidated Substrate
Rocky Coast
Peat or Xylic Substrate
Sublittoral Zone
Bathyal Zone
Abyssal Zone
1
2
3
4
Rocky Coast
5
6
Peat or Xylic Substrate
7
8
9
10
Semi-consolidated Substrate
11
12
13
Sandy Backshore
14
15
16
17
Sandy Shore
18
19
20
21
22
Sublittoral Zone
23
24
25
Bathyal Zone
26
27
28
29
30
Abyssal Zone
Trypanites
Teredolites
Glossifungites
Psilonichnus
Skolithos
Cruziana
Zoophycos
Nereites

Figure 4.1. Trace fossils and their respective ichnofacies and environments (Pemberton and MacEachern, 1995).

4.1.1 Cruziana Ichnofacies

The *Cruziana* ichnofacies includes *Thalassinoides*, *Cylindrichnus*, *Rosselia socialis* and *Planolites*. Although other ichnogenera also compose the *Cruziana* ichnofacies, these specific trace fossils are observed throughout the Venture B-13 core. They are typically representative of mid to distal continental shelf deposition below normal wave base. Wave base is the maximum water depth at which a passing wave may influence sediments (Boggs, 2006) and can be categorised as fair weather deposits

(Wach, 2013). *Planolites* trace fossils are made during intrastratal deposit feeding (Davis *et al.*, 2012). These traces usually have unlined walls and burrow fills that differ in texture from adjacent rock (Pemberton *et al.*, 1992). *Planolites* can be found in various environments from deep marine to freshwater (Pemberton *et al.*, 1992). *Asterosoma* trace fossils were also present. In Venture B-13, a textbook example of *Rosselia socialis* is present (Fig. 4.3). Concentric rings of clay and siltstone surround the central shaft of the *Rosselia* where a ball of silt surrounds a central black shaft (Howell, 2012). These fossils are representative of shallow marine sandstones (Howell, 2012). The organisms forming *Planolites, Thalassinoides, Arenicolites* and *Skolithos* can tolerate salinity-stressed environments (Davis *et al.*, 2012). The organism forming *Planolites* can tolerate oxygen-stressed environments (Davis *et al.*, 2012).

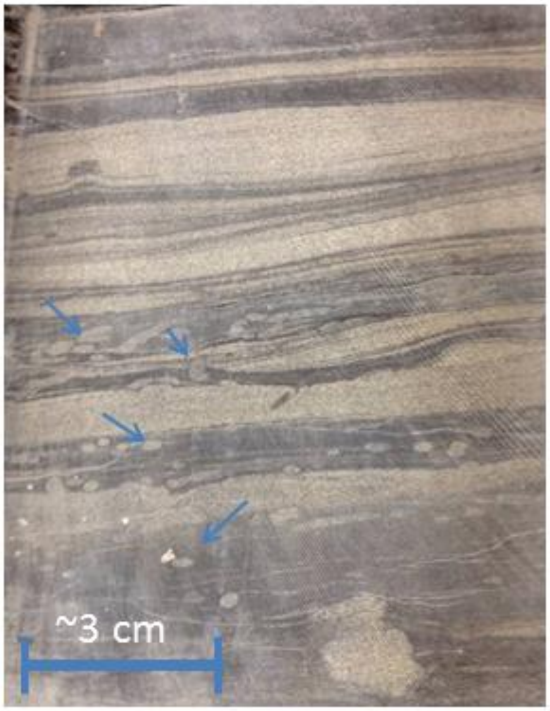

Figure 4.2. Sands and shales from facies 3. Blue arrows indicate *Planolites mortanus* burrows and are concentrated in shale layers that are likely organic rich and deposited in quiet water sedimentation. Cross beds and ripple forms are present. An alternation of strong weak currents are observed, confirming that this is an active depositional environment. Minor flaser bedding is observed within shale laminaee.

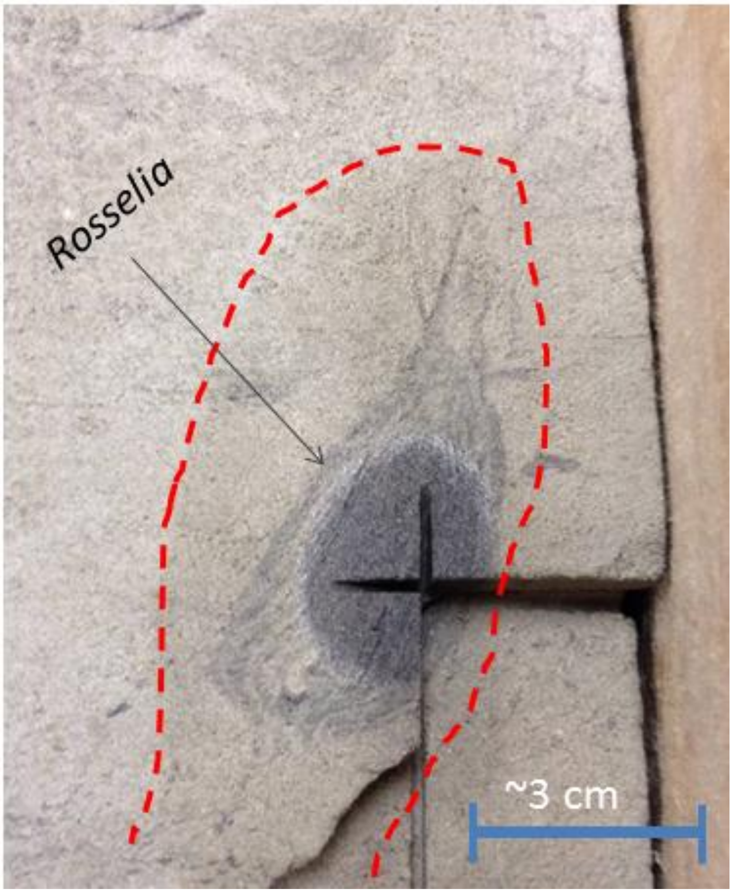

Figure 4.3. Enlargement of a *Rosselia socialis* dwelling burrow of the *Cruziana* inchnofacies. The diagenetic halo is a slightly different colour than the surrounding sandstone

4.1.2 Skolithos Ichnofacies

The *Skolithos* ichnofacies typically comprises *Ophiomorpha*, *Arenicolites* and *Skolithos*. This ichnofacies typically represents a moderate- to high-energy marine environment with a generally low-turbidity and well-oxygenated water column (Dalrymple *et al.*, 2010). *Ophimorpha* burrows represent a near shore environment. Animals found in tidal settings are able to concentrate fine-grained sediments as a result of selective ingestion (Davis *et al.*, 2012). The *Ophiomorpha* burrows with thick mud linings are representative of a subtidal setting and represent the dwelling burrows of suspension-feeding shrimp (Pemberton *et al*., 1992). Traces similar to *Ophiomorpha* but lacking wall lining are attributed to *Thalassinoides* (Bromley, 1990). *Arenicolites* is the dwelling burrow of an annelid generally associated with low energy shoreface or sandy tidal flats (Pemberton *et al.*, 1992). *Skolithos* burrows represent suspension-feeding organisms or passive carnivores that are generally associated with marine or brackish environments (Pemberton *et al*., 1992).

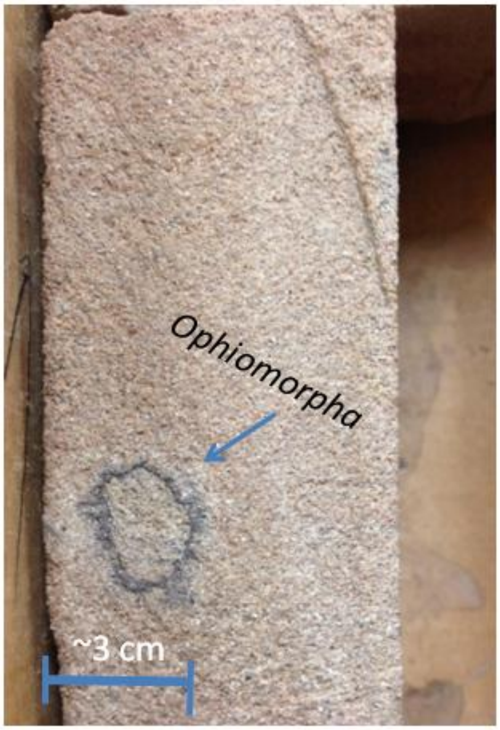

Figure 4.4. Coarse grained argillaceous sandstone of facies 4 with 3 cm *Ophiomorpha nodosa* burrow. Note pelloidal wall linings that support the burrowed structure. These burrows are representative of a tidal setting.

Table 4.1. Trace fossils observed in the Venture B-13 cores and their respective ethologies (Modified from Pemberton et al., 1992)

Trace Fossil	**Ethology**
Ophiomorpha	Dwelling burrow of suspension-feeding shrimp
Cylindrichnus	Suspension feeding dwelling burrow
Planolites	Feeding burrow of deposit-feeder
Arenicolites	Suspension- or filter-feeder
Asterosoma	Selective deposit-feeding
Skolithos	Dwelling burrow of suspension-feeding organism
Rosselia	Dwelling burrow or feeding burrow of a deposit feeder

Table 4.2. Trace fossils and their associated lithofacies compared to average permeability core plug measurements. Permeability measurements will be further discussed in Chapter 5.

Lithofacies	**Trace fossils**	**Range of values (mD)**	**Average permeability from core plugs**
1	None	0.006-0.024	0.01275 mD
2	*Planolites, Asterosoma, Arenicolites, Thalassinoides* (abundant)	0.10-0.16	1.90667 mD
3	*Planolites*, *Skolithos*, and *Ophiomorpha* (abundant)	3.38	3.38 mD
4	*Ophiomorpha and Rosselia socialis* (rare)	0.024- 348	76.136 mD

Skolithos and *Ophiomorpha* are considered dwelling traces (Bromley, 1996). It has also been observed that sediments found surrounding trace fossils demonstrate disturbance as a result of biogenic activity (Bromley, 1996). This is especially applicable to larger trace fossils such as *Ophiomorpha*, *Skolithos* and *Rosselia*. Diagenetic haloes can be present around *Ophiomorpha* and *Rosselia* burrows representing localized zones of oxidation usually related to the presence of organic material. These features show the difference in diagenesis between the wall of the burrow and the infilling sediments (Bromley, 1996).

As observed in Table 4.2, both lithofacies 2 and 3 have high bioturbation values and low permeability values. Lithofacies 1 does not have any trace fossils, but has low a permeability average because of its nature, as described in Chapter 3. Lithofacies 4 has few *Ophiomorpha* burrows and generally high permeability measurements. Low permeability measurements likely occur where burrowing is present. Hence, a higher bioturbation index is related to lower permeability values.

4.2 Summary of Trace fossils

Analysis of trace fossils proved essential in understanding permeability variations throughout the Venture B-13 cores. Diagenetic haloes, present mainly around *Ophiomorpha* burrows, involve cementation in a zone around a burrow, further impacting permeability. Numerous of the discrete traces have muddy linings that affect local permeability. In clean sandstones, three-dimensional burrow connectivity increases permeability and the amount of fluid-flow pathways through rock. However, where both mud and sands are present, high bioturbation leads to sediment mixing, that significantly degrades permeability.

Chapter 5

5.1 Permeability in Venture B-13 Cores

5.1.1 TinyPermII

The tool used to measure permeability for Venture B-13 cores was the TinyPermII from New England Research, Inc. (2013) (Fig. 5.1; Table 5.1). In order to attain permeability measurements, the rubber nozzle is pressed against the core as the syringe knob is pulled towards the operator and air is pulled from the sample. The microcontroller which is connected to the syringe unit measures the syringe volume (the created vacuum pulse), and computes an algorithm for the specific permeability measurement (New England Research, 2013). The permeability values are then displayed on a liquid crystal screen on the microcontroller.

Table 5.1. Physical size of TinyPermII parts (New England Research, 2013).

TineyPerm II Part	Dimensions
Syringe unit	38cm x 12.5cm x 5cm
Microcontroller unit	16.5cm x 11.5cm x 5cm
Interface cable	Variable, up to 3 meters long

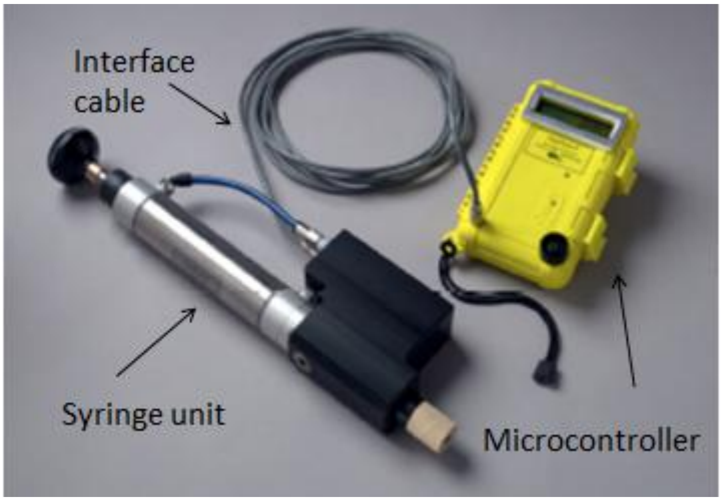

Figure 5.1. TinyPermII from New England Research Inc. The tool consists a syringe unit, interface cable and microcontroller which weighs 1.2kg (New England Research, 2013).

The number displayed on the screen is not given in millidarcies, but must be converted by using calibration charts and tables provided by New England Research Inc.

Horizontal permeability was measured whenever a change in lithofacies was observed. Values retrieved from TinyPermII show a high variation in permeability throughout measured core sections.

5.1.2 Core Plug Permeability

Forty two permeability measurements, based on core plugs sampled at regular intervals by the well operator, were sourced from analyses by Core Laboratories-Canada Limited (File reference #7004-81-13). Horizontal core plugs are samples cut perpendicular to the core axis that are about 2.5 to 3.8 cm in diameter and about 5 cm long (Schlumberger, 2013).

In a laboratory setting, permeability data is collected by using steady-state apparatus. A constant drop in pressure is used to precisely measure flow rate (Doyle, 2006). Equations using Darcy's Law are then used to find the permeability of sample. These measurements are taken through the full diameter of the core for horizontal permeability (K_H)(Doyle, 2006).

5.1.3 TinyPermII and Core Plug Permeability

Measurement results from core plug analyses and the TinyPermII tool are considerably different (on average 2 to 3 orders of magnitude) (Tables 5.2 and 5.3). Values generated by the TinyPermII measuring tool are suspect, possibly due procedural error. Given the sensitivity of the tool, escape of air may have occurred, resulting in erroneous values even though it has been calibrated. In view of these considerations, TinyPermII values were not evaluated as part of this thesis. Since core plug measurements are industry standard attained using calibrated laboratory equipment in a controlled environment, these values will be used as an accurate representation of permeability. Data from core plugs were plotted as depth (m) vs. permeability (mD) curves (Cores 1-4, Figs. 5.2-5.5 respectively).

Average permeability measurements from both core plug data and TinyPermII measurements were assigned to the different lithofacies. Lower permeability values corresponded to shaley sections of the core (lithofacies 2) and higher permeability values corresponded to sandy sections of the core (lithofacies 4). Where increased amounts of pore filling calcite cement were present, permeability was low.

Lithofacies	Core plug average permeability measurement (mD)	Range of values (mD)	Number of values from core plugs
1	0.01275	0.006-0.024	4
2	1.90667	0.10-0.16	3
3	3.38	3.38	1
4	76.136	0.024- 348	28

Table 5.2. Average permeability measurements of lithofacies from core plugs and range of values. The number of values is also included in the table as it is indicative of the certainty of the values.

Lithofacies	TinyPermII average permeability measurement (mD)	Range of values (mD)	Number of values from TinyPermII
1	14.21	3.19- 26.18	4
2	24.25	1.16-24.25	5
3	35.82	8.52- 166.78	8
4	197.64	18.7- 898.6	36

Table 5.3. Average permeability measurements of lithofacies from TinyPermII and range of values. The number of values is also included in the table as it is indicative of the certainty of the values. Range of values for each lithofacies is extremely variable.

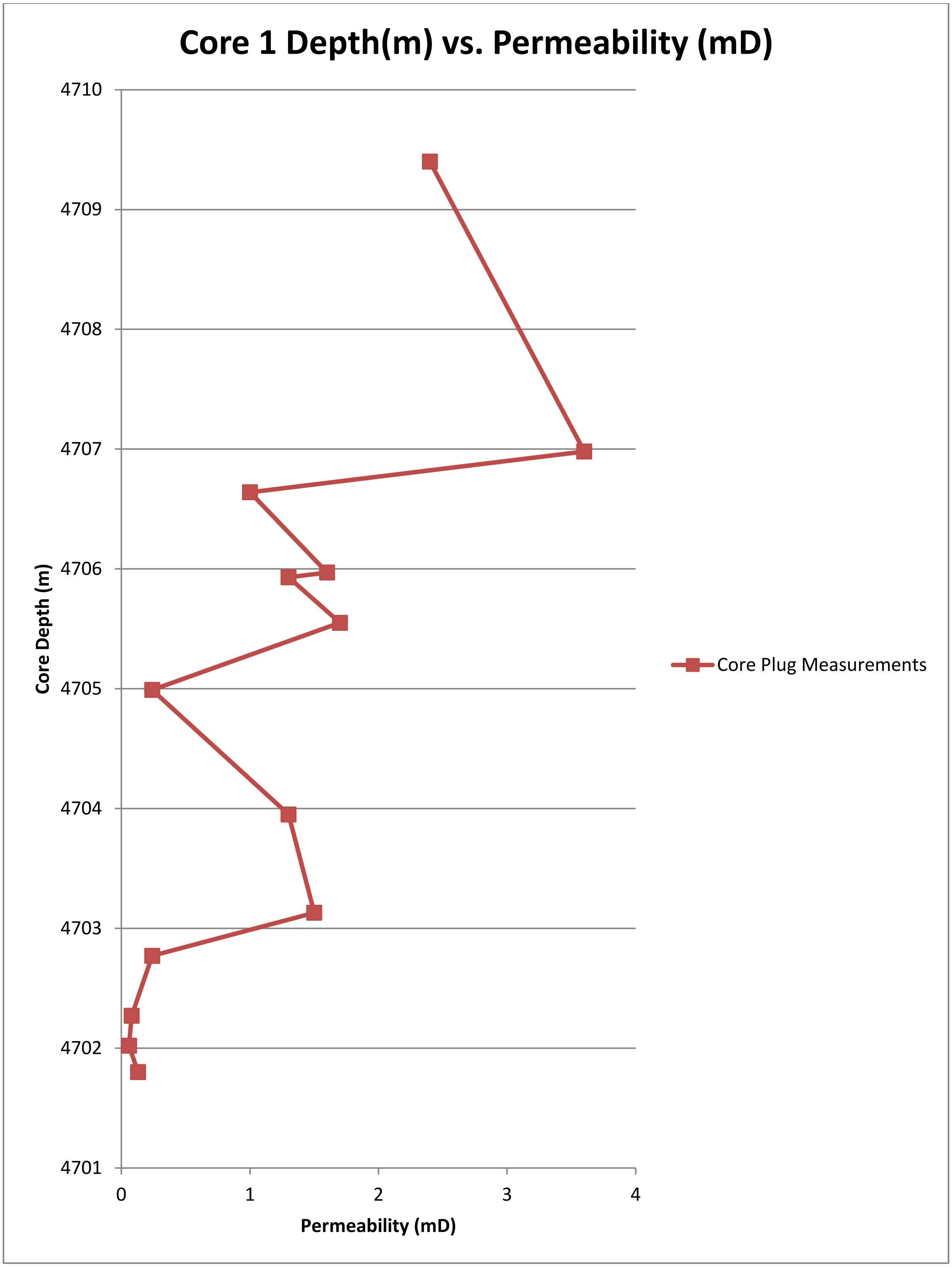

Figure 5.2. Core 1 depth (m) vs. core plug permeability (mD).

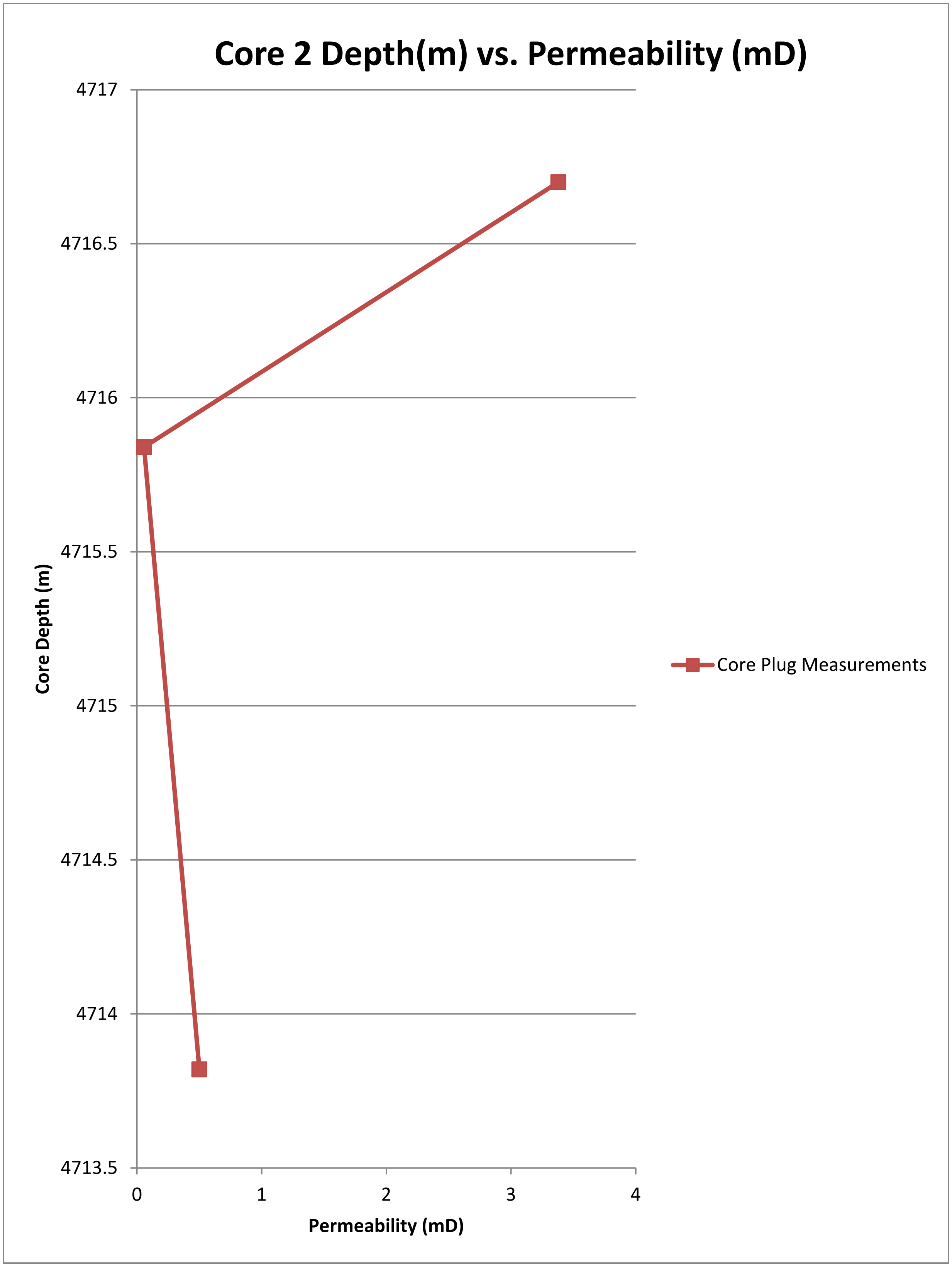

Figure 5.3. Core 2 depth (m) vs. core plug permeability (mD).

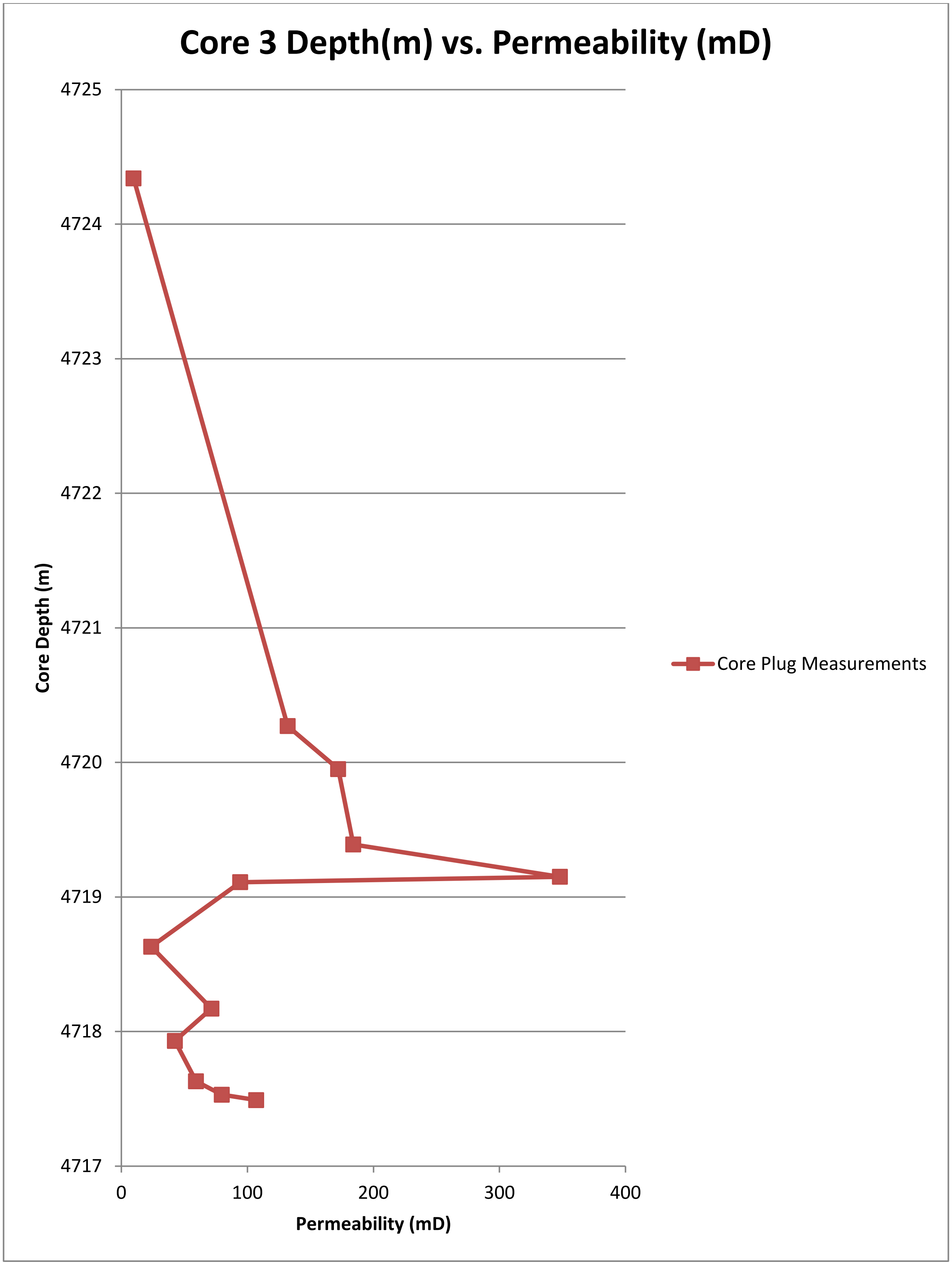

Figure 5.4. Core 3 depth (m) vs. core plug permeability (mD).

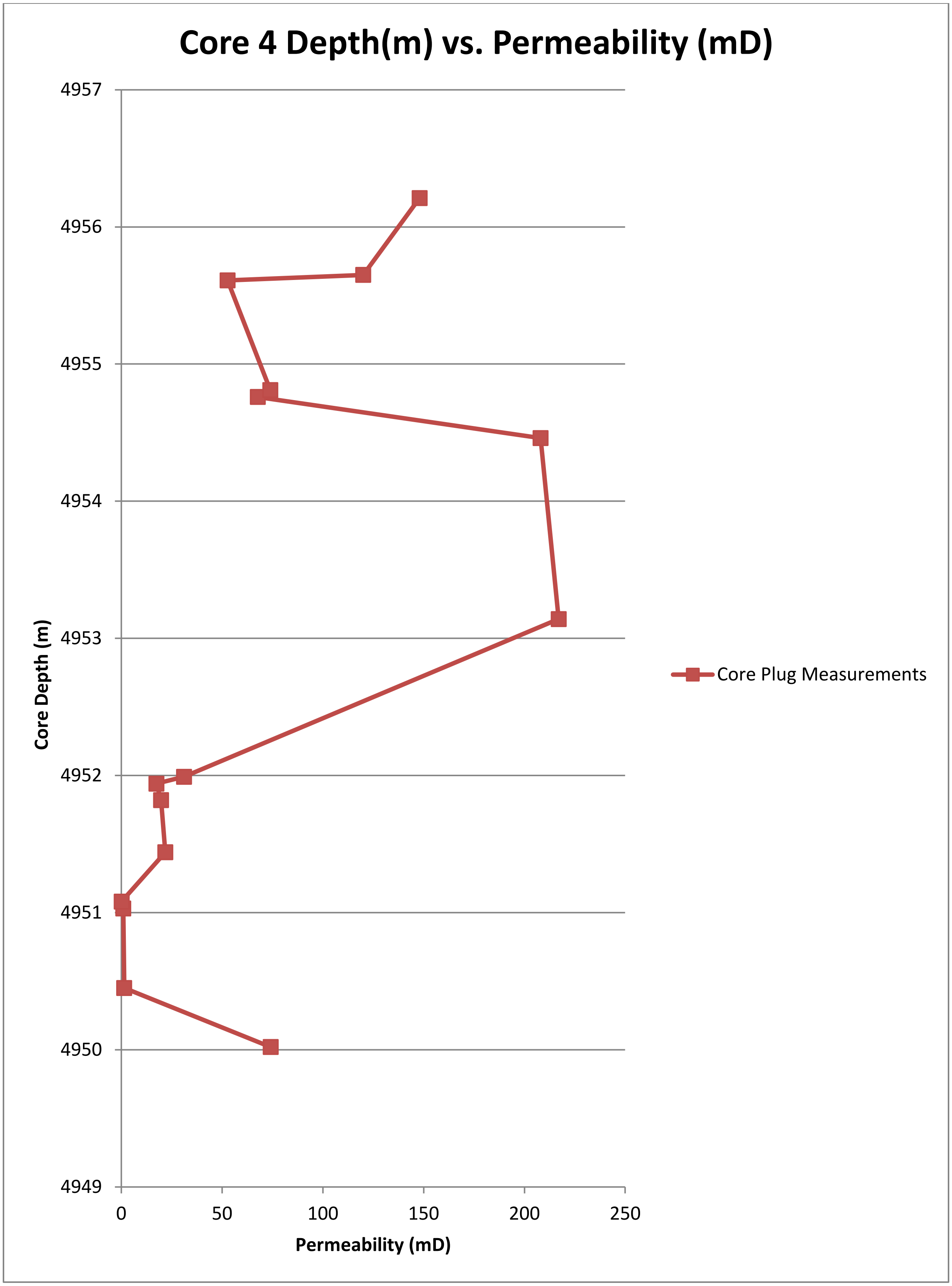

Figure 5.5. Core 4 depth (m) vs. core plug permeability (mD).

5.2 Porosity in Venture B-13

Porosity in Venture B-13 Cores was measured by Core Laboratories-Canada Limited (File reference #7004-81-13) from core plugs and 42 data points were made available.

In a laboratory setting, samples are cleaned and dried to remove drilling fluid. Porosity is measured by applying Boyle's Law: $P_1V_1/T_1=P_2V_2/T_2$. If the temperature remains the same within a closed system, then absolute pressure and volume of confined gas are inversely proportional (Doyle, 2006). In this situation, T remains constant and can be removed from the equation: $P_1V_1 =P_2V_2$. Since a known volume of helium (V_1) is injected at a known pressure (P_1), a resulting pressure may be found and V_2 can be solved (Doyle, 2006). This V_2 value is representative of the grain volume. Once the bulk volume is measured, these two values are subtracted from one another to define pore volumes (Doyle, 2006).

Porosity and depth are plotted in order to observe potential trends. A general increase in porosity is observed with depth for two cores, Core 1 and Core 2,that extend over a 6.0 and 14 m interval respectively. Although porosity loss is expected with increasing depths as a result of compaction, increased burial depth may allow for silicate minerals to dissolve and for organic material to decompose, thereby increasing empty pore space (Boggs, 2006).

Each lithofacies was assigned average porosity values based on core plug measurements. Since lithofacies 4 has the highest number of measured points, it has the most reliable average porosity value. For similar reasons, lithofacies 3 has the least reliable average porosity measurement. Histogram plots of porosity values of Venture B-13 cores are presented in Chapter 2.

Lithofacies	Average porosity measurement from core plugs	Porosity range (core plugs)	Amount of values (#)
1	0.04825	0.039-0.067	4
2	0.1092	0.062-0.067	3
3	0.1720	0.1720	1
4	0.1912	0.039-0.261	28

Table 5.4. Average porosity measurements from core plugs for each lithofacies and the number of values that have been averaged. Note that the majority of the porosity measurements represent lithofacies 4. In contrast, there is only 1 data value for lithofacies 3.

These lithofacies show different porosity values as some sections of the core have undergone increased dissolution during diagenesis. Porosity values increase from lithofacies 1 to 4. Since lithofacies 4 cross-stratified micaceous sands have the highest porosity values, these also have the best reservoir quality. Thin section analysis supports these high porosity values since high amounts of dissolution and low amounts of cementation (10-18%) features were noted. The low porosity values of lithofacies 1 are interpreted to be a result of pore spaces being filled with up to 35% calcite cement and dissolution features are observed from thin sections.

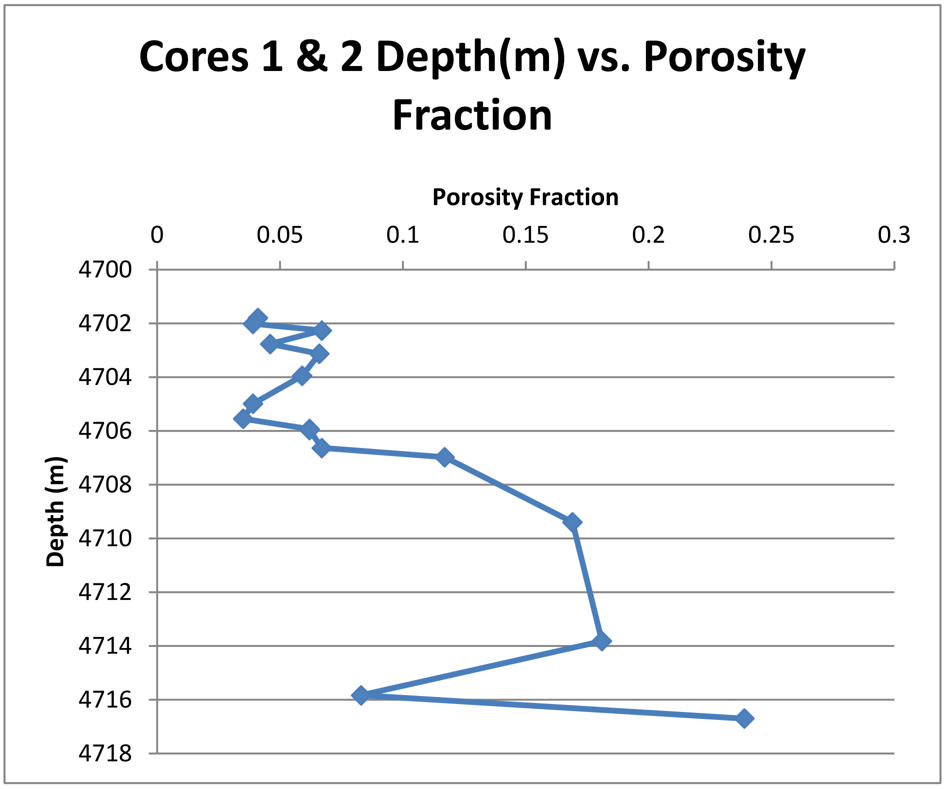

Figure 5.6. Porosity fraction of cores 1&2 plotted against depth of well (m) showing a general increase in porosity with depth.

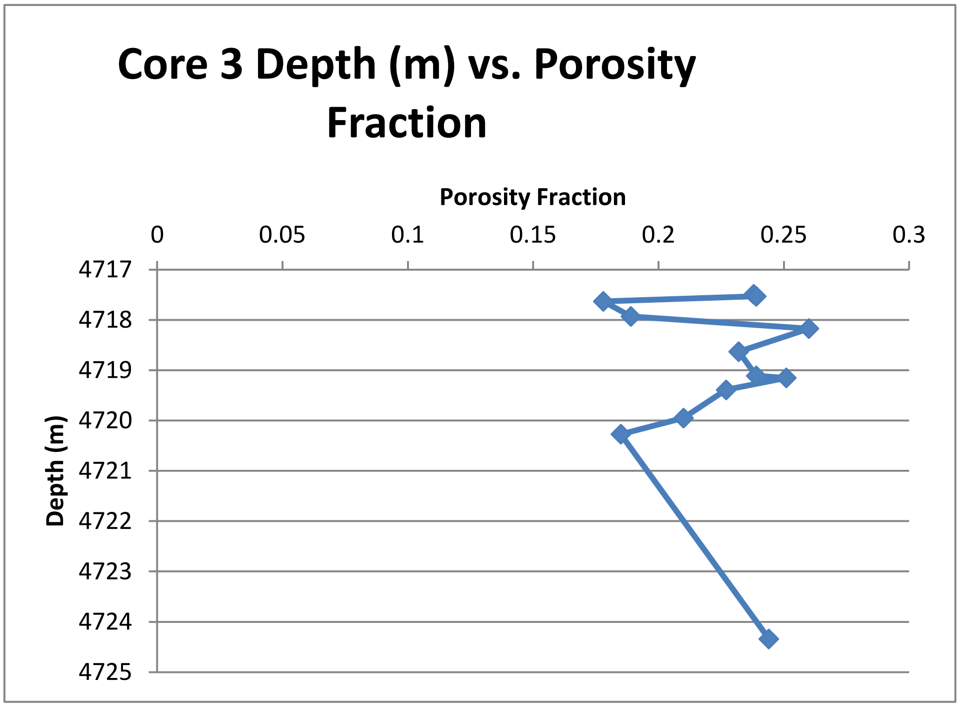

Figure 5.7. Core 3 porosity fraction plotted against depth (m). A cluster of porosity values in the 23-26% porosity range observed.

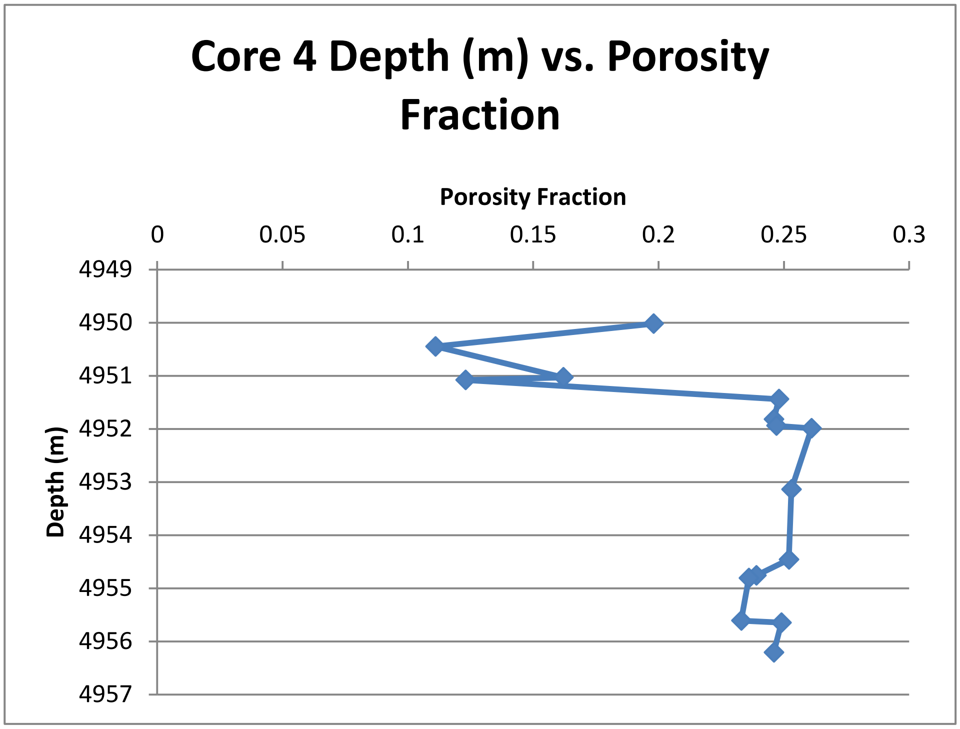

Figure 5.8. Core 4 porosity fraction plotted against depth (m) generally with higher porosity values at increased depths.

5.3 Porosity vs. Permeability

Porosity fractions are plotted against core plug permeability values and a graph with a relatively high R^2 value (0.8248) was created. Proximity of R^2 to a value of 1 indicates a linear trend. Lithofacies are assigned different colours on this graph. Four natural groups/clusters of samples are represented in this diagram: a) A group with about 4-7% porosity and values of about 0.006-0.024 mD associated with lithofacies 1; b) A group with porosity of approximately 6% and permeability of 0.1-0.16 mD associated with lithofacies 2; c) A group with porosity of 11-18% and permeability 0.15-1.4 mD associated with shallower depths of lithofacies 4; d) A group with porosity of 17.8-26% and permeability 9.66-348mD associated with increased depth of lithofacies 4.

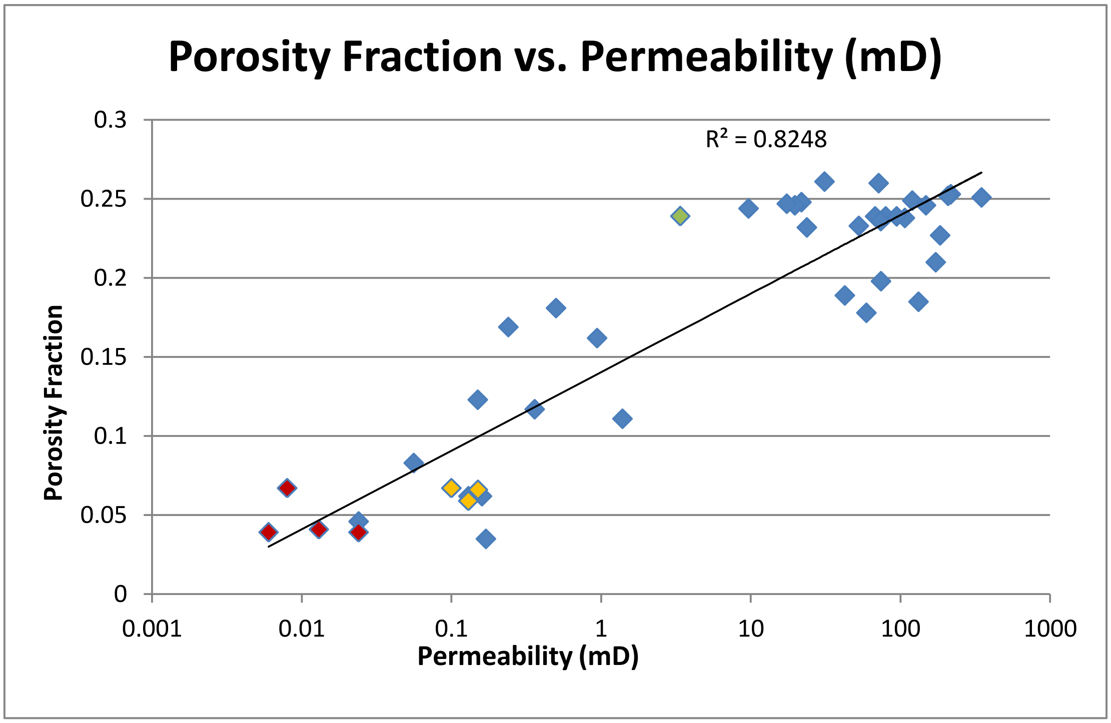

🟥 Lithofacies 1
🟧 Lithofacies 2
🟩 Lithofacies 3
🟦 Lithofacies 4

Figure 5.9. Porosity fraction versus permeability (mD) through Venture B-13. Lithofacies 1 through 4 are assigned specific colours so as to identify clusters.

Chapter 6

6.1 Results

6.1.1 Flow units

A flow unit is a measure of permeability and porosity within a volume of rock, in comparison to strata above or below (Schlumberger, 2013). The identification of lithofacies and analysis of permeability from conventional cores demonstrate that flow units are present at various scales. Properties affecting flow units include grain size, permeability, bioturbation index, cementation, clay content, and mineralogical change. The qualitative assessment of these properties are used to differentiate and characterize the flow units within the cored reservoirs (Chapter 2). They are quantified and the results presented in the following two sets of tables.

The first set of tables, “Potential Differences in Flow Units” (Tables 6.1-6.4), analyses the probability of change in flow units from one depth to another. Numbers in the “relative ranking of flow units” column represent how likely the unit is different from overlaying and underlying strata. Since individual criteria are assigned a number out of 8 and these are all added to give a number indicative of probability of change, values in this column are out of a potential 48 points. The higher the value, the greater the likelihood of change in flow units. Where low values follow one another (3,4,1…), these potentially represent a single flow unit. These are grouped and a blue box is put around them. It is important to note that this section does not quantify the ability to flow within a unit. Low numbers do not indicate a poor flow unit and high numbers do not indicate good flow units.

The second set of tables, “Flow Unit Strength: Influence on Preferential Flow” (Tables 6.5-6.8), compares average core plug permeability values of lithofacies to the sum of assigned values for grain size, clay content, porosity, bioturbation and cementation. A higher sum of values indicates better flow units, whereas a lower sum of values indicates poor flow units. These tables identify flow unit strength.

These values were compared to the assigned permeability to determine if methodology was valid and accurate.

Tables Ranking Potential Differences in Flow Units

Core 1 17.1 m	Depth (m)		Lithology	Grain Size	Permeability	Porosity	Cementation	Bioturbation	Rel. Ranking of flow unit out of 48
	Top	Bottom							
	4709.1	4709	0	1	0	0	1	2	4
	4709	4708.8	0	3	1	0	2	1	7
	4708.8	4708.45	2	4	4	2	5	2	19
	4708.45	4708.23	4	3	8	4	8	0	27
	4708.23	4707.18	2	1	4	2	5	0	14
	4707.18	4706.88	2	1	4	2	5	2	16
	4706.88	4706.23	4	3	8	4	8	2	29
	4706.23	4705.63	4	3	8	2	5	3	25
	4705.63	4704.96	4	3	8	4	8	3	30
	4704.96	4704.91	2	4	4	2	5	2	19
	4704.91	4701.39	2	6	4	2	5	0	19
	4701.39	4700.44	4	6	5	3	8	0	26
	4700.44	4695.94	4	3	1	4	8	1	21
	4695.94	4694.21	4	4	2	4	8	1	23
	4694.213	4693.61	4	1	1	2	4	0	12

Table 6.1. Ranking potential differences in flow units in core 1.

Core 2 5.8 m	Depth (m)		Lithology	Grain Size	Permeability	Porosity	Cementation	Bioturbation	Rel. Ranking of flow unit out of 48
	Top	Bottom							
	4716.2	4716.05	4	1	4	1	2	**0**	12
	4716.05	4714.79	2	2	4	1	2	0	11
	4714.79	4714.45	0	2	0	0	1	1	4
	4714.45	4713.13	2	2	4	4	2	2	16
	4713.13	4712.69	4	2	8	8	4	1	27
	4712.69	4712.36	2	1	4	4	2	1	14
	4712.36	4712.27	4	1	4	4	1	1	15
	4712.27	4712.01	4	3	8	8	2	3	28
	4712.01	4711.81	4	4	8	8	2	1	27
	4711.81	4711.5	4	4	6	8	2	0	24
	4711.5	4711.16	4	2	2	8	1	0	17

Table 6.2. Ranking potential differences in flow units in core 2.

Core 3 18.3	Depth (m)		Lithology	Grain Size	Permeability	Porosity	Cementation	Bioturbation	Rel. Ranking of flow unit out of 48
	Top	Bottom							
	4732.5	4732.21	4	2	2	3	4	1	16
	4732.21	4731.92	4	4	4	6	8	1	27
	4731.92	4731.62	4	4	4	6	8	0	26
	4731.62	4731.15	4	5	4	6	8	2	29
	4731.15	4731.04	4	4	4	6	8	3	29
	4731.04	4729.62	4	2	4	6	8	3	27
	4729.62	4729.34	4	4	4	6	8	3	29
	4729.34	4728.17	4	4	6	6	8	3	31
	4728.17	4724.82	2	1	4	2	8	3	20
	4724.82	4721.418	0	1	0	0	1	2	4
	4721.418	4720.338	2	5	0	0	0	2	9
	4720.338	4719.728	4	3	4	2	4	0	17
	4719.728	4719.658	2	5	8	4	8	0	27
	4719.658	4718.448	0	3	4	2	4	0	13
	4718.448	4717.078	2	2	0	0	0	0	4
	4717.078	4716.359	2	3	4	2	4	0	15
	4716.359	4716.2	4	2	4	2	4	0	16

Table 6.3. Ranking potential differences in flow units in core 3.

Core 4 16.1	**Depth (m)**		**Lithology**	**Grain Size**	**Permeability**	**Porosity**	**Cementation**	**Bioturbation**	**Rel. Ranking of flow unit out of 48**
	Top	**Bottom**							
	4965.1	4964.35	4	1	4	2	4	2	15
	4964.35	4964.19	4	3	4	5	8	1	20
	4964.19	4963.13	4	6	5	4	5	1	21
	4963.13	4962.85	4	6	7	4	2	1	20
	4962.85	4962.176	2	6	4	2	2	1	15
	4962.176	4961.636	0	3	0	1	0	1	4
	4961.636	4960.56	0	0	0	1	0	1	1
	4960.56	4960.16	0	0	0	1	0	0	0
	4960.16	4959.76	0	0	0	1	0	0	0
	4959.76	4958.93	4	0	4	1	1	0	9
	4958.93	4955.2	4	1	7	2	2	1	15
	4955.2	4955	0	2	7	2	2	1	12
	4955	4951.625	0	3	6	2	3	0	12
	4951.62	4950.594	2	2	6	2	3	1	14
	4950.594	4949.0	2	1	4	2	2	1	10

Table 6.4. Ranking potential differences in flow units in core 4.

6.1.2 Flow Unit Strength: Influence on Preferential Flow

The strength of flow units is calculated in the following section as explained in section 2.3.2 of this thesis. Values assigned for ‘permeability’ and ‘ability to flow within unit’ are highlighted in red as they are compared to one another to see if the methodology applied was accurate. High values for permeability should have high flow unit strengths.

Core 1 17.1 m	Depth (m)		Permeability	Grain Size	Clay Content	Porosity	Bioturbation	Cementation	Ability to flow within unit out of 20
	Top	Bottom							
	4709.1	4709	76.13	1	4	3	2	4	14
	4709	4708.8	76.13	2	4	3	4	4	18
	4708.8	4708.45	76.13	3	4	3	3	4	18
	4708.45	4708.23	1.9	0	0	1	1	0	2
	4708.23	4707.18	76.13	1	4	3	1	4	13
	4707.18	4706.88	76.13	1	4	3	3	4	15
	4706.88	4706.23	0.1-1.9	0	0	1	1	0	2
	4706.23	4705.63	76.13	0	4	3	4	4	15
	4705.63	4704.96	1.9	2	0	1	1	0	4
	4704.96	4704.91	76.13	2	4	3	4	4	17
	4704.91	4701.39	76.13	2	4	3	2	4	15
	4701.39	4700.44	1.9	0	0	1	2	0	3
	4700.44	4695.94	0.0127	1	4	0	2	3	10
	4695.94	4694.21	1.9	0	4	1	1	0	6
	4694.213	4693.61	0.01275	2	0	0	0	3	5

Table 6.5. Flow Unit strength through Core 1

Core 2 5.8 m	Depth (m)		Permeability	Grain Size	Clay Content	Porosity	Bioturbation	Cementation	Ability to flow within unit out of 20
	Top	Bottom							
	4716.2	4716.05	3.38	1	3	3	4	3	14
	4716.05	4714.79	0.056- 76.13	1	4	3	4	4	16
	4714.79	4714.45	76.13	1	4	3	3	4	15
	4714.45	4713.13	0.5- 76.13	1	4	3	1	4	13
	4713.13	4712.69	0.01275	2	4	3	2	3	14
	4712.69	4712.36	76.13	1	4	3	1	4	13
	4712.36	4712.27	76.13	1	4	3	4	4	16
	4712.27	4712.01	0.01275	2	4	3	3	3	15
	4712.01	4711.81	76.13	2	4	3	4	4	17
	4711.81	4711.5	0.01275	2	4	3	4	3	16
	4711.5	4711.16	76.13	1	4	3	4	4	16

Table 6.6. Flow Unit strength through Core 2

Core 3 18.3m	Depth (m)		Permeability	Grain Size	Clay Content	Porosity	Bioturbation	Cementation	Ability to flow within unit out of 20
	Top	Bottom							
	4732.5	4732.21	3.38	1	3	3	3	3	13
	4732.21	4731.92	1.9	0	0	1	4	0	5
	4731.92	4731.62	3.38	2	3	3	3	3	14
	4731.62	4731.15	1.9	1	0	1	3	0	5
	4731.15	4731.04	3.38	1	3	3	1	3	11
	4731.04	4729.62	1.9	0	0	3	4	0	7
	4729.62	4729.34	3.38	2	3	1	1	3	10
	4729.34	4728.17	1.9	1	0	3	4	0	8
	4728.17	4724.82	76.13	3	4	3	1	4	16
	4724.82	4721.41	9.66-76.13	2	4	3	4	4	17
	4721.41	4720.33	76.13	3	4	3	2	4	16
	4720.33	4719.72	172	0	4	3	4	4	15
	4719.72	4719.65	1.9	3	0	1	4	0	8
	4719.65	4718.44	348	3	4	3	4	4	18
	4718.44	4717.07	79.7	1	4	3	4	4	16
	4717.07	4716.35	107	1	4	3	4	4	16
	4716.35	4716.2	0.0127	0	0	1	4	0	5

Table 6.7. Flow Unit strength through Core 3

Core 4 16.1	Depth (m)		Permeability	Grain Size	Clay Content	Porosity	Bioturbation	Cementation	Ability to flow within unit out of 20
	Top	Bottom							
	4965.1	4964.35	76	1	4	4	4	4	16
	4964.35	4964.19	1.9	0	0	2	2	0	3
	4964.19	4963.13	50	2	3	4	3	3	14
	4963.13	4962.85	76	2	4	4	4	4	17
	4962.85	4962.176	3.38	1	3	4	3	3	13
	4962.176	4961.636	3.38	1	3	4	4	3	14
	4961.636	4960.56	3.38	1	3	4	3	3	13
	4960.56	4960.16	3.38	2	3	4	4	3	15
	4960.16	4959.76	3.38	1	3	4	4	3	14
	4959.76	4958.93	50	2	3	4	4	3	15
	4958.93	4955.2	52.7-120	2	4	4	3	4	16
	4955.2	4955	3.3	1	3	4	4	3	14
	4955	4951.625	50-67.7	2	3	4	3	3	14
	4951.62	4950.594	50	1	3	4	3	3	13
	4950.594	4949.0	74.1	0	4	4	4	4	15

Table 6.8. Flow Unit strength through Core 4

Core descriptions assist in providing a visual representation of the variation of flow units strength (FUS) with depth. They also give information on bed thickness, sedimentary structures, bioturbation index, trace fossils and ichnofacies. Flow unit strengths were assigned values out of 20 (Tables 32, 33, 34, 35). Each number, from 1 to 20 was then given a specific colour and represented on the core description sheet.

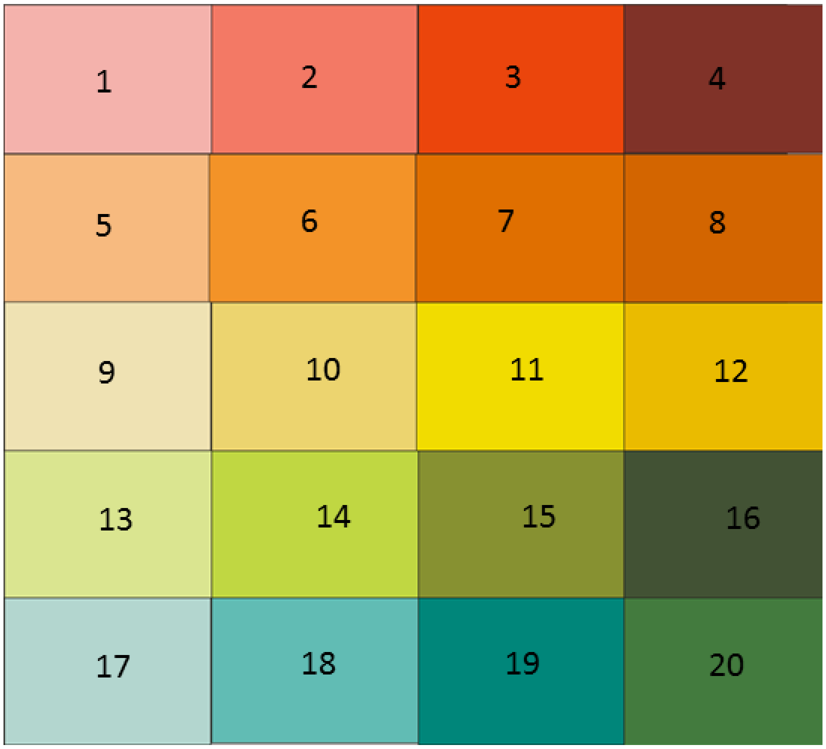

1	2	3	4
5	6	7	8
9	10	11	12
13	14	15	16
17	18	19	20

Figure 6.1. Colors assigned to flow unit strength values. : 1=highest / best, 20=lowest / worst.

Legend

sharp	Contact between beds
≡	Parallel shale laminae
●	Calcite nodules
	Symmetrical ripples
	Wavey laminae
Massive	

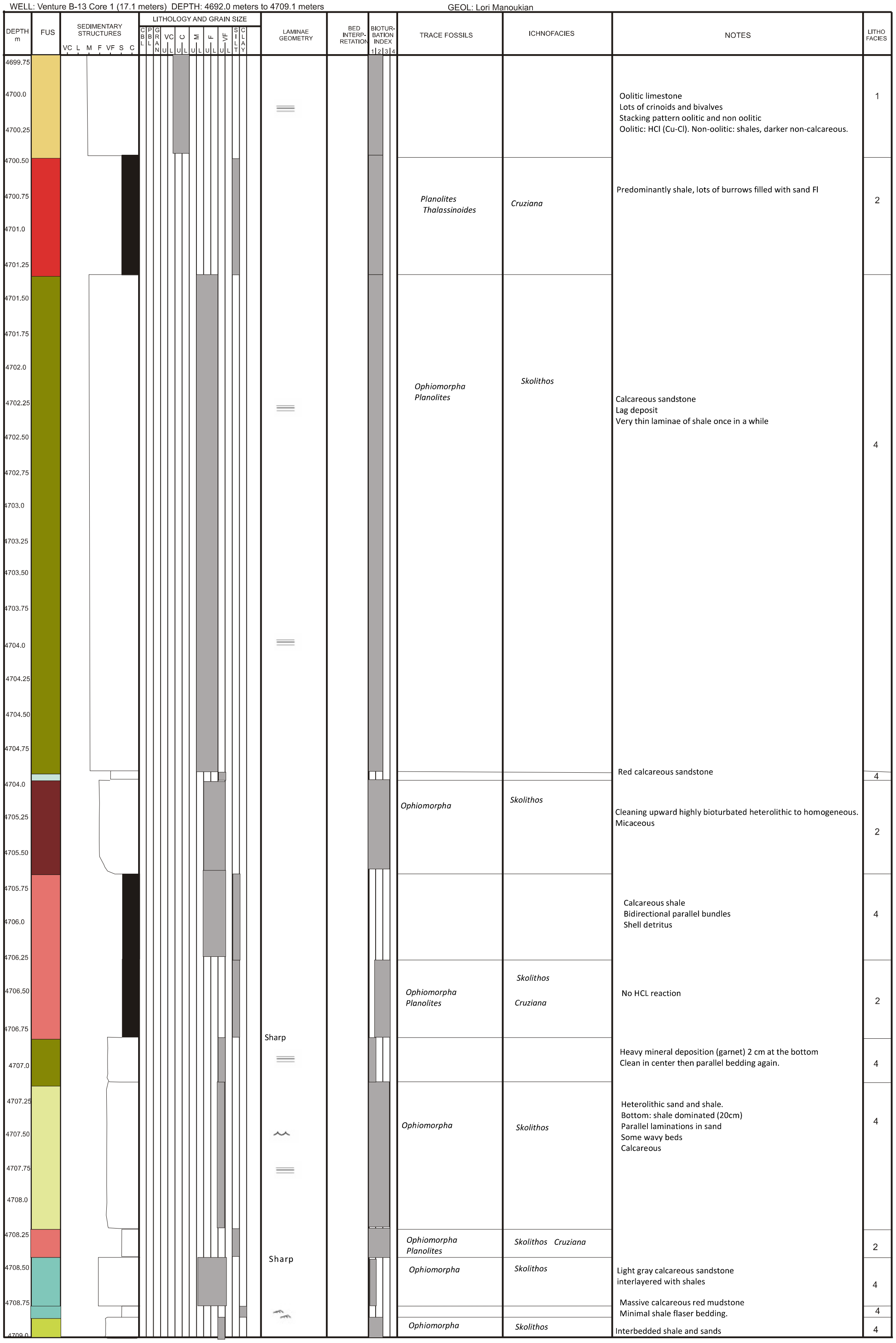
WELL: Venture B-13 Core 1 (17.1 meters) DEPTH: 4692.0 meters to 4709.1 meters
GEOL: Lori Manoukian
DEPTH m
FUS
SEDIMENTARY STRUCTURES
VC L M F VF S C
LITHOLOGY AND GRAIN SIZE
CBL PBL GRAN VC C M F VF SILT CLAY
U L U L U L U L U L
LAMINAE GEOMETRY
BED INTERP-RETATION
BIOTUR-BATION INDEX
1 2 3 4
TRACE FOSSILS
ICHNOFACIES
NOTES
LITHO FACIES
4699.75
4700.0
4700.25
4700.50
4700.75
4701.0
4701.25
4701.50
4701.75
4702.0
4702.25
4702.50
4702.75
4703.0
4703.25
4703.50
4703.75
4704.0
4704.25
4704.50
4704.75
4704.0
4705.25
4705.50
4705.75
4706.0
4706.25
4706.50
4706.75
4707.0
4707.25
4707.50
4707.75
4708.0
4708.25
4708.50
4708.75
4709.0
Planolites
Thalassinoides
Cruziana
Ophiomorpha
Planolites
Skolithos
Ophiomorpha
Skolithos
Skolithos
Ophiomorpha
Planolites
Cruziana
Sharp
Ophiomorpha
Skolithos
Ophiomorpha
Planolites
Skolithos Cruziana
Sharp
Ophiomorpha
Skolithos
Ophiomorpha
Skolithos
1
2
4
4
2
4
2
4
4
2
4
4
4

Oolitic limestone
Lots of crinoids and bivalves
Stacking pattern oolitic and non oolitic
Oolitic: HCl (Cu-Cl). Non-oolitic: shales, darker non-calcareous.

Predominantly shale, lots of burrows filled with sand Fl

Calcareous sandstone
Lag deposit
Very thin laminae of shale once in a while

Red calcareous sandstone

Cleaning upward highly bioturbated heterolithic to homogeneous.
Micaceous

Calcareous shale
Bidirectional parallel bundles
Shell detritus

No HCL reaction

Heavy mineral deposition (garnet) 2 cm at the bottom
Clean in center then parallel bedding again.

Heterolithic sand and shale.
Bottom: shale dominated (20cm)
Parallel laminations in sand
Some wavy beds
Calcareous

Light gray calcareous sandstone
interlayered with shales

Massive calcareous red mudstone
Minimal shale flaser bedding.

Interbedded shale and sands

Figure 6.2. Core 1 description sheet

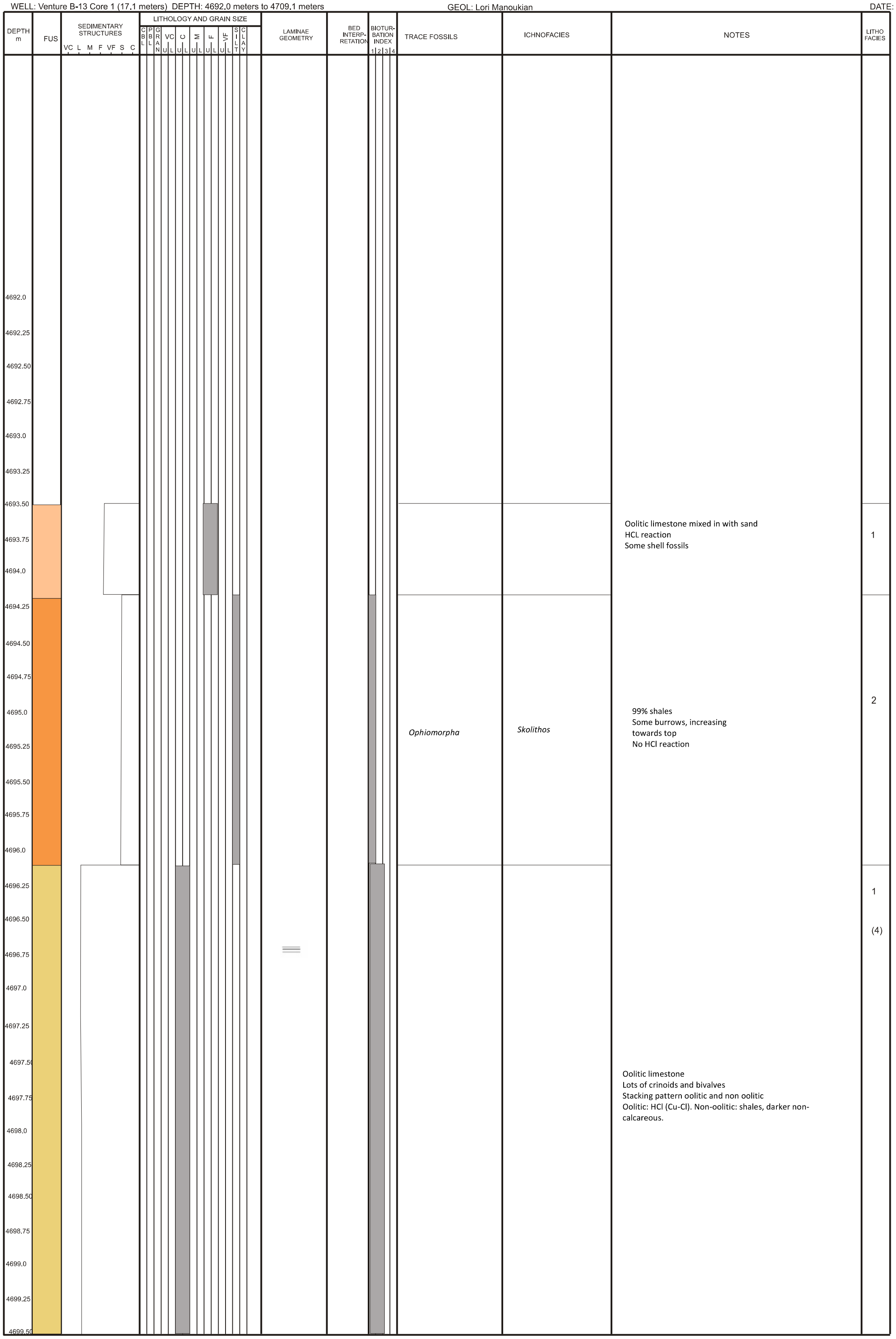

Oolitic limestone mixed in with sand
HCL reaction
Some shell fossils

99% shales
Some burrows, increasing towards top
No HCl reaction

Oolitic limestone
Lots of crinoids and bivalves
Stacking pattern oolitic and non oolitic
Oolitic: HCl (Cu-Cl). Non-oolitic: shales, darker non-calcareous.

Figure 6.2. Core 1 description sheet
]

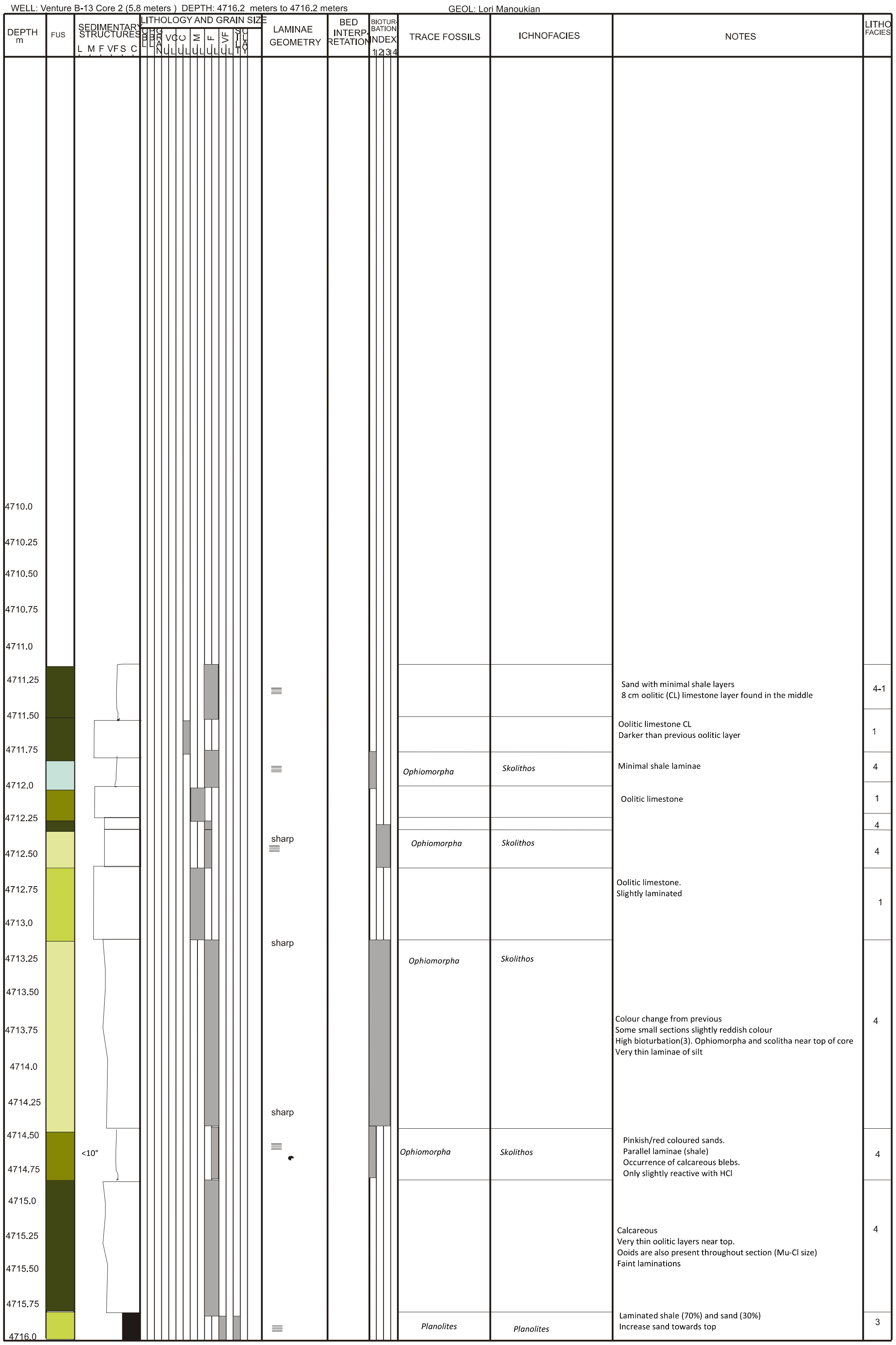
WELL: Venture B-13 Core 2 (5.8 meters) DEPTH: 4716.2 meters to 4716.2 meters
GEOL: Lori Manoukian
DEPTH m
FUS
SEDIMENTARY STRUCTURES
L M F VF S C
LITHOLOGY AND GRAIN SIZE
VC C M F VF
U L U L U L U L U L
SILT
CLAY
LAMINAE GEOMETRY
BED INTERPRETATION
BIOTURBATION INDEX
1 2 3 4
TRACE FOSSILS
ICHNOFACIES
NOTES
LITHO FACIES
4710.0
4710.25
4710.50
4710.75
4711.0
4711.25
4711.50
4711.75
4712.0
4712.25
4712.50
4712.75
4713.0
4713.25
4713.50
4713.75
4714.0
4714.25
4714.50
4714.75
4715.0
4715.25
4715.50
4715.75
4716.0
sharp
sharp
sharp
<10°
Ophiomorpha
Skolithos
Ophiomorpha
Skolithos
Ophiomorpha
Skolithos
Ophiomorpha
Skolithos
Planolites
Planolites
Sand with minimal shale layers
8 cm oolitic (CL) limestone layer found in the middle
4-1
Oolitic limestone CL
Darker than previous oolitic layer
1
Minimal shale laminae
4
Oolitic limestone
1
4
4
Oolitic limestone.
Slightly laminated
1
Colour change from previous
Some small sections slightly reddish colour
High bioturbation(3). Ophiomorpha and scolitha near top of core
Very thin laminae of silt
4
Pinkish/red coloured sands.
Parallel laminae (shale)
Occurrence of calcareous blebs.
Only slightly reactive with HCl
4
Calcareous
Very thin oolitic layers near top.
Ooids are also present throughout section (Mu-Cl size)
Faint laminations
4
Laminated shale (70%) and sand (30%)
Increase sand towards top
3

Figure 6.3. Core 2 description sheet

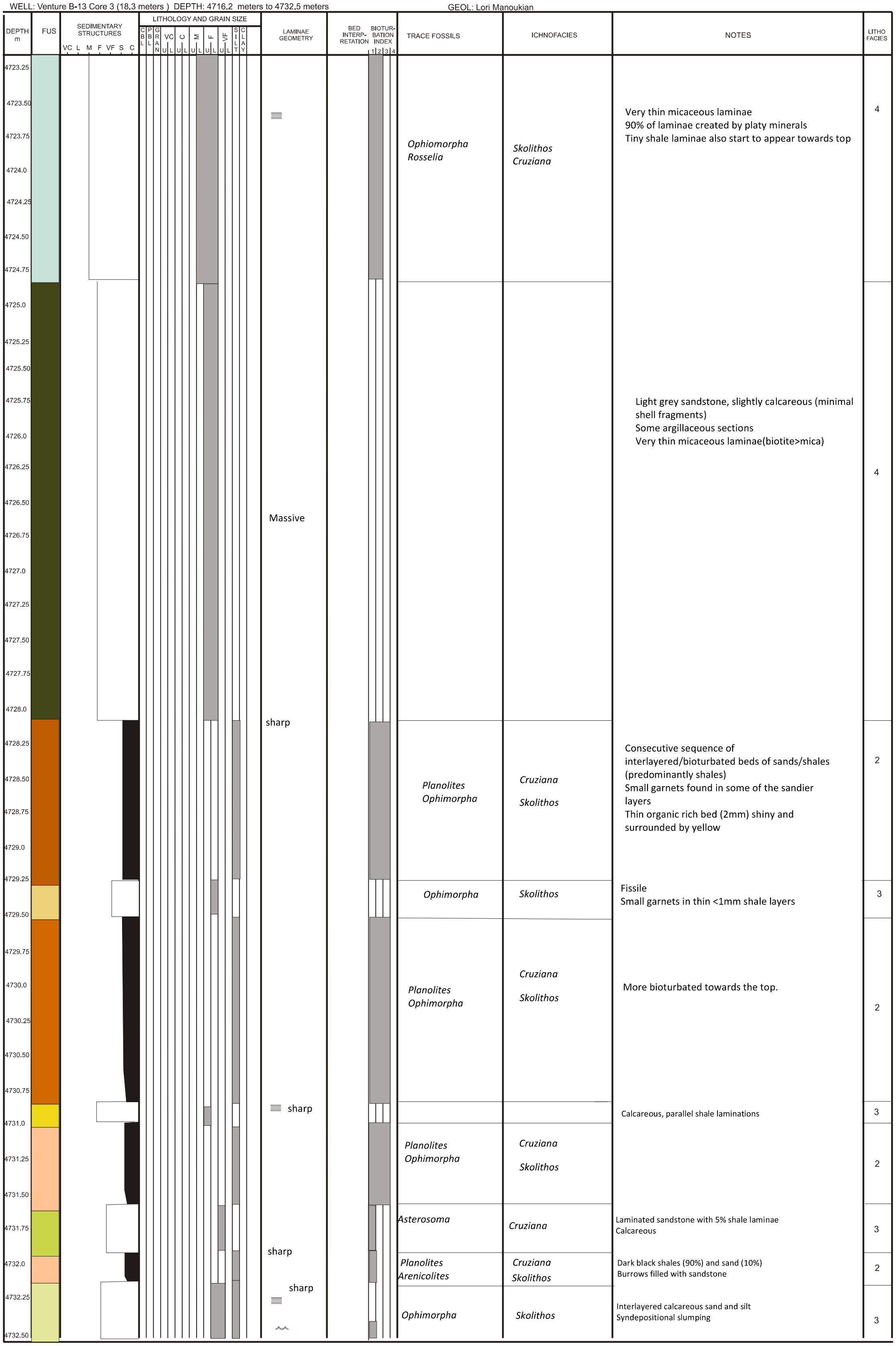
WELL: Venture B-13 Core 3 (18.3 meters) DEPTH: 4716.2 meters to 4732.5 meters
GEOL: Lori Manoukian
DEPTH m
FUS
SEDIMENTARY STRUCTURES
VC L M F VF S C
LITHOLOGY AND GRAIN SIZE
CBL
PBL
GRAN
VC
C
M
F
VF
SILT
CLAY
U L
LAMINAE GEOMETRY
BED INTERP-RETATION
BIOTUR-BATION INDEX
1 2 3 4
TRACE FOSSILS
ICHNOFACIES
NOTES
LITHO FACIES
4723.25
4723.50
4723.75
4724.0
4724.25
4724.50
4724.75
4725.0
4725.25
4725.50
4725.75
4726.0
4726.25
4726.50
4726.75
4727.0
4727.25
4727.50
4727.75
4728.0
4728.25
4728.50
4728.75
4729.0
4729.25
4729.50
4729.75
4730.0
4730.25
4730.50
4730.75
4731.0
4731.25
4731.50
4731.75
4732.0
4732.25
4732.50
Massive
sharp
sharp
sharp
sharp
Ophiomorpha
Rosselia
Skolithos
Cruziana
4
4
Planolites
Ophimorpha
Cruziana
Skolithos
2
Ophimorpha
Skolithos
3
Planolites
Ophimorpha
Cruziana
Skolithos
2
3
Planolites
Ophimorpha
Cruziana
Skolithos
2
Asterosoma
Cruziana
3
Planolites
Arenicolites
Cruziana
Skolithos
2
Ophimorpha
Skolithos
3

Very thin micaceous laminae
90% of laminae created by platy minerals
Tiny shale laminae also start to appear towards top

Light grey sandstone, slightly calcareous (minimal shell fragments)
Some argillaceous sections
Very thin micaceous laminae(biotite>mica)

Consecutive sequence of interlayered/bioturbated beds of sands/shales (predominantly shales)
Small garnets found in some of the sandier layers
Thin organic rich bed (2mm) shiny and surrounded by yellow

Fissile
Small garnets in thin <1mm shale layers

More bioturbated towards the top.

Calcareous, parallel shale laminations

Laminated sandstone with 5% shale laminae
Calcareous

Dark black shales (90%) and sand (10%)
Burrows filled with sandstone

Interlayered calcareous sand and silt
Syndepositional slumping

Figure 6.4. Core 3 description sheet

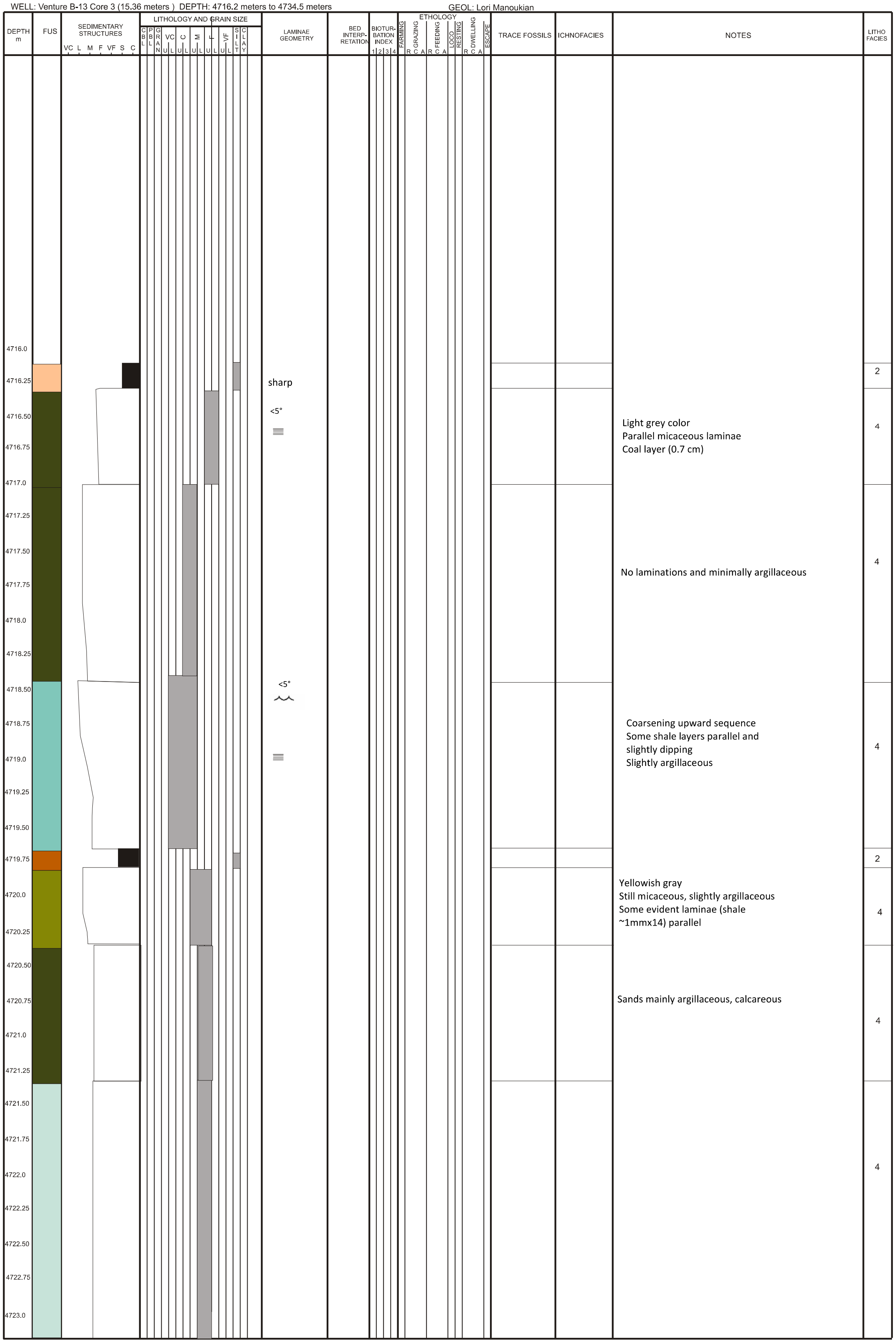
WELL: Venture B-13 Core 3 (15.36 meters) DEPTH: 4716.2 meters to 4734.5 meters
GEOL: Lori Manoukian
DEPTH m
FUS
SEDIMENTARY STRUCTURES
VC L M F VF S C
LITHOLOGY AND GRAIN SIZE
CBL
PBL
GRAN
VC
C
M
F
VF
SILT
CLAY
U L
LAMINAE GEOMETRY
BED INTERP-RETATION
BIOTUR-BATION INDEX
1 2 3 4
ETHOLOGY
FARMING
GRAZING
FEEDING
LOCO RESTING
DWELLING
ESCAPE
R C A
TRACE FOSSILS
ICHNOFACIES
NOTES
LITHO FACIES
4716.0
4716.25
4716.50
4716.75
4717.0
4717.25
4717.50
4717.75
4718.0
4718.25
4718.50
4718.75
4719.0
4719.25
4719.50
4719.75
4720.0
4720.25
4720.50
4720.75
4721.0
4721.25
4721.50
4721.75
4722.0
4722.25
4722.50
4722.75
4723.0
sharp
<5°
<5°
2
4
4
4
2
4
4
4

Light grey color
Parallel micaceous laminae
Coal layer (0.7 cm)

No laminations and minimally argillaceous

Coarsening upward sequence
Some shale layers parallel and
slightly dipping
Slightly argillaceous

Yellowish gray
Still micaceous, slightly argillaceous
Some evident laminae (shale
~1mmx14) parallel

Sands mainly argillaceous, calcareous

Figure 6.4. Core 3 description sheet

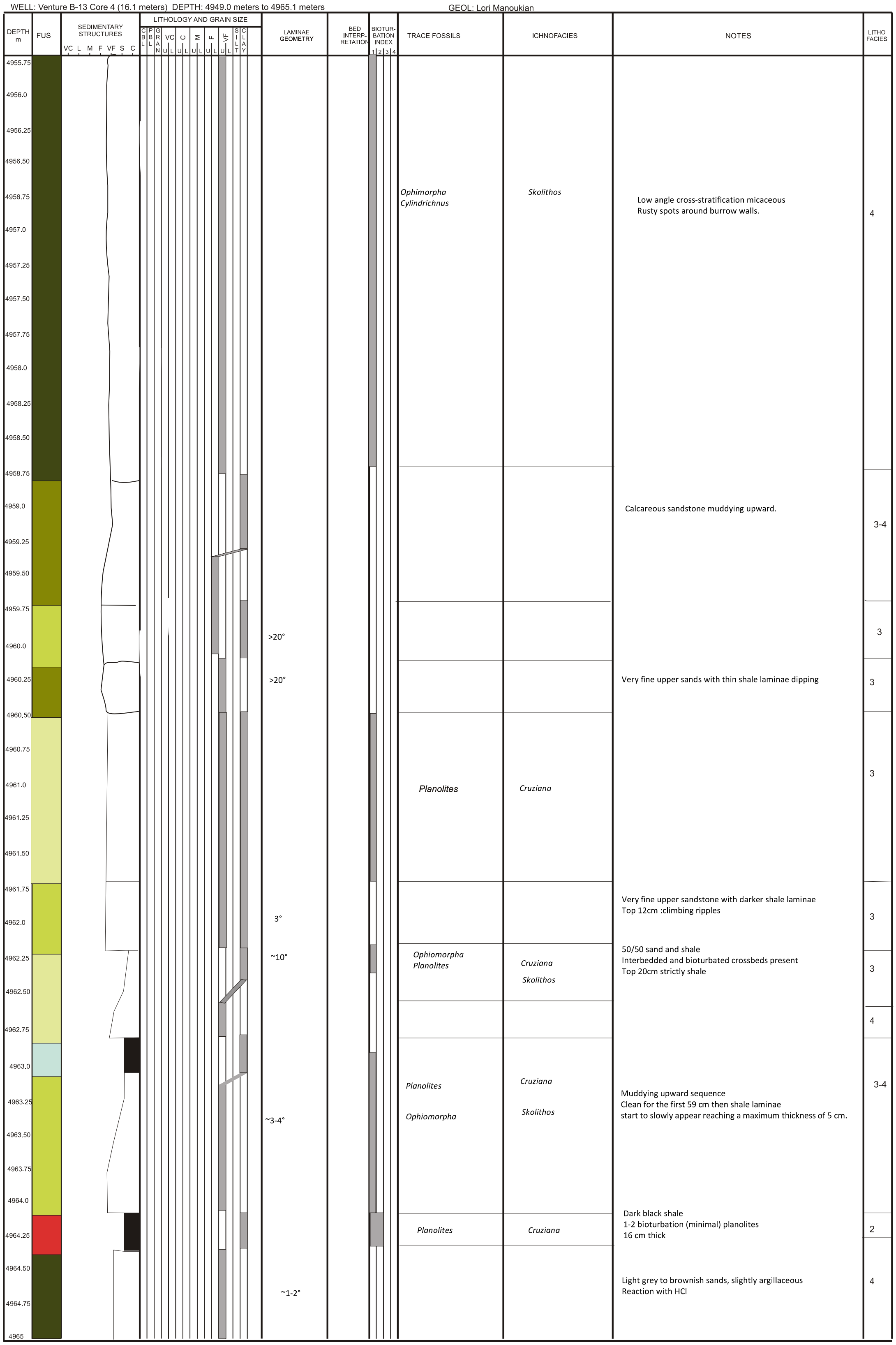
WELL: Venture B-13 Core 4 (16.1 meters) DEPTH: 4949.0 meters to 4965.1 meters
GEOL: Lori Manoukian
DEPTH m
FUS
SEDIMENTARY STRUCTURES
VC L M F VF S C
LITHOLOGY AND GRAIN SIZE
CBL PBL GRAN VC C M F VF SILT CLAY
U L U L U L U L U L
LAMINAE GEOMETRY
BED INTERP-RETATION
BIOTUR-BATION INDEX
1 2 3 4
TRACE FOSSILS
ICHNOFACIES
NOTES
LITHO FACIES
4955.75
4956.0
4956.25
4956.50
4956.75
4957.0
4957.25
4957.50
4957.75
4958.0
4958.25
4958.50
4958.75
4959.0
4959.25
4959.50
4959.75
4960.0
4960.25
4960.50
4960.75
4961.0
4961.25
4961.50
4961.75
4962.0
4962.25
4962.50
4962.75
4963.0
4963.25
4963.50
4963.75
4964.0
4964.25
4964.50
4964.75
4965
>20°
>20°
3°
~10°
~3-4°
~1-2°
Ophimorpha
Cylindrichnus
Skolithos
4
3-4
3
3
Planolites
Cruziana
3
3
Ophiomorpha
Planolites
Cruziana
Skolithos
3
4
Planolites
Ophiomorpha
Cruziana
Skolithos
3-4
Planolites
Cruziana
2
4

Low angle cross-stratification micaceous
Rusty spots around burrow walls.

Calcareous sandstone muddying upward.

Very fine upper sands with thin shale laminae dipping

Very fine upper sandstone with darker shale laminae
Top 12cm :climbing ripples

50/50 sand and shale
Interbedded and bioturbated crossbeds present
Top 20cm strictly shale

Muddying upward sequence
Clean for the first 59 cm then shale laminae
start to slowly appear reaching a maximum thickness of 5 cm.

Dark black shale
1-2 bioturbation (minimal) planolites
16 cm thick

Light grey to brownish sands, slightly argillaceous
Reaction with HCl

Figure 6.5. Core 4 description sheet

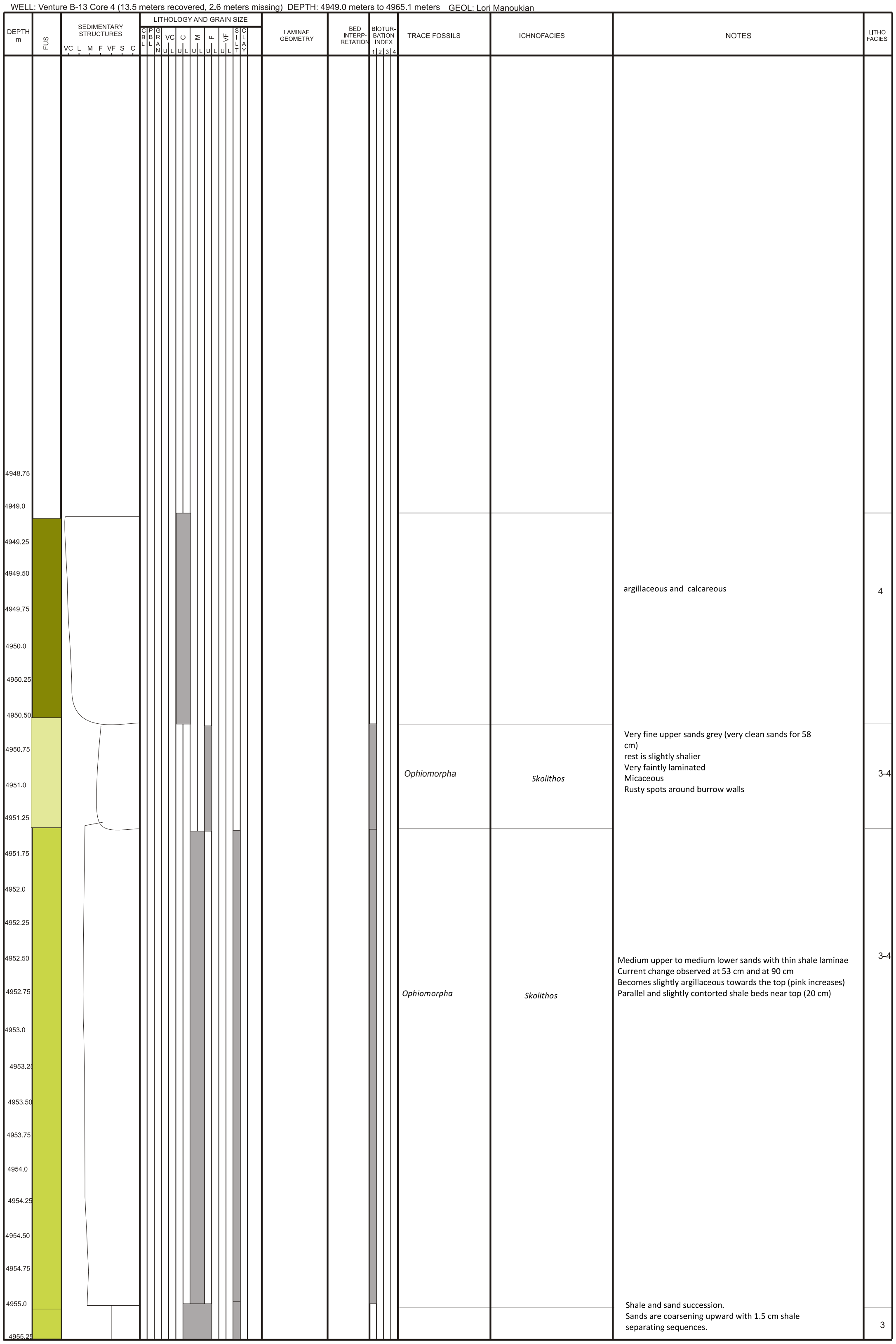
WELL: Venture B-13 Core 4 (13.5 meters recovered, 2.6 meters missing) DEPTH: 4949.0 meters to 4965.1 meters GEOL: Lori Manoukian
DEPTH m
FUS
SEDIMENTARY STRUCTURES
VC L M F VF S C
LITHOLOGY AND GRAIN SIZE
CBL
PBL
GRAN
VC U L
C U L
M U L
F U L
VF U L
SILT
CLAY
LAMINAE GEOMETRY
BED INTERP-RETATION
BIOTUR-BATION INDEX
1 2 3 4
TRACE FOSSILS
ICHNOFACIES
NOTES
LITHO FACIES
4948.75
4949.0
4949.25
4949.50
4949.75
4950.0
4950.25
4950.50
4950.75
4951.0
4951.25
4951.75
4952.0
4952.25
4952.50
4952.75
4953.0
4953.25
4953.50
4953.75
4954.0
4954.25
4954.50
4954.75
4955.0
4955.25
argillaceous and calcareous
4
Ophiomorpha
Skolithos
Very fine upper sands grey (very clean sands for 58 cm)
rest is slightly shalier
Very faintly laminated
Micaceous
Rusty spots around burrow walls
3-4
Ophiomorpha
Skolithos
Medium upper to medium lower sands with thin shale laminae
Current change observed at 53 cm and at 90 cm
Becomes slightly argillaceous towards the top (pink increases)
Parallel and slightly contorted shale beds near top (20 cm)
3-4
Shale and sand succession.
Sands are coarsening upward with 1.5 cm shale separating sequences.
3

Figure 6.5. Core 4 description sheet

Chapter 7

7.1 Discussion

7.1.1 Porosity

The dominant type of porosity of the Lower Missisauga Formation, as determined from representative cores, is intergranular and secondary. Interestingly, a general increase in porosity is observed with depth. The highest porosity is 26.1 % at a depth of 4951.99m (Core 4) and the lowest porosity is 3.9% at depths of 4704.99m (Core 1) and 4702.02m (Core 1). Values as high as 26% at nearly 5km depth are remarkable, and represent an unusual situation. This is explained by an increase of diagenetic processes with depth. In particular, dissolution of carbonate cement has created a large volume of secondary porosity within the sandstones of the Venture Field. Specifically, secondary porosity at depths below 4000m is achieved mainly by ferroan sparry calcite dissolution, and minor secondary porosity is created by dissolution of framework grains or clay alteration (Jansa and Noguera, 1990). Although syndepositional fracturing within the deeper Lower Missisauga Formation might explain unusually high porosity and permeability in some samples, there was no sign in thin sections of highly fractured rock. Lastly, as observed in thin section paragenesis (Chapter 3), the enhancement of porosity is possibly the result of numerous diagenetic events that overlapped in time (Jansa and Noguera, 1990). Furthermore, it was noticed that lithofacies with authigenic chlorite have higher porosity values. Silica overgrowths on detrital quartz grains are non-existent with the presence of chlorite that precluded quartz growth and in these cases preserved the original porosity (Drummond, 1990).

7.1.2 Horizontal Permeability

Core plug permeability measurements showed no trends with increased depth; however, values did increase from facies 1 to facies 4. The oolitic limestone(1) has the lowest permeability and is a weak flow unit, followed by shales (2), heterolithic and cyclic sandstone and shale (3), and finally facies 4 cross-stratified micaceous sandstone. As such, facies 4 would be the best flow unit and possibly the highest quality reservoir rock. Furthermore, since lithofacies 4 has the highest amount of data points, it provides the researcher with the most accurate permeability result. Lithofacies 3 only had one data point, therefore the permeability value assigned will have a great margin of error. The highest permeability value encountered in the Venture B-13 cores is 208 mD (lithofacies 4, Core 4), and the lowest 0.006 mD (lithofacies 1, Core 1). Variations in permeability values are observed in scales from a single well core to a thin section. This serves as evidence for influence of numerous factors on flow unit strength including: grain size, porosity, cementation, bioturbation, and the amount of clay minerals. Based on this study's results, a larger grain size and higher porosity coincide with higher permeability values. Low cementation and clay minerals, and high bioturbation decrease permeability values.

7.1.3 Porosity vs. Permeability

Porosity and permeability are co-dependent factors that influence flow within volumes of rock. Available data of porosity and permeability from the Venture B-13 conventional cores show a log-normal trend with an R^2 value of 0.8248. The plot of reservoir properties of the four lithofacies in Figure 5.9 indicates that that lithofacies 1 has the lowest permeability and porosity measurements, followed by lithofacies 2. However, two clusters of values from lithofacies 4 were observed. One group had porosity values ranging from 11 to 18% and permeability values from 0.15 to 1.4 mD, and the other group had porosity values ranging from 17.8-26% and permeability values from 9.66 to 348mD. The lower porosity/permeability values of lithofacies 4 are associated with shallower depths and higher porosity/permeability values with increased depths due to diagenesis.

7.1.4 Flow Unit Differentiation

Tables ranking potential differences in flow units were created incorporating change in grain size, lithology, permeability, cementation and bioturbation. Units were given a number out of a potential 48. Overall, 58 flow units were identified, with 45 identified as major flow units. The highest individual flow unit value was 30 out of a possible 48. Seemingly low values indicate that potential flow unit differentiation is not located at specific intervals in the well cores. In certain cases, flow unit divisions are not clearly defined and may be found within a zone. The lowest value is “0” indicating that there is no change between overlying and underlying lithologies. Values below 15 would indicate poor flow unit differentiation. Accuracy of the applied methodology may be improved by adding additional variables such as grain shape, and pore throat size or geometry. Moreover, since cementation is variable at a microscopic scale, the margin of error for the cementation column may be greater than the rest of the criteria. The thickest of these potential flow units is 3.4 m and the thinnest of these flow units is approximately 5cm. It is important to note that although volumes of rock have been assigned fixed permeability values, these are microscopically variable. An increased amount of permeability data points would improve accuracy of this methodology.

7.1.5 Flow Unit Characterization

Core plug permeability averages were assigned to lithofacies assemblages and were subsequently compared to calculated potential flow ability. Grain size, clay content, cementation, porosity and bioturbation data were used to quantify flow quality within rock units. Flow units were assigned a value out of 20. A total of 56 flow units identified in the previous section were thoroughly analysed with respect to their strength. Generally, low permeability measurements associated with low calculated flow potential values and high permeability measurements associated with high calculated flow potential values. Where this was not the case, more accurate values of permeability are needed. The highest value was an 18 out of 20 representative of a good flow unit, and the lowest was a 2 out 20 representative of a poor flow unit. Finally, lithofacies cementation and clay content averages were used in these tables, the values assigned for “ability to flow” column may have a large margin of error. By adding colors indicative of flow unit strength onto core description sheets, change in strength was easily observed.

7.2 Conclusions

Core of the Lower Missisauga Formation reservoir sands from the Venture B-13 well demonstrate a wide range of permeability and porosity values throughout core. This study has explored numerous factors that affect fluctuations in permeability and porosity allowing the formulation of flow units such as clay content, cementation, bioturbation and grain size.

Description of approximately 57 meters of core allowed for the identification of the following lithofacies (Table 7.1) and microlithofacies (Table 7.2):

Table 7.1. Lithofacies identified in the Venture B-13 cores and interpreted depositional environments.

Lithofacies	Name	Interpreted depositional environments
1	Oolitic limestone	Shallow marine, sub-tidal zone
2	Shale	Shallow marine open shelf
3	Heterolithic and cyclic sandstones and shales	Tide influenced, nearshore shallow marine shelf
4	Cross-stratified calcareous and micaceous Sandstone	Shoreface deposits

Table 7.2. Microlithofacies identified in the Venture B-13 cores and associated lithofacies.

Microlithofacies	Lithofacies Association	Thin Sections
Bio-oosparite	1	4692.2m, 4693 m, 4695.62 m, 4698 m
Oobiosparite	1	4704.85m, 4711.40m
Burrowed clay	2	4708.14m
Interbedded siltstone and clay	3	4708.14m and 4716.25m
Fine to medium-grained calcareous sandstone with ooids and shell fragments	4	4699.66 m, 4703.01m
Very fine- to medium-grained calcareous sandstone	4	4718.70m, 4718.75m
Fine- to coarse-grained calcareous silt	4	4693.64 m, 4707.80m, 4708.20m, 4711.95m, 4727.60m, 4730.20 m, 4730.67m, 4749.76m

Table 7.3. Average lithofacies porosity and permeability measurements from the Venture B-13 cores.

Lithofacies	Average porosity measurement from core plugs	Core plug average permeability measurement (mD)
1	0.04825	0.01275
2	0.1092	1.90667
3	0.1720	3.38
4	0.1912	76.136

From core plug measurements, average porosity and permeability measurements were identified for all lithofacies (Table 7.3). Data show that porosity and permeability increase from lithofacies 1 to 4. As such, cross-stratified calcareous and micaceous sandstones of lithofacies 4 are the best quality reservoir, whereas oolitic limestones (lithofacies 1) and shales (lithofacies 2) have extremely low to no porosity and act as baffles or barriers to flow.

Plotting values of porosity against permeability showed a linear trend and increased flow unit potential with depth. Diagenesis is the main contributor in creation of porosity within the Lower Missisauga Formation. Data and thin section analysis show that alteration of sand body as a result of dissolution and diagenesis has considerably increased porosity values at greater depths. Lithofacies 4 shows evidence of late diagenesis, whereas lithofacies 1 shows evidence of early diagenesis.

Throughout the Venture B-13 cores, the appearance of trace fossils is correlated to low permeability intervals. The mud linings of trace fossils within clean sands of lithofacies 4 and diagenetic haloes have created zones of low permeability. Furthermore, where bioturbation is high, mud and sand are highly mixed, further lowering permeability values. Analysis of trace fossils also aided in the interpretation of paleoenvironments.

Application of methodologies integrating semi-quantitative values of porosity, permeability, bioturbation, and clay and cement content permitted the identification of 56 minor flow units and 48 major flow units within the Venture B-13 cores. The majority of these flow units demonstrated medium to high preferential flow. From one flow unit to the next, values assigned to specific criteria showed variations, though in some cases the flow unit strength was the same and not affected. In such situations, finer scale variations can be resolved through other analyses. Average core plug permeability values generally correspond to calculated flow potential of unit. The accuracy of this method may be improved with an increased number of permeability data points.

The flow of fluids through the Missisauga Formation is being controlled at a scale of meters or less. For current and future gas or oil production from this and other formation reservoirs must be understood and exploited effectively, the resolution of modelling and completion must be at this fine scale.

7.3 Future Work

For the gas-producing Sable Subbasin, a high resolution reservoir model of the Missisauga Formation could be created using this thesis' flow unit identification methodology. If applied to the greater Sable Subbasin area, this high resolution reservoir model for the Missisauga Formation could be identified in and linked to specific signatures in petrophysical well log data to classify flow units throughout the Missisauga Formation in the Venture B-13 well. It could also be extended to other wells in the Venture Field and integrated with reservoir production data. However, as seen on Figure 1.6, the resolution of petrophysical data is likely not high enough to identify small scale heterogeneities. Baffles and barriers in the reservoir may be identified and hydrocarbon preferential flow identified. For a more accurate definition of reservoir flow units in all Venture B-13 cores, it is recommended that more core plugs be obtained and analysed for their porosity and permeability. Finally, grain shape and angularity should also be analysed in future work as these have direct impact on porosity values.

References

Boggs, S. 2006. *Principles of sedimentology and stratigraphy*. (4th ed.). Upper Saddle River: Pearson Prentice Hall.

Bromley, R.G. 1990. *Trace fossils: Biology and Taphonomy*. Institute of Historical Geology and Palaeontology, University of Copenhagen, Denmark.

Bromley, G. R. 1996. *Trace fossils: Biology, taphonomy and applications*. (2nd ed.). London, England: Chapman & Hall. Retrieved from http://books.google.ca/books?id=ngZI35A1os0C&pg=PA179&dq=ophiomorpha&hl=en&sa=X&ei=K0wEUebmFOLB0AGyuYH4DA&ved=0CDUQ6AEwAQ.

Calvo, J.P., Rodriguez-Pascua, M., Martin-Velazquez, S., Jimenez, S., & De Vicente,G. 2002. Microdeformation of lacustrine laminite sequences from Late Miocene formations of SE Spain:an interpretation of loop bedding. *Journal of Sedimentary Research*. Vol. 45 (2), pp279-292. Retrieved from http://onlinelibrary.wiley.com/doi/10.1046/j.1365-3091.1998.00145.x/abstract.

Canada Nova Scotia Offshore Petroleum Board. 2013. Call for bids: Regional geology overview. Retrieved from http://www.callforbids.cnsopb.ns.ca/2008/02/regional_geology.html.

Canada Nova Scotia Offshore Petroleum Board. 2013. Offshore activity: Production data. Retrieved from http://www.cnsopb.ns.ca/offshore-activity/production-data.

Colletta, B., Monnier, G., Rabary, G., Doublet, S., & Letouzey, P. 2011. Offshore Nova Scotia Play Fairway analysis: 2D basin modeling results. Offshore Technology Conference, Houston Texas, USA.

Cummings, Don I; R. William C. Arnott. (2005) Growth-faulted shelf-margin deltas: a new (but old) play type, offshore Nova Scotia. *Bulletin of Canadian Petroleum Geology*. Vol. 53, 3, pp 211-236.

Dalrymple, R.W. 2010. *Facies Models*. (4th ed.). Geological Association of Canada. Kingston, Ontario.

Davis, A. R., & Dalrymple, R. W. 2012. *Principles of sedimentology*. New York, NY: Springer Science. Retrieved from http://books.google.ca/books?id=hyuIYTTjFL4C&pg=PA69&lpg=PA69&dq=cylindrichnus&source=bl&ots=FR8SbAsqL&sig=T1bpLc1BATj1epSUZ3YquA3nJSI&hl=en&sa=X&ei=hFzvUIaQLKqx0QGN8ICgAQ&ved=0CFoQ6AEwCQ.

Doyle, S. 2006. Permeability, porosity, and depositional environment and their effect on reservoir quality in the Cretaceous Bluesky Formation Whitecourt, Alberta. Unpublished BSc thesis, Dalhousie University Earth Sciences.

Drummond, K.J., 1990. *Geology of Venture, a Geopressured Gas Field, Offshore Nova Scotia.* In: M.T. Halbouty (Ed.), *Giant Oil and Gas Fields of the Decade 1978-1988.* American Association of Petroleum Geologists, Memoir 54, p.55-71.

Geomore. 2012. Porosity and permeability. Retrieved from http://www.geomore.com/porosity-and-permeability-2/.

Guild, P. W., 1981. Preliminary metallogenic map of North America: A numerical listing of deposits (858-A). *U.S Geological Survey* Retrieved from website: http://books.google.ca/books?id=YTrwAAAAMAAJ&pg=RA1-PA71&lpg=RA1-PA71&dq=missisauga formation&source=bl&ots=GHacIzOAdw&sig=FGCoC9oaF5AsJsa0UMFqjUk7ls0&hl=en&sa=X&ei=rxAdUfe5EMiP0QGlnoDIAw&ved=0CFIQ6AEwBg.

Hansen ,D.M., Shimeld, J.W., Williamson, M.A.,& Lykke-Andersen, H. 2004 Development of a major polygonal fault system in Upper Cretaceous chalk and Cenozoic mudrocks of the Sable Subbasin, Canadian Atlantic margin. *Marine and Petroleum Geology* Vol.21, pp1205–1219.

Hohn, M. E. 2012. Petroleum geology and reservoir characterization of the Upper Devonian Gordon sandstone, Jacksonburg-Stringtown oil field, northwestern West Virginia (B-45). *West Virginia Geological and Economical Survey*. Retrieved from website: http://www.wvgs.wvnet.edu/www/news/Bulletin45Summary.pdf.

Ings, S.J., MacRae, A.R., Shimeld, J.W., & Pe-Piper, G. 2005. Diagenesis and porosity reduction in the Late Cretaceous Wyandot Formation, offshore Nova Scotia: a comparison with Norwegian North Sea Chalks." *Bulletin of Canadian Petroleum Geology.* Vol 53, pp237-249.

Jansa, L.F., & Noguera V.H. (1990). Geology and Diagenetic History of Overpressured Sandstone Reservoirs, Venture Gas Field, Offshore Nova Scotia, Canada. *The American Association of Petroleum Geologists.* Vol. 74, No 10, pp1640-1658.

Jansa, L.F. and Wade, J.A., 1975. Paleogeography and sedimentation in the Mesozoic and Cenozoic, southeastern Canada. In: C.J. Yorath, E.R. Parker and D.J. Glass (Eds.), Canada's Offshore Margins and Petroleum Exploration. Canadian Society of Petroleum Geologists, Memoir 4, p.79-102.

Hyne, N. J., 2001. Nontechnical Guide to Petroleum Geology, Exploration, and Production, 2nd Edition. *PennWell Corporation*. Retrieved from http://books.google.ca/books?id=D4I-G0DcTcUC&printsec=frontcover&source=gbs_ge_summary_r&cad=0#v=onepage&q&f=false.

Kidston, G.A., Brown, D.E., Smith, B.M, & Althiem, B. 2005. The Upper Jurassic Abenaki Formation offshore Nova Scotia: A seismic and geologic perspective. *Canada Nova Scotia Offshore Petroleum Board*, Canada.

Karim, A., Pe-Piper, G., Piper, D. 2009. Controls on diagenesis of Lower Cretaceous reservoir sandstones in the western Sable Subbasin, offshore Nova Scotia. *Journal of Sedimentology*. Department of Geology, Saint Mary's University, Halifax.

La Croix, A.D., Gingras, M.K., Dashtgard, S.E., Pemberton, S.G., 2012. Computer modeling bioturbation: the creation of porous and permeable fluid-flow pathways. American Association of Petroleum Geologists Bulletin. Vol 96, pp545–556.

McIver, N. L.. 1971. Cenozoic and Mesozoic Stratigraphy of the Nova Scotia Shelf. *Canadian Journal of Earth Sciences,* Vol. 9, pp 54- 70.

Mukhopadhyay, P.K., Brown, D.E., Kidston, D.G., Bowman, T.D., Faber, J., & Harvey,P.J. 2003. Petroleum Systems of Deepwater Scotian Basin, Eastern Canada: Challenges for Finding Oil versus Gas Provinces. *Offshore Technology Conference*.

New England Research, Inc. 2003. *TinypermII*. Retrieved from http://ner.com/laboratory-systems/tinyperm-ii.html

Pearson, N.J., & Gingras, M.K. 2006. An ichnological and sedimentological facies model for muddy point-bar deposits. *Journal of Sedimentary Research.* Vol.76, No. 5 pp771-782. Retrieved from http://jsedres.sepmonline.org/content/76/5/771

Pemberton, S.G. & MacEachern, J.A., Frey, R.W. 1992. Trace fossil facies models: Evironmental and allostratigraphic significance (Facies Models: response to sea leavl change). Edited by Walker, R.G. and James, N.P. *Geological Association of Canada*, St. John's, pp47-73.

Ramm,M., & Bjorlykke, K. 1993. Porosity/depth trends in reservoir sandstones: Assessing the quantitative effects of varying pore-pressure, temperature history and mineralogy, Norwegian shelf data. Retrieved from http://www.minersoc.org/pages/Archive-CM/Volume_29/29-4-475.pdf.

Reading, H.G. 1978. *Sedimentary Environments and Facies*. Elsevier, New York.

Sable Offshore Energy. 1996. Development Plan: Geology, geophysics and petrophysics. Unpublished report submitted to and available through the Canada Nova Scotia Offshore Petroleum Board), 230p.

Schlumberger Oilfield Glossary. 2013. Retrieved from http://www.glossary.oilfield.slb.com/

Shepherd, M., 2009. Production data and layering. *Oil Field Production Geology*: American Association of Petroleum Geologists Memoir 91, p.131-144.

Terry, R.D. , Chilingarian, G.V., 1955. Summary of " Concerning some additional aids in studying sedimentary formations" by M.S. Shvestsov. *Journal of Sedimentary Research*., Vol. 25(3), pp229-234.

Tsikouras, B., Pe-Piper, G., Piper, D. J. W., & Schaffer, M. 2011. Varietal heavy mineral analysis of sediment provenance, lower cretaceous scotian basin, Eastern Canada. *Sedimentary Geology*, Vol *238*(3-4), pp150-165. Retrieved from http://www.sciencedirect.com/science/article/pii/S0037073811000650.

Wach, G. 2007. Trinidad field guide. Dahousie University Department of Earth Sciences.

Wade, J. A. 1991. Scotian shelf lithostratigraphy: Missisauga formation. Geological Survey of Canada, Atlantic Geosciences Center. Retrieved from website: ftp://ftp2.cits.rncan.gc.ca/pub/geott/ess_pubs/210/210642/gscecbas_ss-210642_b_1991_nt01.pdf.

Wade, J.A. and MacLean, B.C., 1990. Chapter 5 - The geology of the southeastern margin of Canada, Part 2: Aspects of the geology of the Scotian Basin from recent seismic and well data. In: M.J. Keen and G.L. Williams (Eds.), Geology of Canada No.2 - Geology of the continental margin of eastern Canada. Geological Survey of Canada, p.190-238 (also Geological Society of America, The Geology of North America, Vol.I-1).

Wade, J.A., MacLean, B.C. and Williams, G.L.; 1995. Mesozoic and Cenozoic stratigraphy, eastern Scotian Shelf: new interpretations. Canadian Journal of Earth Sciences, vol.32, no.9, pp.1462-1473.

Appendix A: Pictures of Core Boxes

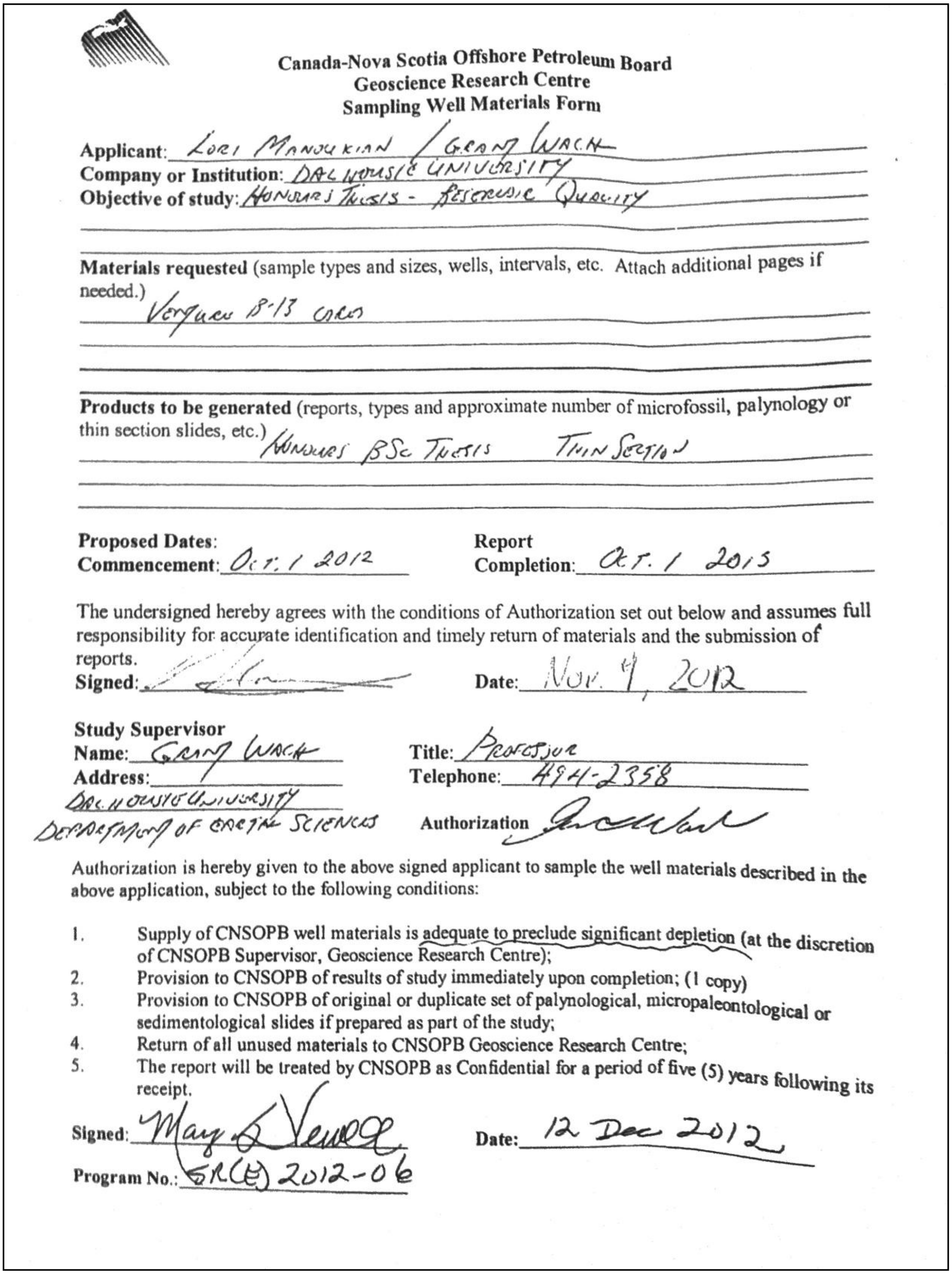

Canada-Nova Scotia Offshore Petroleum Board
Geoscience Research Centre
Sampling Well Materials Form

Applicant: LORI MANOUKIAN / GRANT WACH
Company or Institution: DALHOUSIE UNIVERSITY
Objective of study: HONOURS THESIS - RESERVOIR QUALITY

Materials requested (sample types and sizes, wells, intervals, etc. Attach additional pages if needed.) Venture B-13 cores

Products to be generated (reports, types and approximate number of microfossil, palynology or thin section slides, etc.) HONOURS BSc THESIS THIN SECTION

Proposed Dates:
Commencement: Oct. 1 2012
Report Completion: Oct. 1 2015

The undersigned hereby agrees with the conditions of Authorization set out below and assumes full responsibility for accurate identification and timely return of materials and the submission of reports.

Signed:
Date: Nov. 9, 2012

Study Supervisor
Name: GRANT WACH
Title: PROFESSOR
Address: DALHOUSIE UNIVERSITY DEPARTMENT OF EARTH SCIENCES
Telephone: 494-2358
Authorization

Authorization is hereby given to the above signed applicant to sample the well materials described in the above application, subject to the following conditions:

1. Supply of CNSOPB well materials is adequate to preclude significant depletion (at the discretion of CNSOPB Supervisor, Geoscience Research Centre);
2. Provision to CNSOPB of results of study immediately upon completion; (1 copy)
3. Provision to CNSOPB of original or duplicate set of palynological, micropaleontological or sedimentological slides if prepared as part of the study;
4. Return of all unused materials to CNSOPB Geoscience Research Centre;
5. The report will be treated by CNSOPB as Confidential for a period of five (5) years following its receipt.

Signed: Mary L Newell
Date: 12 Dec 2012
Program No.: GR(E) 2012-06

Mobil Texaco Pex Venture B-13: **Core 1**

Recovered: 17.3 m

Boxes 1 to 4: 4692.00m to 4697.29m

Boxes 5 to 8: 4697.29m to 4702.38m

Boxes 9 to 11: 4702.38m to 4706.28m

Boxes 12 to 13: 4706.28m to 4709.1m

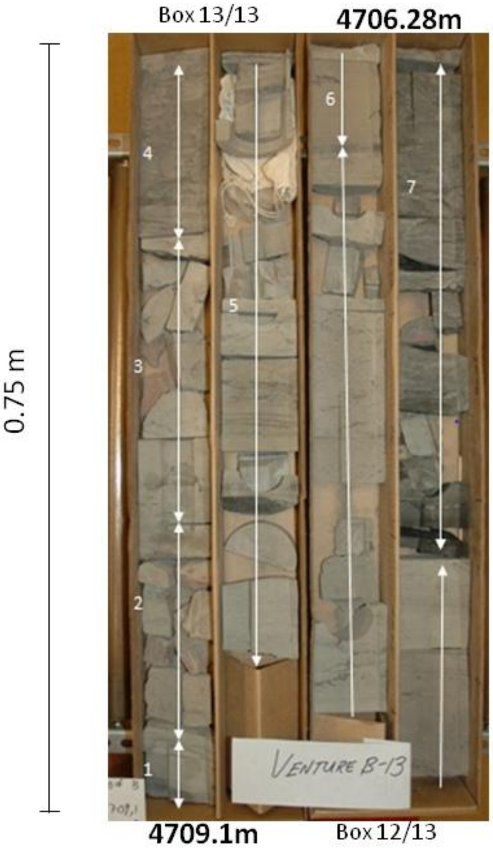
Box 13/13
4706.28m
0.75 m
4
3
2
1
5
6
7
VENTURE B-13
4709.1m
Box 12/13

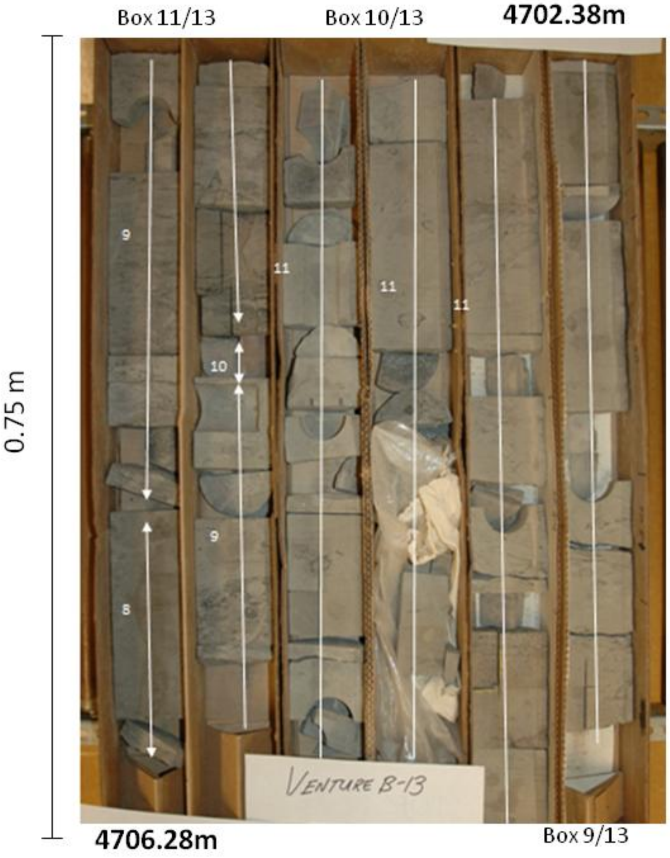
Box 11/13
Box 10/13
4702.38m
0.75 m
9
10
9
8
11
11
11
VENTURE B-13
4706.28m
Box 9/13

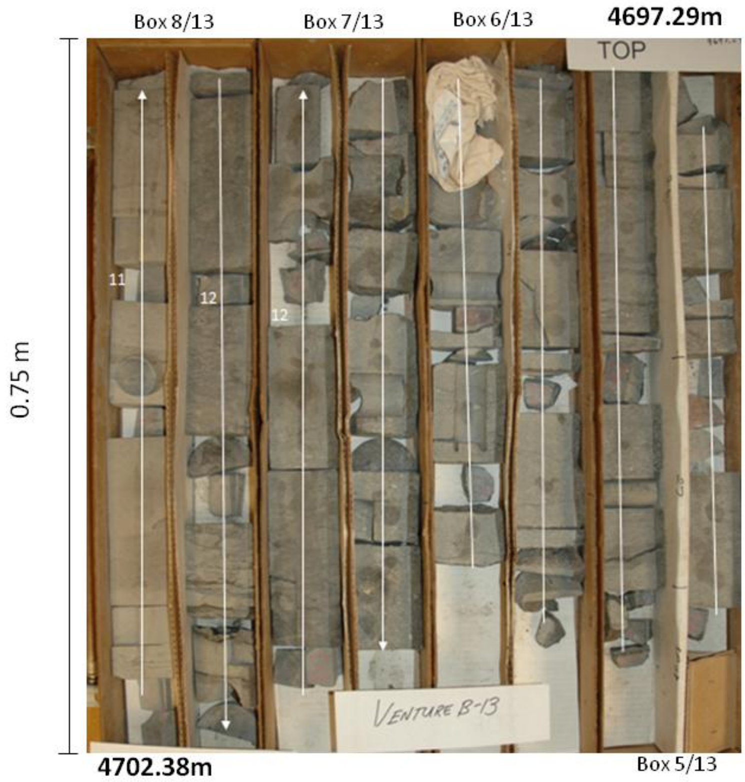
Box 8/13
Box 7/13
Box 6/13
4697.29m
TOP
0.75 m
11
12
12
VENTURE B-13
4702.38m
Box 5/13

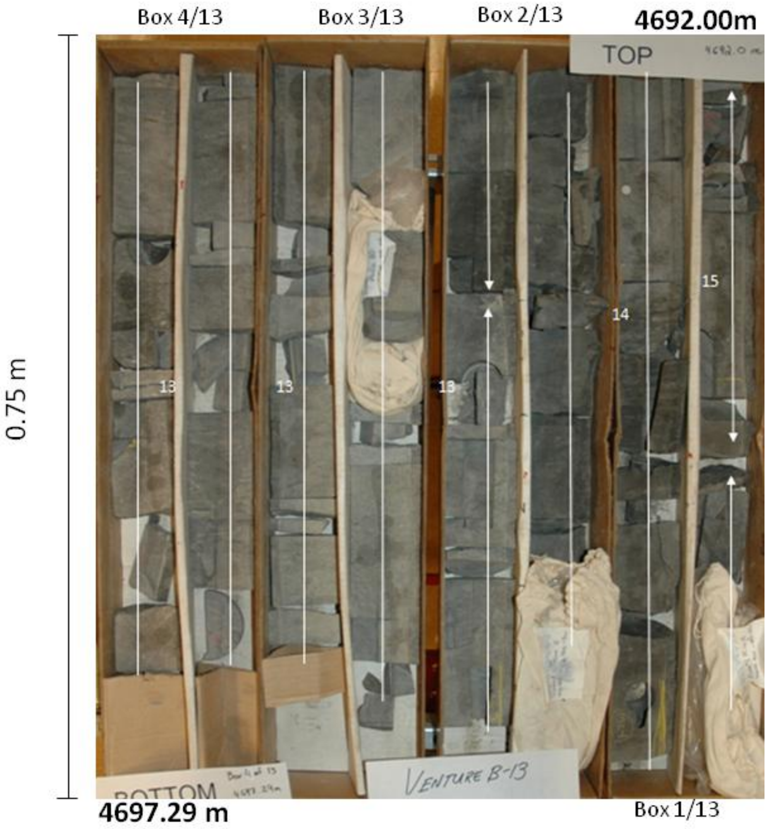
Box 4/13
Box 3/13
Box 2/13
4692.00m
TOP
0.75 m
13
13
13
14
15
BOTTOM
VENTURE B-13
4697.29 m
Box 1/13

Depth interval for numbered sections Core 1

Assigned number to core section	Depth Interval (m)
1	4709.10 to 4709.00
2	4709.00 to 4708.80
3	4708.80 to 4708.45
4	4708.45 to 4708.23
5	4708.23 to 4707.18
6	4707.18 to 4706.88
7	4706.88 to 4706.23
8	4706.23 to 4705.63
9	4705.63 to 4704.96
10	4704.96 to 4704.91
11	4704.91 to 4701.39
12	4701.39 to 4700.44
13	4700.44 to 4695.94
14	4695.94 to 4694.21
15	4694.21 to 4693.61

Description of core intervals for Core 2 (more detail on core-logging sheets)

1- Interbedded shale and very fine upper sands with *Ophiomorpha* burrows (BI:1).
2- Massive calcareous red Mudstone with minor shale Flaser bedding.
3- Light gray calcareous sandstone interlayered with shales. Coarse lower to fine upper *Skolithos* and *Ophiomorpha* burrows creating a bioturbation index of 1.A sharp contact is evident with overlaying beds.
4- Bioturbated shale (BI: 3) with *Ophiomorpha* and *Planolites* burrows.
5- Heterolithic sandstone and shale.
The bottom 20 cm are shale dominated bioturbated(BI: 3) with parallel laminations sandstone.
The shallow sections of this section is a very fine uppe, calcareous sandstone with some wavy beds (BI: 2)
6- Calcareous sandstone (very fine upper) with thin and parallel shale laminae. A bioturbation index of 1 is identified and a thin (2cm) bed of heavy minerals at the bottom of this section.
7- This section is composed of dark shale highlighting an obvious change in lithology.
A bioturbation index of 2 to 3 is apparent. There is no reaction with hydrochloric acid.
8- A primary composition of calcareous shale with shell fragments is observed. This section is slightly lighter in colour than section 5. Furthermore, no bioturbation is observed; however, evidence of bidirectional Flow is identified.
9- Cleaning upward highly bioturbated heterolithic to homogeneous sands (vFu-Fu) with a coarsening upward sequence observed. Biotite and mica Flakes may be seen and the lithology is lighter in colour than section8.
10- This is a red calcareous Fun upper (Fu) sandstone.
11- Calcareous sandstone Fu-FL that seems relatively clean when compared to rest of core.

Very thin laminae of shale are observed throughout. Lastly, *Skolithos*, *Planolites* and *Ophiomorpha* burrows are present throughout this section.

12- This section is predominantly shale with *Planolites* and *Thalassinoides* burrows filled with fine lower sandstone.

13- Interbedded oolitic limestone and non-calcareous shales. Crinoids and bivalves shell fragments were also observed.

14- Burrowed black shales with increased bioturbation towards top of section. No reaction with hydrochloric acid.

15- Oolitic limestone mixed with fine upper and fine lower sandstone. No bioturbation is observed in this section; however, some shell fossils were present.

Mobil Texaco Pex Venture B-13: **Core 2**

Recovered: 5.8m

Boxes 1 to 3: 4710.42m to 4714.00m

Boxes 4 to 5: 4714.00m to 4715.51m

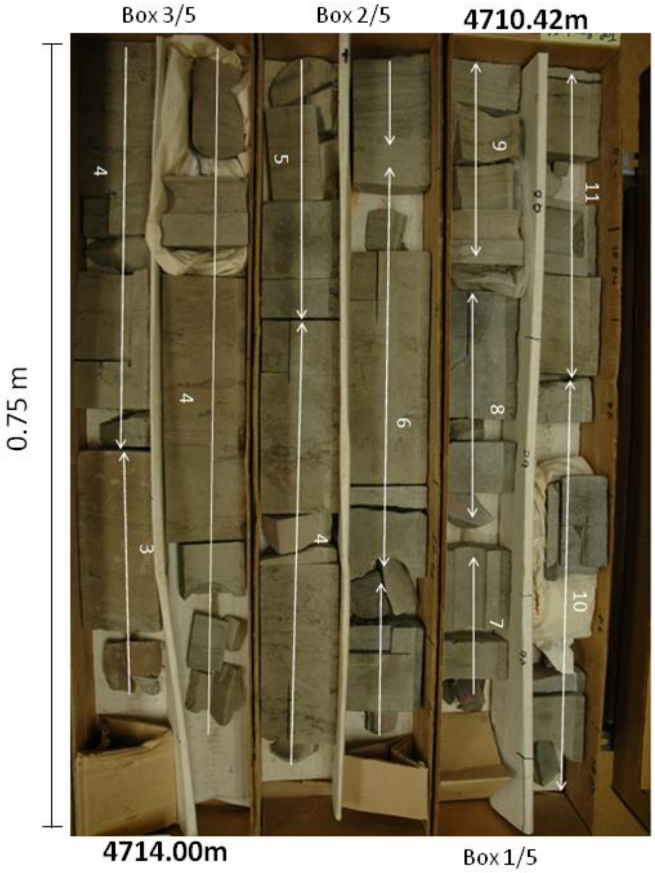
Box 3/5
Box 2/5
4710.42m
0.75 m
4
4
3
5
4
6
9
8
7
11
10
4714.00m
Box 1/5

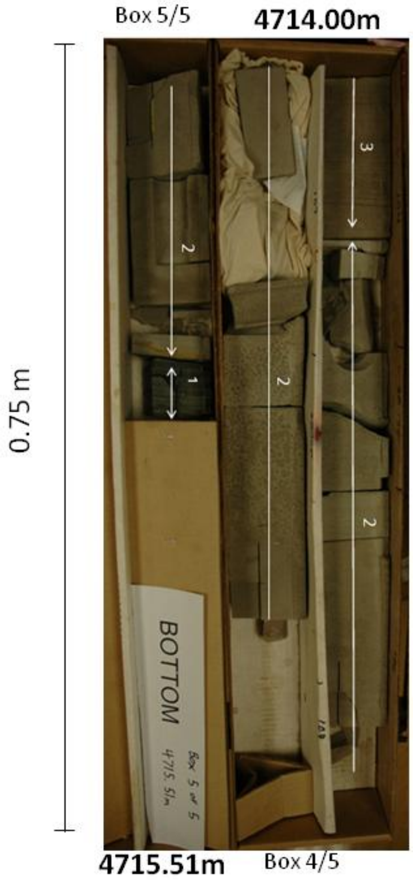
Box 5/5
4714.00m
0.75 m
2
1
2
3
2
BOTTOM
Box 5 of 5
4715.51m
4715.51m
Box 4/5

Depth interval for numbered sections of Core 2

Assigned number to core section	Depth Interval (m)
1	4716.2 to 4716.05
2	4716.05 to 4714.79
3	4714.79 to 4714.45
4	4714.45 to 4713.13
5	4713.13 to 4712.69
6	4712.69 to 4712.36
7	4712.36 to 4712.27
8	4712.27 to 4712.01
9	4712.01 to 4711.81
10	4711.81 to 4711.50
11	4711.50 to 4711.16

Description of core intervals in Core 2 (more detail on core-logging sheets)

1- Laminated shale (70%) and fine upper to medium lower sandstone (30%) are observed here. An increase of sand towards top of this section is evident.
2- Fine lower to fine upper, calcareous sandstone gritty feel with faint micaceous laminations were described for this section. There are very thin oolitic layers near top. Minimal amounts of these ooids are also present throughout section (Mu-Cl size).
A sharp contact with 3 is identified.
3- Fine lower sands with parallel shale laminations. Occurrence of calcareous blebs and *Skolithos* and *Ophiomorpha* burrows (BI: 1)
4- A colour change may be seen from previous section with some small sections showing a reddish tinge. High bioturbation (BI:3) with an increased amount of *Ophiomorpha* and *Skolithos* near the top of the core. A sharp contact with 5 is identified.
5- Black oolitic limestone with medium upper to medium lower nuclei. Crinoids and shell fragments found throughout this section.
6- Fine upper sandstone with some very thin parallel micaceous laminations. A bioturbation index of 2-3 was assigned with fairly abundant *Ophiomorpha* burrows.
There is a very sharp change from section 6 to 7.
7- Thin interbedded fine-lower sandstone and shale with ooids near bottom (3cm).
8- Dark oolitic limestone with medium upper to medium lower nuclei
9- Fine upper to fine lower sands with minimal shale laminae and *Ophiomorpha* burrows.
10- Oolitic limestone with coarse lower nuclei. This section is darker than previous oolitic section.
11- Fine upper to fine lower sand with minimal shale layers. At 15 cm, there is an 8 cm thick oolitic (CL) limestone layer.

Mobil Texaco Pex Venture B-13: **Core 3**

Recovered: 18.0m

Boxes 1 to 3: 4716.20m to 4720.00m

Boxes 4 to 6: 4720.00m to 4723.87m

Boxes 7 to 9: 4723.87m to 4727.89m

Boxes 10 to 11: 4727.89m to 4730.69m

Boxes 12 to 13: 4730.69m to 4732.45m

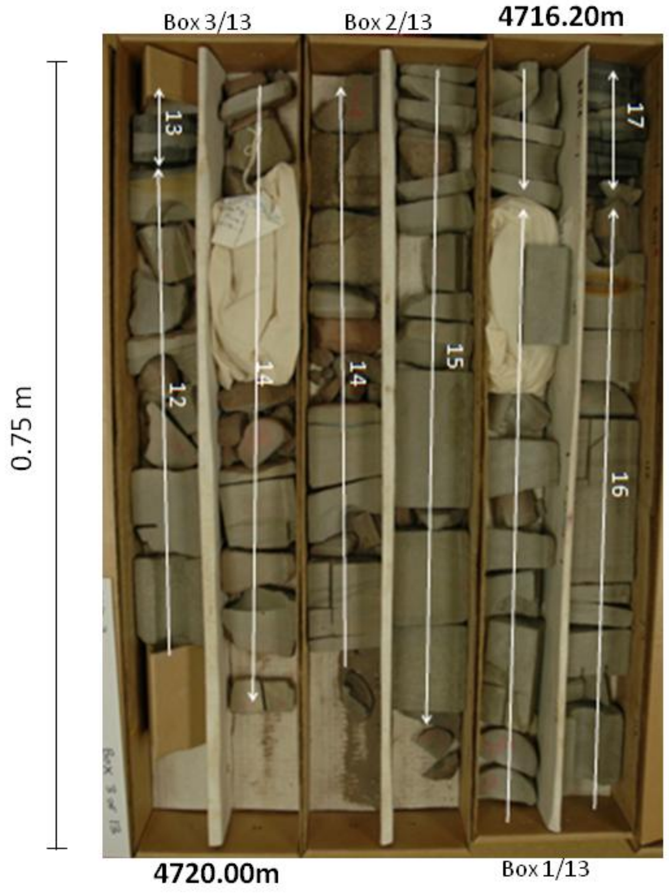
Box 3/13
Box 2/13
4716.20m
0.75 m
13
12
14
14
15
17
16
4720.00m
Box 1/13

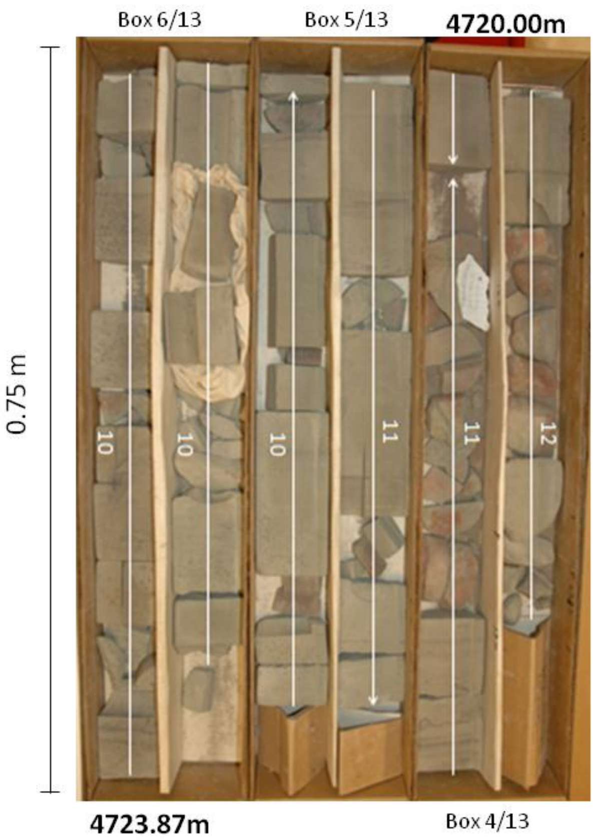
Box 6/13
Box 5/13
4720.00m
0.75 m
10
10
10
11
11
12
4723.87m
Box 4/13

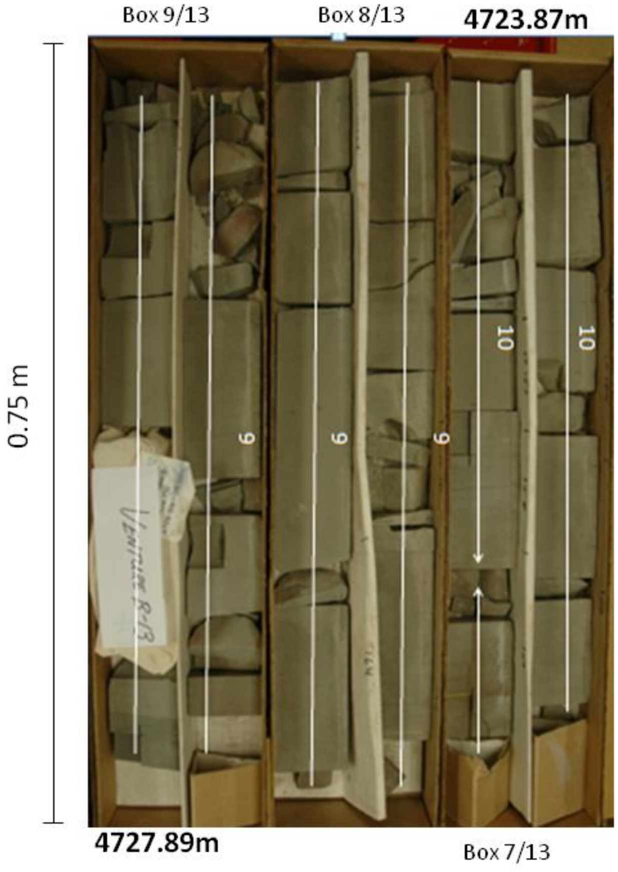
Box 9/13
Box 8/13
4723.87m
0.75 m
9
9
9
10
10
4727.89m
Box 7/13

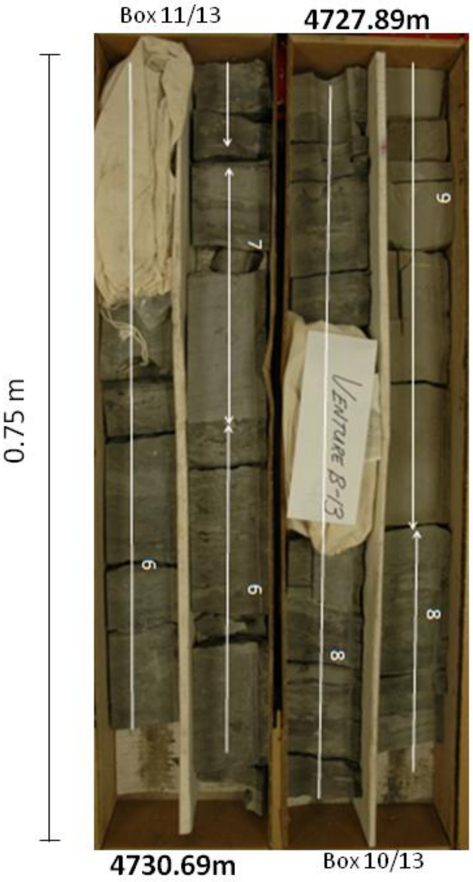
Box 11/13
4727.89m
0.75 m
7
9
9
Venture B-13
9
8
8
4730.69m
Box 10/13

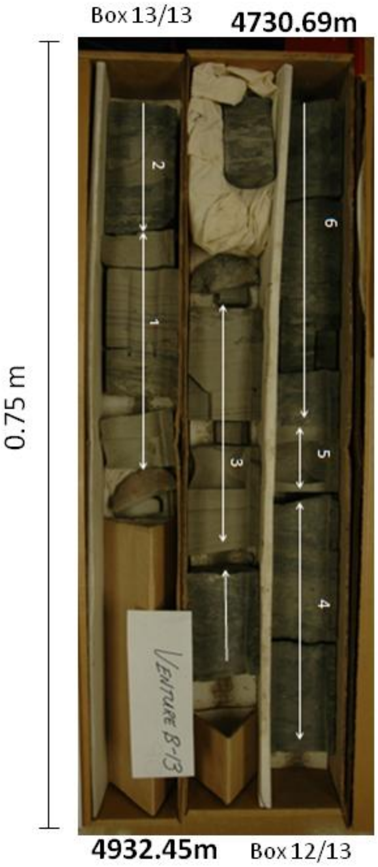
Box 13/13
4730.69m
0.75 m
2
1
3
6
5
4
Venture B-13
4932.45m
Box 12/13

Depth interval for numbered sections Core 3

Assigned number to core section	Depth Interval (m)
1	4732.50 to 4732.21
2	4732.21 to 4731.92
3	4731.92 to 4731.62
4	4731.62 to 4731.15
5	4731.15 to 4731.04
6	4731.04 to 4729.62
7	4729.62 to 4729.34
8	4729.34 to 4728.17
9	4728.17 to 4724.82
10	4724.82 to 4721.41
11	4721.41 to 4720.33
12	4720.33 to 4719.72
13	4719.72 to 4719.65
14	4719.65 to 4718.44
15	4718.44 to 4717.07
16	4717.07 to 4716.35
17	4716.35 to 4716.21

Description of core intervals for Core 3(more detail on core-logging sheets)

1- Fine upper, light grey sandstone interbedded with black silt laminae that are parallel towards top and borrowed towards the bottom of this section. Syndepositional slumping and loop bedding also present. Slightly argillaceous and calcareous sandstone with a red tinge in some sections as well. Possible rhythmic bedding (tidal couplets and bundles) observed.

2- A sharp change in lithology is observed from previous section. These are black shales (90%) interbedded with fine upper sandsone. *Arenicolites* and *Planolites* burrows are identified within the shale

3- Calcareous fine upper sandstone with *Asterosoma* and *Skolithos* burrows.

4- Highly bioturbated shales(BI :3) with *Planolites* and *Ophimorpha* burrows.

5- Fine upper calcareous sandstone with parallel shale laminations. A sharp change is observed with previous section.

6- Shale with a sharp scoured contact with sands from 5. A bioturbation index 2-3 is found throughout the section with increased bioturbation towards the top.

7- Fine Upper sandstone with faint fissile shale laminae and *Planolites* and *Ophiomorpha* burrows. Small garnets are found in thin <1mm shale layers

8- Consecutive sequence of interlayered/bioturbated beds of sands and shales (predominantly shales). Small garnets are found in some of the sandier layers.

   Thin organic bed (2mm) shiny and surrounded by yellow.

9- Fine-upper to fine-lower light grey, calcareous sandstone with minimal shell fragments. Muscovite and biotite are present throughout this section in thin laminae. Some argillaceous sections are also observed.

10- Same as 9, but slightly more pronounced dark laminae. A gradational change from fine upper to medium lower sandstone with high amounts of muscovite was present. Towards the top of the section, shale laminae begin to appear. Occurrence of garnets, as well as *Ophiomorpha* and *Rosselia socialis* burrows are characteristics of this section.

11- Coarser grained calcareous and argillaceous sandstone with good porosity.

12- Yellow to gray coarse grained micaceous sandstone. Some parallel shale laminae were evident (shale ~1mmx20).

13- Black shale with no observable bioturbation.

14- Coarsening upward sequence (medium upper to coarse upper) of sandstone.

   The shale laminae in this section are parallel and slightly dipping (<3^{o}).

15- Coarse lower to coarse upper sandstone. No laminations and minimally argillaceous.

16- Sharp erosive change from previous section. Light grey with fine upper to medium lower grained sands and parallel micaceous laminae.

17- Shale with no observable bioturbation

Mobil Texaco Pex Venture B-13: **Core 4**

Recovered: 18.3m

Boxes 1 to 3: 4949.00m to 4952.67m

Boxes 4 to 6: 4952.67m to 4955.98m

Boxes 7 to 9: 4955.98m to 4959.82m

Boxes 10 to 11: 4959.82m to 4962.66m

Boxes 12 to 13: 4962.66m to 4965.10m

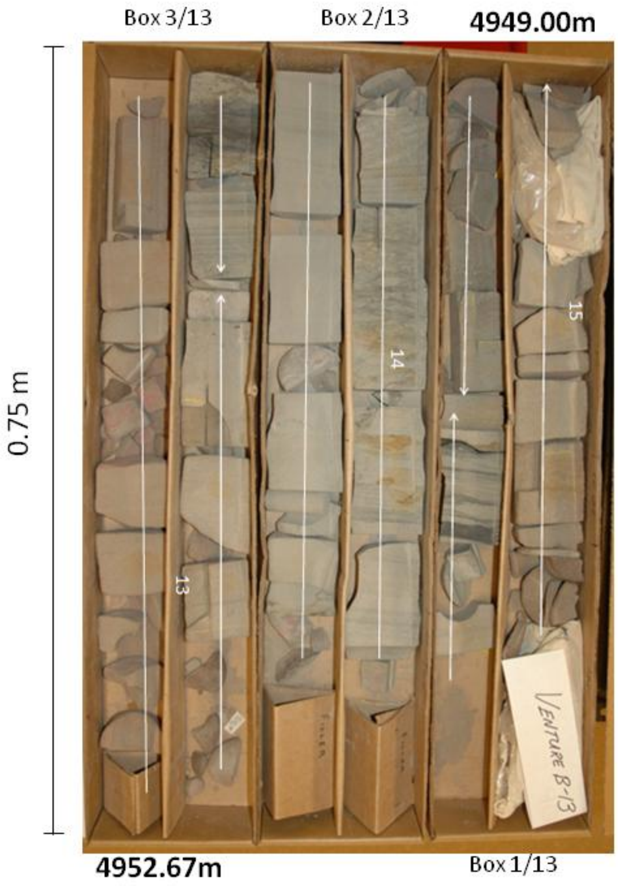
Box 3/13
Box 2/13
4949.00m
0.75 m
13
14
15
Venture B-13
4952.67m
Box 1/13

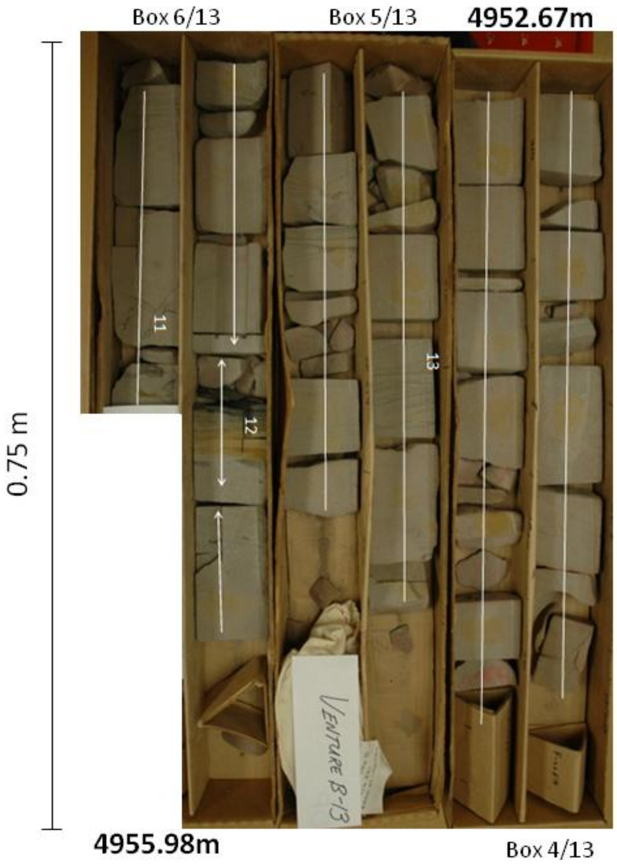
Box 6/13
Box 5/13
4952.67m
0.75 m
11
12
13
Venture B-13
4955.98m
Box 4/13

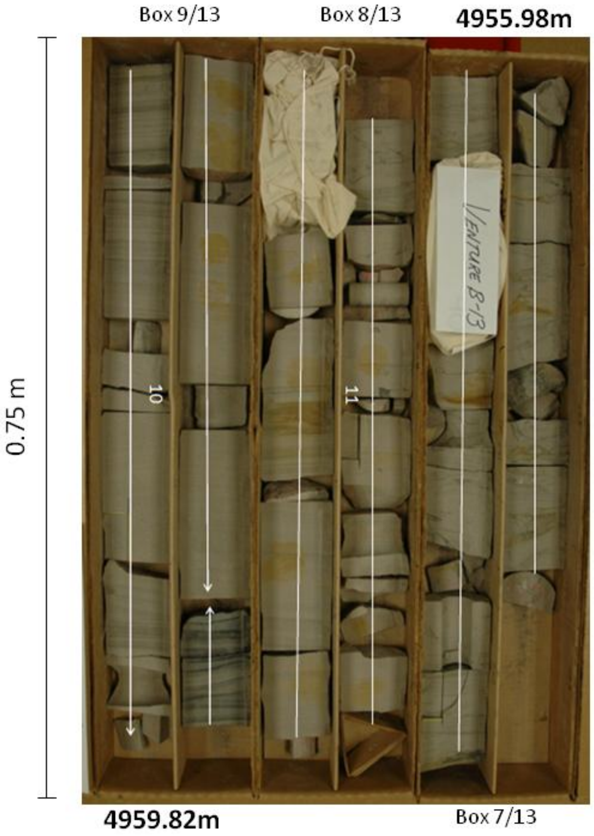
Box 9/13
Box 8/13
4955.98m
0.75 m
10
11
Venture B-13
4959.82m
Box 7/13

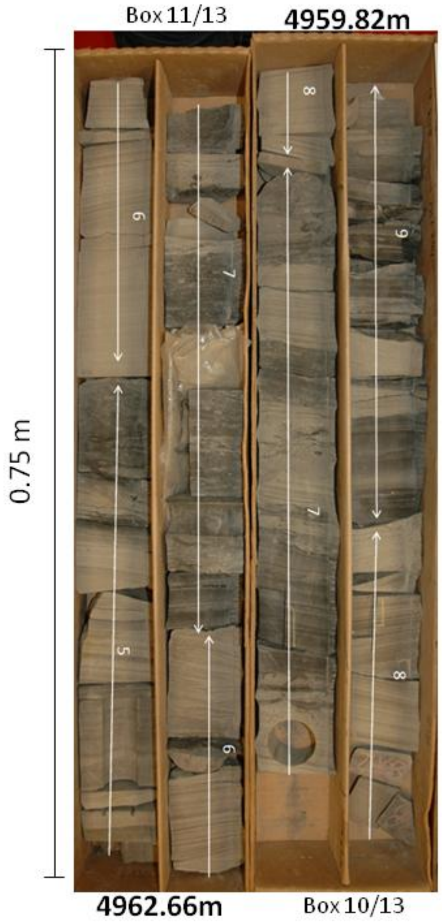
Box 11/13
4959.82m
0.75 m
9
8
7
6
5
4962.66m
Box 10/13

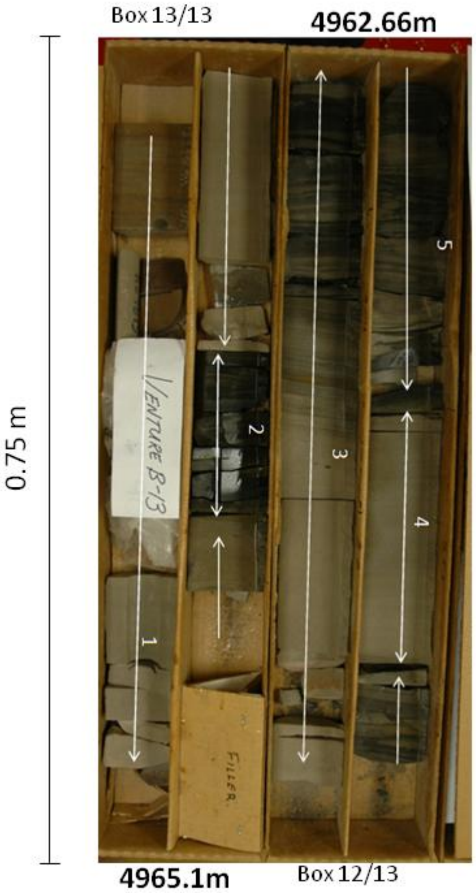
Box 13/13
4962.66m
0.75 m
VENTURE B-13
FILLER
1
2
3
4
5
4965.1m
Box 12/13

Depth interval for numbered sections Core 4

Assigned number to core section	Depth Interval (m)
1	4965.1 to 4964.35
2	4964.35 to 4964.19
3	4964.19 to 4963.13
4	4963.13 to 4962.85
5	4962.85 to 4962.17
6	4962.17 to 4961.63
7	4961.66 to 4960.56
8	4960.56 to 4960.16
9	4960.16 to 4959.76
10	4959.76 to 4958.93
11	4958.93 to 4955.20
12	4955.20 to 4955.00
13	4955.00 to 4951.62
14	4951.62 to 4950.59
15	4950.59 to 4949.12

Description of core intervals for Core 4 (more detail on core-logging sheets)

1- Light grey to brown, very fine upper calcareous sandstone with parallel shale laminae dipping ~1-2°. No bioturbation was observed.

2- Dark shale with a bioturbation of 1-2 (*Planolites* burrows)

3- Very fine upper sands fining upward. Parallel shale laminae appear after 59 cm, reaching a maximum thickness of 5 cm. These laminae dip ~3-4°. *Planolites* and *Ophimorpha* burrows are present; however, there is low bioturbation.

4- Very fine upper sand

5- Equal amounts of sandstone and shale (50%) interbedded. Bioturbated crossbeds present dipping ~10° towards top. Ophiomorpha and Planolites burrows observed. Sections 4 and 5 may be combined to create a fining upward sequence.

6- Very fine upper sandstone with darker shale laminae, parallel and dipping 3°.
Climbing ripples observed on top 12cm of section.

7- Same as number 5, except the shale layers are thicker, contorted at 38 cm (for 13cm) and the sandstone layer is similar to number 6.

8- Very fine upper sands with beds demonstrating opposing dip.

9- Shale and interbedded sandstone. Shale laminae show dips greater than 20°.

Relatively thick shale layers reaching 5 cm.

10- Fine upper calcareous sandstone similar to number 3 demonstrating a fining upward sequence.

11- Very fine grained micaceous sandstone with low angle cross-stratification. Diagenetic haloes around burrow walls. The top 132 cm of this section are burrowed (*Ophimorpha* and *Cylindrichnus*)

12- Fine upper to coarse lower shale and sand succession. Sands are coarsening upward with 1.5 cm shale separating sequences.

13- Medium upper to medium lower sands with thin shale laminae and *Ophiomorpha* burrows (BI: 1-2). Beds with opposing dip are observed at 53 cm and at 90 cm.

The sandstone of this section becomes slightly argillaceous towards the top. Lastly, parallel and slightly contorted shale beds begin to appear near the top 20 cm of this section.

14- Very fine upper, micaceous grey sands. The bioturbation index is 1-2 and diagenetic haloes are observed.

15- Coarse upper to coarse lower calcareous and argillaceous sands.

Appendix B: Horizontal core plug data points

Core number	Sample number	Depth (m)	Permeability (mD)	Porosity (%)
1	1	4701.8	0.013	4.1
1	2	4702.02	0.006	3.9
1	3	4702.27	0.008	6.7
1	4	4702.77	0.024	4.6
1	5	4703.13	0.15	6.6
1	6	4703.95	0.13	5.9
1	7	4704.99	0.024	3.9
1	8	4705.55	0.17	3.5
1	9	4705.93	0.13	6.2
1	10	4705.97	0.16	6.2
1	11	4706.64	0.1	6.7
1	12	4706.98	0.36	11.7
1	13	4709.4	0.24	16.9
2	14	4713.82	0.5	18.1
2	15	4715.84	0.056	8.3
2	16	4716.7	3.38	23.9
3	17	4717.49	107	23.8
3	18	4717.53	79.7	23.9
3	19	4717.63	59.2	17.8
3	20	4717.93	42.5	18.9
3	21	4718.17	71.5	26
3	22	4718.63	23.7	23.2
3	23	4719.11	94.3	23.9
3	24	4719.15	348	25.1
3	25	4719.39	184	22.7
3	26	4719.95	172	21
3	27	4720.27	132	18.5
3	28	4724.34	9.66	24.4
4	29	4950.02	74.1	19.8
4	30	4950.45	1.39	11.1
4	31	4951.03	0.94	16.2
4	32	4951.08	0.15	12.3
4	33	4951.44	21.8	24.8
4	34	4951.82	19.7	24.6
4	35	4951.94	17.4	24.7
4	36	4951.99	31.1	26.1
4	37	4953.14	217	25.3
4	38	4954.46	208	25.2
4	39	4954.76	67.7	23.9
4	40	4954.81	73.9	23.6
4	41	4955.61	52.7	23.3
4	42	4955.65	120	24.9

Appendix C: Thin section data points

Sample	Core	Depth (m)
1	1	4692.2
2	1	4693
3	1	4693.64
4	1	4695.62
5	1	4698
6	1	4699.66
7	1	4703.01
8	1	4704.85
9	1	4707.40
10	1	4707.80
11	1	4708.14
12	1	4708.20
13	2	4711.40
14	2	4711.95
15	3	4716.25
16	3	4718.70
17	3	4718.75
18	3	4727.60
19	3	4730.20
20	3	4730.67
21	3	4749.76

Thin sections sampled from Canada Nova Scotia Offshore Petroleum board.

Sample name	Core	Thin section depth (m)	Polished thin section depth (m)
GW 001 2013	4	4952.14	4952.14
GW 002 2013	4	4952.34	4952.34
GW 003 2013	4	4961.44	4961.44
GW 004 2013	4	4963.64	4963.64
GW 005 2013	4	4963.95	4963.95
GW 006 2013	4	4964.37	4964.37